MATERIAL PROCESSING USING A CO_2 LASER

By

RAJESH IYER

Bachelor of Engineering

Visvesvaraya Regional Engineering College,

Nagpur, India

1991

Submitted to the Faculty of the
Graduate College of the
Oklahoma State University
in partial fulfillment of
the requirements for
the Degree of
MASTER OF SCIENCE
May, 1997

MATERIAL PROCESSING USING A

CO_2 LASER

Thesis Approved:

R Komanduri

Thesis Adviser

Don A. Tucca

Ronald L. Dougherty

Thomas C. Collins

Dean of the Graduate College

ACKNOWLEDGEMENTS

I would like to acknowledge my indebtedness to my adviser, Professor R. Komanduri, for his guidance, encouragement and support throughout the graduate program.

I would like to express my gratitude to Dr. D. A. Lucca and Dr. R. Dougherty for agreeing to serve in my thesis committee, and for their suggestions and reviews of this thesis.

My sincere thanks to Professor Hou for helping me with the heat transfer modeling and his constant encouragement during this project.

Thanks are due to my colleagues in the lab, in particular, Mike Scharf and Jeff Ericksson. This acknowledgement would be incomplete without mentioning special thanks to Mallika for helping me with the SEM and XRD analysis. I would like to thank Dr. Ali Noori Khajavi for his help and guidance throughout the course of this project.

Last, but certainly not the least, my thanks to Jerry Dale and his associates, for helping me build the beam delivery system, for the moral support they gave me in times of difficulties and for their role in helping me maintain the laser facilities.

TABLE OF CONTENTS

LIST OF TABLES

Table Page

LIST OF FIGURES

Figure Page

SUMMARY

The last two decades has seen an enormous surge of interest in ceramic materials, and as a result there have been significant advances in their development and usage. Many applications take advantage of their inherent properties, such as high hardness and strength at elevated temperatures, chemical stability, low friction and high wear resistance. Despite their outstanding properties, as compared to metals, ceramics have gained only partial acceptance in industrial applications, mainly due to the difficulties and high cost of their production and processing. Thus, there has been a constant quest to find other machining processes, to process these advanced materials. As one of the various alternative processes, laser beam machining is being adapted for the processing of ceramics. Lasers present a number of advantages over other methods. It is a non-contact, toolless process, thus eliminating tool wear, machine-tool deflections, vibrations and cutting forces.

Although an attractive alternative to conventional techniques, laser processing of ceramics has not been very successful to date. Thermal cracking of the specimen, loss of strength due to micro and macrocracking on the specimen surface, formation of recast layer on the machined surface etc. are some of the problems associated with laser machining which need to be investigated in depth.

In the present investigation, a 1500 W CO_2 laser was used to study the material processing using a laser. Both theoretical and experimental

studies were conducted to understand the phenomena associated with laser machining.

The first task was the setting up of the equipment and its auxiliaries. The CO_2 laser machining center was designed to give the researcher ease of operation, flexibility to conduct a variety of experiments without modifying the setup and a sturdy arrangement to give accurate results with good repeatability.

For the preliminary tests, a beam delivery system was designed and fabricated indigenously in the lab. This beam delivery system was used to initiate laser assisted machining (LAM) tests on steel and aluminum specimen. LAM tests were carried out with special emphasis on selection of proper absorptive coating to increase the absorptivity of metals to CO_2 laser beam. To protect the operating personnel from stray, reflecting beam from the workpiece surface, a vinyl protection screen was provided around the test area. An exhaust system was installed to expel any gases released during the machining tests. The toolholder on the lathe was modified to hold a piezoelectric dynamometer. This allowed on-line measurement of cutting forces during the laser assisted machining tests.

The original beam delivery system was later replaced with a state-of-the-art articulated arm to provide seven degrees of freedom of movement in the delivery of the beam to the workpiece.

Drilling tests were carried out on ceramics, cemented carbides, and metals to investigate the effect of CO_2 laser beam in material processing.

Grooving tests were performed using a computer numerically controlled (CNC) x-y table. The nature of the recast layer and the mechanism of material removal by laser ablation were studied for silicon nitride work material.

To develop the laser machining model, certain thermophysical properties need to be determined. One of these properties is the material removal temperature at the laser wavelength. A simple technique was devised to predict the material removal temperature of hot pressed silicon nitride. This technique can be used to predict the material removal temperature for any material. Results obtained by this method were found to be in good agreement with literature.

Another important parameter to be determined is the beam profile and the focused beam spot size. This was determined with a simple, inexpensive setup. The results obtained from this technique were found to be adequate for use in the modeling calculations.

A heat transfer model was developed for the laser drilling process considering the effect of variable intensity with increase in the hole depth. The experimental results were found to be in good agreement with the theoretical results obtained from the model.

CHAPTER 1

INTRODUCTION

Since the invention of the laser in 1960, it has found diverse applications in engineering and industry. The fact that a laser provides concentrated energy in a small area has led to one of the most important applications of the lasers today, namely, materials processing. Some of the applications in this area are welding, drilling, cutting, scribing, and heat treatment. Materials that have been processed successfully include metals and their alloys, metal matrix composites, polymers, ceramics and other materials such as wood, paper and Kevlar (Duley, 1983).

Ceramics are refractory materials which exhibit high hardness and brittleness. They withstand high temperatures, are corrosion resistant and have a high strength-to-weight ratio. Unfortunately, their hardness and brittleness make them difficult to machine by conventional processes, which has severely limited their use in industry. The development of efficient and cost-effective manufacturing techniques for structural ceramics would lead to more widespread use of these products with substantial technological advantages in many areas (Grigoryants, 1994).

Ceramics are used today in high temperature applications such as dies, furnaces and regenerators (Grigoryants, 1991). However the use of these ceramics is still quite limited due to the prohibitive cost of machining them in their fired state (Affolter et al., 1987). Hence they are machined in

their green (or unfired) state and used in applications where close tolerances are not required. Ceramics which are hot pressed or sintered from fine powder cannot be easily machined. Diamond abrasive is needed to grind such ceramics (Chryssolouris,1991). Even with diamond tools the machining rates are very low and the ceramic workpiece tends to chip due to brittle fracture during material removal. Large tool forces may be encountered thereby necessitating the use of extremely rigid, high precision machine tools to prevent tool chatter which causes poor tolerances, rough surfaces and rapid fracture of tools (Chryssolouris, 1991).

Lasers may be the logical solution for machining of ceramics because it is a non-contact process and is independent of the hardness of the workpiece. No rigid machine tools are required and the same laser workstation can be used for machining and processing other materials as well. No additional requirements, such as the workpiece being electrically conductive or need for any evacuated chamber is needed. However, the optical and thermal properties of the work material for a given wavelength of the laser are important. The optical properties are important as the material removal is by an optical beam and the thermal properties are important as it is a thermal process. Thus lasers can offer many benefits for machining of ceramics.

Even though laser machining of ceramics is an attractive proposition, both technically and commercially, it has not been very successful to date. Some of the problems associated with the laser machining of ceramics can be summarized as follows (Duley, 1983):

- Laser beam induces thermal stress on the workpiece and shatters it especially if the workpiece is thick.
- The strength of the material can decrease after laser machining due to formation of micro and macro cracks on its surface.
- Redeposition of material takes place along the walls of the groove or cut region.
- Quality of cut is very poor due to slag and burr formation.
- There is some heat affected zone (HAZ) around the cut /groove.

If the above listed problems have to be eliminated, it is necessary to understand in detail the process of laser machining of ceramics. Lasers have been used successfully in metal alloy applications. However the quantitative understanding of the physical mechanisms governing the process is lacking. Optimal cutting parameters have been determined by trial and error methods with qualitative and empirical guidelines for optimizing the process (Chen et al., 1996). The use of lasers for cutting newly developed materials requires extensive efforts to obtain the desired results. Many times these efforts prove futile, but nevertheless efforts need to be continued to understand the intricacies of the process.

A number of different phenomena occur during the laser machining process (Chryssolouris, 1991). These include absorption of the laser radiation by the material, conduction heat losses, effect of assist gases during processing etc. However, there is very limited literature in the area of laser machining of ceramics which would explain the contribution of

these phenomena quantitatively. Though experiments have been successfully performed on metals, the same results may not be applicable to ceramics because of different material properties. Thus it is important to quantify these effects for ceramic materials in order to machine them.

Laser machining is a very complex process. The laser processing operation is an outcome of many parameters, properties, and phenomena. These parameters may vary randomly and hence may not be amenable to analytical treatment. For example, fluctuation of the laser power due to lasing instabilities, formation of plasma on the workpiece surface etc are a few of the several random process variations taking place during laser machining. · The deterministic components of the laser machining process are phenomena such as heat conduction, sublimation, beam spot size, etc. These deterministic phenomena can be successfully modelled thus reducing the number of trials required to optimally process a new material. However, the success of modelling would depend on several complex parameters, such as % reflectance, latent heat of melting, thermal conductivity, diffusivity, spot size etc., which are difficult to measure and are not readily available.

The three commonly used lasers for materials processing applications are CO_2 lasers, Nd-YAG lasers, and excimer lasers. The first two types remove material by thermal processes such as melting and evaporation whereas the excimer lasers remove material by breaking the molecular bonds with high energy ultra-violet photons (Duley, 1976).

The effect of laser and material parameters on the outcome of the laser machining process will be discussed qualitatively in the following sections (Chryssolouris, 1991).

1.1 Laser Parameters

1.1.1 Lens Focal Length and Position

The principal advantage of the laser is that the laser energy is collimated and has a high power density (~ 1500 W/cm^2) . This power density can be substantially increased through optical focusing using a plano-convex lens to yield fluxes of the order of 10^6 W/cm^2. This results in melting and evaporation in a few microseconds for most materials. Most laser machining units have the ability to change the focal length and position of the focusing lens with respect to the surface of the workpiece. This control over the spot size has several advantages. For instance, laser butt welding requires larger spot size than laser cutting or laser drilling. Drilling of holes of different diameters can be accomplished by varying the focal length and/or varying the focal position of the lens. The depth of focus of the given lens increases with the focal length of the lens. Thus, in order to drill very deep holes of a specific taper tolerance, it may be necessary to increase the focal length of the lens. A substantial improvement in the material removal rate, hole taper and cut quality is often possible by varying the focal position and focal length of the lens.

1.1.2 Beam Profile

The intensity distribution of the laser beam is referred to as the laser beam profile. Lasers for manufacturing applications usually exhibit a Gaussian or a doughnut mode (Hecht, 1992). The spatial intensity distribution of a Gaussian laser beam, I(r), can be represented by a Gaussian curve of the form, $I(r) = Io \exp (-2r^2/w_0^2)$ where w_0 is the radius of the laser beam at the beam waist. Doughnut mode refers to lasers which have a beam profile of the form $I(r) = I_0 r^2 \exp (-2r^2/w_0^2)$. A burn pattern on plexiglass, using a doughnut mode laser beam, yields a doughnut shaped hole. Doughnut mode beams are usually generated by fast axial flow CO_2 lasers. Gaussian beams are generated by slow flow, CO_2 lasers and Nd-YAG lasers. Laser beams used for manufacturing applications do not conform precisely to either of these descriptions. These terms are used to qualitatively indicate the type of the laser beam profile. Laser beam quality can be quantified by a beam quality parameter, M^2. The value of M^2 for a Gaussian laser beam is 1 and increases as the beam profile differs from the Gaussian beam resulting in a larger spot size at the focal plane. Any increase in the spot size results in lower intensity, lower cutting speeds, greater kerf widths etc. The intensity distribution at the workpiece is critical and is sometimes possible to accomplish a given task only with a high quality beam rather than a high power, low quality beam.

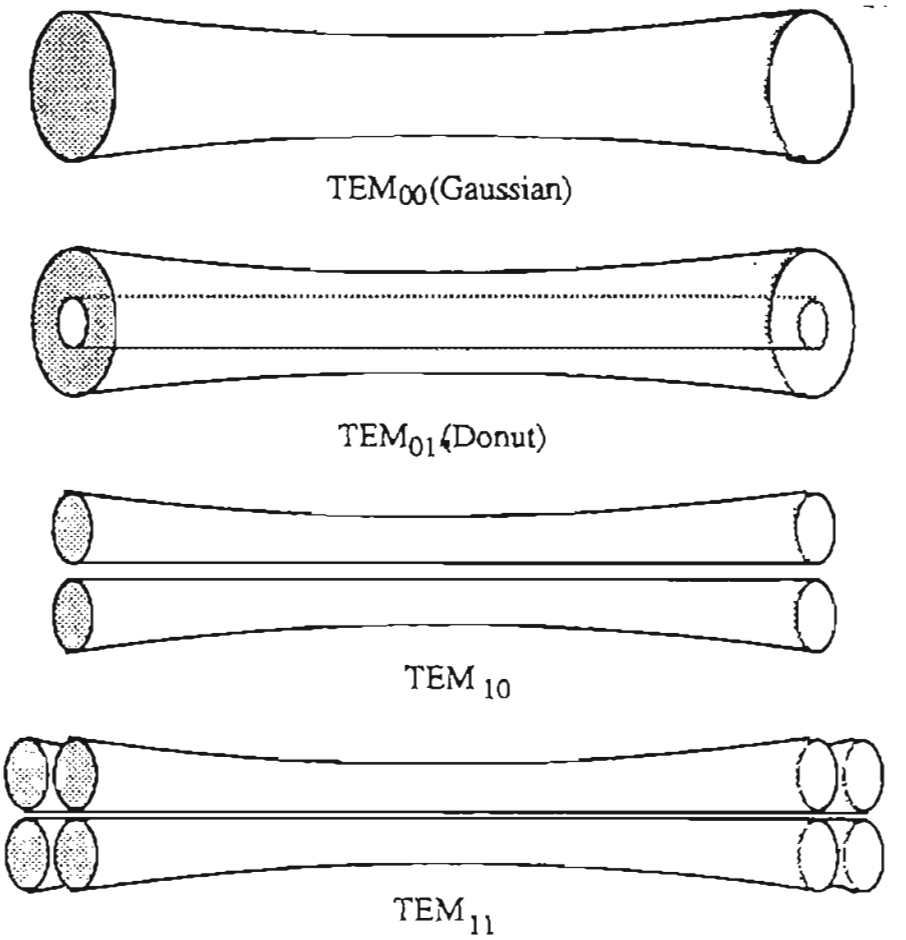

Figure1.1.2.1 TEM Modes (after Chryssolouris,1991)

1.1.3 Laser Power and Pulsing

The laser power determines the rate of heat input to the workpiece. Most high power lasers have a built-in power meter to measure the power output of the laser. The losses through transmissive and reflective optics are usually small and this reading approximately indicates the laser power available at the workpiece surface. Most lasers can be pulsed; this means that the energy emerging from the laser varies temporally according to some specific wave form. This results in an increase in the peak power supplied to the workpiece with no substantial change in the average power. Further, the pulsing frequency and the duty cycle (ratio of laser on time to pulse period) can also be varied. The pulse shapes are usually triangular or square waveforms.

The power output of the laser beam determines the depth of cut during laser cutting and penetration depth during laser welding (Hecht, 1992). The pulsing of the laser beam has a strong impact on cut quality. Some materials like alumina can be cut with a pulsed laser beam and not a continuous wave (CW) laser beam. The pulsing of the laser beam has several advantages. A pulsed beam provides an increased local heating rate which results in less heat losses and more active cutting. The off duration of the laser beam helps to cool the surface and heat the bulk material which relieves thermal stresses built up in the material. If some molten material is present, this may be blown away with gas assist during the off duration of the laser. If this were not removed it may be necessary to evaporate this molten material resulting in higher specific energy consumption and lower cutting speeds.

1.1.4 Laser Scanning Speed.

One of the primary considerations for any machining process is time. High cutting speed results in greater throughput and processing capability. The cutting of the workpiece with a laser can be accomplished by moving either the laser beam or the workpiece. Moving the laser beam is often more convenient for large workpieces and for automating the process. As the power is increased an equal increase in scanning speed assures a constant rate of energy deposition per unit area of the surface. However, at high scanning speeds, the heat absorbed at the surface of the workpiece has less time to be conducted away into the medium. This results in lower heat losses, higher material removal rates and smaller heat affected zones. High traverse speeds also result in steeper temperature gradients thus increasing the susceptibility to thermal shock. At low scanning speeds, there may be some refilling of the groove/cut, at least for ablative type materials such as silicon carbide, carbon etc.

1.1.5 Nozzle and Assist gas

Lasers used for machining generally have different nozzles available through which pressurized gases are directed at the interaction zone (Chryssolouris, 1991). The shape of the nozzle is important and can be varied. The flow rate, the pressure, and the composition of the assist gases can also be varied. The distance between the nozzle and the workpiece surface can be adjusted for optimal efficiency. The gases usually flow coaxial to the laser beam. The primary purpose of a nozzle is to protect the focusing lens from backsplatter, while cutting or welding metals. The

pressurized gases emerging from the nozzle blow the debris away and prevent it from depositing on the focusing lens. The removal of the debris from the path of the laser beam by using a coaxial nozzle also assists in increasing the direct irradiation of the beam to the workpiece thus reducing the absorption and scattering by the debris. An axi-symmetric nozzle is also used to clip an elliptical laser beam (due to poor beam quality) to make it circular.

One of the functions of an assist gas is to blow away the molten material out of the cutting zone. Also, during laser welding a plasma is formed which attaches to the top of the workpiece and prevents any laser energy from reaching the surface. This cools down the workpiece until the plasma detaches and the process starts all over again. Assist gases like argon and helium can reduce (or even suppress) the formation of such an attenuating plasma, due to their high ionization potential. They also prevent oxidation at high temperatures . However, in case of cutting steels, oxygen enhances the removal rates through exothermal reaction, without substantial reduction in the quality of cut. However, the use of oxygen is kept minimal, as the combustion reaction is difficult to control and may lead to poor quality.

1.2 Material Parameters

The material to be processed by the laser also plays an important role in the outcome of the process (Chryssolouris, 1991). The different material properties and their affect on the outcome of the process is discussed briefly in the following sections.

1.2.1 Material Absorptance

The primary requirement for any laser induced material removal to occur is that the laser beam must be absorbed by the material. This absorption may be surface absorption for optically thick materials or volumetric absorption for optically thin materials. Volumetric absorption may lead to material removal through sub-surface explosions as compared to the melting/ablative type material removal associated with surface absorption. Surface absorption is more common and occurs within a few micrometers of the surface. Surface absorption is characterized by the absorptance (e) of the material at the laser wavelength. As the absorptance increases, more of the laser energy is absorbed by the medium rather than being reflected away. Once material removal is initiated, the laser beam is trapped inside the resulting cavity (which acts like a black body) resulting in a higher absorption.

The absorptance of a material varies significantly with the wavelength, angle of incidence, beam polarization, temperature, surface roughness and contamination. The dependence of absorptance on wavelength often determines the type of laser to be used for a particular material. The variation with angle of incidence leads to uniform holes/cuts, since the absorptance tends to decrease as the angle of incidence increases. The absorptance of the material may be very different depending upon whether the laser beam is polarized or not. A polarized beam results in the depth of cut being strongly dependent on the direction of traverse. Consequently, most lasers are fitted with a circular polarization unit to avoid this problem. The value of absorptance can change substantially with

temperature, making it difficult to model the process. The surface roughness of the material (during the process) may be substantially different from the virgin material due to melt formation, oxidation, separation of alloying elements etc. The surface of the material may get modified by contamination thus changing the absorptance of the material. Contamination may result from the remnants of cutting fluids from other machining operations, dust, surface oxidation etc.

1.2.2 Material Removal Temperature

The material removal temperature (T_{rem}) is defined to be the temperature at which active material removal takes place (Duley, 1983). In a conventional sense this may be viewed as the boiling/ sublimation/ decomposition point of the material, i.e., the temperature at which the sum of the partial pressures of the vapors emanating from the heated material equals the ambient pressure. The material removal temperature is identical to the boiling point for some materials. For others, it may be substantially different. Most materials melt before boiling and a substantial portion of the melt is blown away by the assist gas. Some other materials decompose upon heating into liquid and vapor phases. The violent boiling of the vapors may be sufficient to remove the liquid phase. Further, any change in the ambient pressure results in a change of this temperature. For instance, the production of the vapors may be so rapid that there is a pressure buildup at the surface which increases the material removal temperature. This quantity may also be affected by the assist gas used during the process which affects the kinetics, thermodynamics, and the by-products of the process.

1.2.3 Energy Required for Material Removal

The energy required for material removal is defined to be the additional energy required to remove material after it reaches the material removal temperature. This may be viewed in a conventional sense as identical to the latent heat required for the change of state from solid to vapor. This term can, however, also be used to account for other phenomena. For some materials it is the heat of decomposition; for others, it is the latent heat for melting. In the case of oxygen assisted cutting of wood, it may even be close to zero, since the oxidation reaction of wood is exothermic. Some materials decompose over a wide range of temperatures with very different products, possibly consuming different amounts of energy. The precise reactions which occur depend on the specific kinetics and thermodynamics and are quite difficult to predict or measure.

1.2.4 Specific Heat

The minimum requirement for any material to be removed thermally is that the material be heated up to the removal temperature, T_{rem}, and then consumes an amount of energy equal to the latent energy in order to be removed. The specific heat (c) determines how much energy is required per unit mass to raise the temperature of the material from the ambient temperature to T_{rem}. As the specific heat increases a larger amount of energy is utilized to heat the material to a given temperature. Ceramics typically have about three times the specific heat of metals (Duley, 1983).

1.2.5 Thermal Conductivity

The pulse durations considered in this study are long (> 20 x 10^{-5} s) compared to the energy relaxation time (10^{-6} to 10^{-13} s) of molecular vibrations. Hence Fourier's law of heat conduction is applicable for the study of laser machining (Duley, 1983). A large value of thermal conductivity (λ) results in heating the whole workpiece rather than rapid heating of a small zone; this results in a smaller depth of cut and lower cutting speeds, and is undesirable. The thermal conductivity of ceramics usually decreases with temperature. For instance, the thermal conductivity of silicon carbide reduces by a factor of ten from room temperature to 3000 K (Roy et al., 1991). This variation needs to be included to accurately model the laser machining process. Some composite materials exhibit substantially different conductivities in different directions (anisotropic) causing additional problems in modeling laser processing.

1.2.6 Thermal Diffusivity

The thermal diffusivity (κ) is a measure of the speed of heat propagation through the medium and is related to the thermal conductivity (λ), density (ρ) and specific heat (c) of the material. The effects of thermal diffusivity on the laser machining process can be deduced from the arguments given above for thermal conductivity and specific heat, since the density of the material is usually fairly constant.

In the present study, some of the problems, phenomena and processes associated with the laser interaction with different materials has

been investigated. A 1500 W CO_2 laser is used for this purpose. Different material processing operations such as drilling, grooving and laser assisted machining have been dealt with both theoretically and experimentally. Chapter 2 covers the literature review of the various laser machining processes. Chapter 3 outlines the problem statement. The experimental setup used for laser processing is presented in Chapter 4. Chapters 5 and 6 discuss the techniques used to determine the beam profile, focused beam spot size, and the material removal temperature. Laser drilling is presented in Chapter 7, and theoretical modelling of the laser drilling process in Chapter 8. Laser assisted machining has been described in Chapter 9. The recast layer formation has been described in Chapter 10. Grooving tests and the material removal mechanism in silicon nitride have been presented in Chapter 11. The conclusions from this study have been outlined in Chapter 12. Future work has been presented in Chapter 13. The code developed for the thermal analysis is presented in the Appendix.

CHAPTER 2

LITERATURE REVIEW

2.1 Introduction

During the past thirty years a number of papers have appeared dealing with experimental and theoretical aspects of laser drilling, scribing, and cutting. Most of these papers have dealt with CO_2 or Nd-YAG laser processing of metals and their alloys. Comprehensive reviews of different aspects of laser processing have been given in two books by Duley the first one covering the literature up to 1974 (Duley, 1974), the second one upto 1982 (Duley, 1982) and by Von Allmen (1987), covering the literature upto 1986. A review of the large body of Soviet publications has been presented by Uglov and Kokora (1977). Current reviews of the literature available on laser processing of materials have been given by Modest (1990), Chryssolouris (1991), Steen (1991), and Grigoryants (1994).

This discussion of the literature on laser machining will proceed as follows. In the first section experimental papers dealing with laser drilling, scribing and cutting of materials are discussed. This is followed by a review of the theoretical work on modeling of the laser machining process. Accurate measurements of material, process and laser parameters during laser processing are critical to the understanding and modeling of the process. This is often the determining factor in the success or failure of a model. Thus, in the last two sections, some of the literature available on in-situ measurements of these parameters is discussed.

2.2 Experimental Studies

Laser drilling was one of the earliest applications of high power lasers. Ready (1963) investigated the effects of vaporizing material with a laser to produce a hole. He determined that the effect of a very large pulse (10^{10} W/cm^2) on carbon black leads to subsurface superheating and eventually a thermal explosion. Longfellow (1971) has studied the high speed drilling in alumina substrates with a CO_2 laser. He used a massive hollow copper box with a vacuum port in the base as the fixture for holding the alumina substrate. The coaxial assist gas forces the fused alumina into the vacuum system during the laser drilling operation thus giving close tolerances holes.

Gonsalves and Duley (1971) performed experiments on CO_2 laser drilling of stainless steel sheets in air and in vacuum. They found that the time required for drilling in vacuum was three times larger than that in air and hypothesized that this was due to a substantial change in absorptance during heating in air. Duley and Gonsalves (1972) studied CO_2 laser drilling of fused quartz and found that the holes in quartz had a larger taper than the holes in stainless steel. They attributed this to the difference in the properties between metals and refractory oxides. They also presented an analytical method to extrapolate their results to other refractory oxides.

Chen et al. (1996) studied the effects of laser peak power, pulse duration and wavelength in the drilling of three advanced materials: NiAl, N5 and SiC CMC. It was demonstrated that cracking in NiAl was greatly reduced when high peak power, short laser pulses were used. Recast

layers in all three materials were generally thinner when high peak powers, short pulse durations or long pulse bursts were employed.

Durand et al. (1996) used a short pulsed Nd-YAG laser for machining silicon nitride. The cuts were made crack free and exhibited promising characteristics for precision laser machining of such materials. They analyzed the cut kerf geometry and modeled it as a function of energy density. Their model proved fairly accurate for lower level energy densities, but the amount of material removed was found to increase with an increase in energy density up to a maximum point followed by a decrease with finite increase in energy density.

Bar-Isaac et al. (1974) studied pulsed ruby laser drilling of copper, aluminum, and lead for different focal positions. They measured the hole depth at different times and found moderate agreement with their model, assuming that the heat conduction effects were negligible. Scribing of alumina was considered by Paek and Zaleckas (1975). They compared the performance of the CO_2 and Nd-YAG lasers noting that the YAG laser gave a smoother edge but left unwanted debris on the surface. This was attributed to the absorption coefficient being lower at shorter wavelengths resulting in sub-surface evaporation and explosive removal of particles, rather than surface evaporation. Lukacs et al. (1995) have made preliminary studies in the copper-vapor laser cutting of silicon wafers and PZT.

Von Allmen (1976) drilled copper samples with Nd-YAG pulsed laser. He studied the phenomenon of liquid explosion and identified four regimes: (i) at intensities below 10^5 W/cm^2 the drilling mechanism is

evaporation; (ii) in the range 10^5 - 5 x 10^6 W/cm^2 there is a region of instability, causing oscillatory behavior; (iii) above 5 x 10^6 W/cm^2 the power is high enough for liquid expulsion and the drilling is stable; and (iv) above 10^9 W/cm^2 the laser beam is partially blocked due to absorption of the laser beam by the super saturated vapor and plasma above the material.

Wallace et al. (1983,1986) demonstrated the feasibility of several shaping operations based on overlapping grooves, including turning, threading and milling hot pressed silicon nitride. They also studied the effects of laser beam polarization on the shape of the groove and its dependence on the scanning direction of the laser beam. Affolter and Schmid (1987) studied the laser machining of various ceramics such as aluminum oxide, silicon carbide, silicon nitride etc. with a Nd-YAG laser. They found best results were obtained with high powers and short pulse times. They also found extensive micro cracking and expected a serious reduction of mechanical strength due to laser machining.

Sheng and Liu (1995) have discussed a laser based technique for finishing axisymmetric parts which allows efficient finishing of polymers and ceramics without tool wear, tool breakage or cutting forces. The process consists of a laser beam impinging tangentially on to the surface of a cylindrical workpiece. Asperities on the workpiece can be removed through vaporization (for plastic and composite materials) or melting (for ceramics and metals). Thus a flexible machine tool can be developed to grind parts of differing geometries and materials by changing process parameters instead of setups or machines, as well as integrate primary machining and secondary finishing in one machine tool. The precision of

the laser finishing can be enhanced by using oblique beam impingement angles. The paper presents the elements of the laser machine tool and preliminary results on the parametric dependencies for laser finishing of polymer workpieces. The operating parameters which affect the surface finish are the rotational speed of the workpiece, feed, beam power and oblique beam angle.

Yamamoto and Yamamoto (1987) studied laser cutting of silicon nitride with a CO_2 laser. They found that flexural strength of the laser cut material was only 35 % of the flexural strength of the uncut material. They attributed this to the microcracking during the laser cutting process. Saifi and Borutta (1975) have discussed the laser scribing parameters for aluminum oxide which optimize the flexural strength for annealed and unannealed substrates while allowing easy separation of the ceramic along the scribed line. Laser parameters such as pulse length, peak pulse power and spacing between successively drilled blind holes have been investigated. The force is measured using a piezoelectric transducer. The flexural strength is measured using a 4-point loading fixture. The authors found that increasing the pulse length > 0.8 ms did not decrease the separation force markedly, however, thermally induced cracking was observed near the scribed region. In certain applications, annealing of the ceramic substrate would be necessary after scribing to relieve the thermal stresses. This causes grain growth and resintering of material in the blind holes causing an increase in the separation force. Study of high magnification SEM's of the scribed region showed columnar grains. For larger pulse lengths the columnar grains are deeper and scribing induced cracks are visible on surface and in cross section. The authors have

concluded that short pulse lengths with high peak power gives better results in terms of lower separation force and better flexural strength retention during the scribing process.

Wallace et al. (1986) studied the characteristics of the groove formed in hot-pressed Si_3N_4 with a CO_2 laser beam at normal incidence angle when the workpiece is moved with respect to the laser beam. They observed that the groove curves out of the plane defined by the velocity direction of the workpiece. The curved cross sections change from one side of the plane to the other if the velocity direction is reversed. This effect is more prominent at the lowest velocities and highest incident powers. The cross section was shown to vary systematically with the angle between the velocity direction and the direction of the electric vector of the incident beam, which was found to be partially polarized. They have proposed a mechanism for the curved cross section effect based on the existence of a significant difference in reflectance between the transverse electric (TE) and transverse magnetic (TM) reflections from the groove walls in Si_3N_4 for large angles of incidence. Calculations of the values of reflectance for the TM and TE reflections as a function of the angle of incidence show the existence of a large difference for the CO_2 beam wavelength of 10.6 μm.

Eberl et al. (1992) machined three-dimensional pockets into materials, such as silicon nitride using multiple pass scribing and elaborate feedback control loops. Trubelja et al. (1992) studied laser scribing and cutting of carbon fibers in silicon carbide matrix composite with special emphasis on strength reduction and material removal mechanism. They found that extensive redeposit on the groove surface was β-SiC and carbon.

They also found that the laser-cut samples retained 80 % of the strength of diamond cut samples. Full strength was recovered after removing 180 μm from the surface of the laser-cut material.

Trubelja et al (1994) have studied the CO_2 laser scribing and cutting on a carbon fiber-silicon carbide -matrix (C/SiC) composite containing 45% vol. of carbon fibers. Scribing and cutting were performed in continuous wave (CW) mode using laser powers between 750 and 1500 watts, specimen translation speeds between 0.5 to 4 cm/sec and laser spot size of 300 mm in diameter. Analyzing the groove depth and width as a function of laser power and specimen translation velocity, the authors have observed that the fibers and matrix end abruptly and there is an extensive refilling of the groove. This is attributed to the ablative decomposition of this material, with the evaporated material recondensing downstream of the laser beam. SEM examination of the groove cross section also showed extensive redeposition of carbon and silicon carbide. X-ray and Raman spectroscopy analysis of the laser cut surfaces showed the presence of β-SiC and graphitic carbon formed by the condensation from the vapor phase. It was also observed that there was a decrease in the bend strength of the laser cut surface by 20% compared to the corresponding strength of diamond cut material. This was attributed to the existence of heat affected zone (HAZ). But removal of this zone by grinding, facilitates in recovering the strength of the material.

Zhang et al. (1996) have studied the effects of laser machining on ceramics in terms of surface morphology, flexural strength and its variances under various machining conditions. Weibull modulus 'm' is

introduced to measure the degree of variation in strength. The authors conducted their test on SiAlON 501, which is a silicon nitride composite material. The beam parameters varied in the experiment were the pulse frequency, pulse energy (E), and the feed rate. Machining was performed under a coaxial jet of compressed air. The experimental results indicate that micro-cracks and thermally affected layer increase with increasing pulse energy E and feed rate of the ceramic workpiece but decrease very little when the pulse frequency was varied from 18 to 30 Hz. Formation of cracks result from the high power intensity of the laser beam, with very steep temperature gradients being created in the material, that causes high localized thermal stress wave. Further stress arises from recoil pressure due to evaporating surface atoms. Finally, resolidification further imposes stress, which at the end, exceeds the fracturing limit of extremely brittle ceramics. Thermal stress (σ) is roughly estimated by the equation:

$$\sigma = E\alpha\Delta T$$

where E=Young's modulus,

α=Coefficient of thermal expansion,

ΔT=Temperature rise.

In laser machining of ceramics, the maximum theoretically estimated value of σ is about 5-25 GNm^{-2} which far exceeds the bend strength of ceramics. Hence the microcracks are not avoidable. The authors have also found that the mean flexural strength is only about 40% of the original value of the material which they reason is due to the thick thermally affected layer and the cracks in it caused by thermal shock.

Lunau et al.(1969) studied the effects of assist gas jet while cutting with a CO_2 laser. This was motivated by the need to increase cutting efficiency since metals have a high reflectance at 10.6 μm. They found that the use of assist gas increases penetration by up to 20%. It also made the cut width less tapered. They attributed these effects to the transfer of heat from the vaporized material to the uncut material at the bottom. Duley and Gonsalves (1974) studied oxygen-assisted cutting of stainless steel and found that oxygen assist increased the minimum cutting speed by factors ranging from 1.5 to 2.5 for different thicknesses. However, there is an optimum level of gas flow beyond which the minimum cutting speed decreases. They also found that this optimal flow rate was independent of the laser power. They presented some sample calculations to show that the cooling effect of the assist gas is insignificant and that the exothermic oxidation of iron is insufficient to provide such a large increase in the minimum cutting speed. They speculated that the increase may be due to the ability to remove material at temperatures below the melting point which is somehow caused by the addition of oxygen.

In laser cutting, an erosion front (liquid gas region) forms at the momentary end of the cut. The material removal rate is dictated by laser heating, exothermic reactions and shear force between the gas flow and the molten layer. Standard coaxial gas -assisted laser cutting for thicker steels does not provide satisfactory performance since the oxide dross clings to the bottom edge of the cut and forms a hard burr. This phenomenon is more prominently observed in the laser machining of stainless steel due to the low fluidity of the melt and the high melting point of chromium oxide, which restrains oxygen diffusion into the molten cutting front. One solution

to this problem is to use high pressure gas in the coaxial nozzle. However this leads to fracture of the focussing lens and the formation of a Mach shock disc (MSD), which causes large variations in the effective gas pressure acting on the workpiece. The principle of the off-axial gas jet is to provide straight non-turbulent flow to the cutting erosion front, causing further oxidation reactions and transferring momentum to the molten slag and dross. Ilavarasan and Molian (1995) have studied the laser cutting of thick sectioned steels using gas flow impingement on the erosion front. The investigators have developed an off-axial gas jet that extends the laser's effectiveness by improving the rate at which the parts can be machined, producing high quality surfaces, enhancing the cutting thickness, and adding the range of materials that can be machined. Molian (1993) has developed a dual-beam technique involving two CO_2 gas lasers with a power capacity of 1.5 kW each to cut steel and superalloy. It was found that dual beams were capable of enhancing the cutting thickness and speed without deteriorating the quality of cut.

Thomassen and Olsen (1983) investigated the effects of nozzle pressure and cutting speed on the quality of cut in steels. They found that different effects are observed in mild steel and stainless steel, although they are similar materials. Powell et al. (1985) showed that the striations which occur during gas-assisted laser cutting are due to a periodic formation of melt phase. They showed that the roughness due to these striations can be minimized by pulsing the laser at twice the frequency of striations. Schuocker (1986) presented a model for calculating dynamic effects (such as striations) during reactive-gas-assisted laser cutting. He also presented

a method to calculate the energy gain due to reactions occuring at the interaction zone using a simple mass and energy balance.

Fieret et al.(1987) present an overview of supersonic gas assist effects in laser cutting. They found that the maximum cutting speed is positively correlated to cutting pressures. Further, the occurrence of a Mach shock disc with the possible formation of a vortex ring can be associated with poor cutting performance.

Laser machining of glass and glass-ceramic matrix composite has been investigated by several researchers recently. Finucane and Black (1996) have examined the various laser cutting parameters required to generate a cut surface in glass which will require minimal post treatment to be carried out. The results obtained by them through their numerous experiments on various stained glass was used to generate a database giving the various parameter settings. Tuersley et al. (1996) carried out tests to emphasize the influence of SiC fibre glass-ceramic matrix phase's ability to couple with the 1.06 μm emission of the Nd-YAG laser. Allcock et al. (1995) have investigated the CO_2 laser marking of soda-lime and borosilicate glasses as a function of laser fluence and pulse duration. Various fracture mechanisms have been analyzed by them. Residual surface stress following rapid laser heating has been identified as the most likely cause of microcracking. Gas phase products evolved during the interaction of the laser with glass has also been evaluated using spectroscopy of the luminous plume and fast photography techniques.

Besides ceramics and metals, lasers have been extensively used in the cutting of composites like wood and wood based products . However not

much literature is available on the mechanism of cutting wood using lasers. Lijun Li and Mazumder (1991) have studied the physical mechanism and theory of cutting wood with a laser with respect to the laser beam absorption and penetration, gas-jet assistance, and the characteristics of wood materials. Formulas for the basic relationships have also been derived. The process of cutting wood is accompanied by an exothermic reaction of distillation of wood. In the case of thin layer cutting, the laser beam directly hits and vaporizes the wood. However, thick-lumber cutting is mainly a hot gas jet ignited and sustained distillation process.

When wood is heated, its distillation is initiated at around 573 deg K. This is an exothermic reaction. Combustible and incombustible gases are formed and a loose residue, charcoal is left behind. Charcoal is vaporized by further heating. Combustion takes place when oxygen reacts with the products of distillation at a high temperature. In the case of gas-jet-assisted laser cutting of wood, the laser beam raises the temperature of wood to the distillation temperature and the gas jet purges the distilled and vaporized products. The gas jet gets hot because of its interaction with the distilled and vaporized gases. This hot gas jet ignites and sustains the distillation of wood. Thus the energy required to heat the wood to reach its distillation temperature is self-generated. Nitrogen or compressed air is used as assist gas in the laser cutting of wood. The authors have developed the model for both thin layer cutting which is a direct vaporization process and the thick lumber cutting which is basically a distillation process. Based on their study, the authors conclude that direct vaporization of wood by laser beam is more efficient than cutting by hot gas jet. Thick lumber cutting can be made possible using the direct vaporization process by using

large focal length lens. Besides, they have also concluded that using high velocity of the gas jet improves the performance of the cutting process. The increased velocity of the gas jet increases both the shear stress of the jet to the cutting front and the convective heat transfer between the gas jet and the kerf material, thus accelerating the cutting process.

Peters and Banas (1976) have studied the feasibility of using multikilowatt CO_2 lasers to cut wood since higher power offers higher cutting speed thereby reducing the surface charring normally associated with lower cutting speeds. The authors have tried a variety of wood, varying in density, moisture content and thickness. They have found that cutting speed increased with the decrease in thickness of the sample and with an increase in the laser power. Cutting speed also increased with a decrease in the material density. They have also developed relationships between cutting speed and power and speed and density. Characteristics of the cut surface were studied qualitatively and were found to vary from a slight browning at high cutting speeds (around 125 fpm) to shallow charring at low cutting speeds (15 fpm).

McMillin and Harry (1971) have conducted a factorial experiment with two replications, to understand the effect of laser cutting on southern pinewood, with varying moisture content, specific gravity, thickness and direction of cutting. The study has indicated that the feed rate does not depend on the orientation of the grain in wood. Thus, when cutting complicated line profiles or holes, the feed rate need not be varied with changes in the cutting direction. The feed rate decreased with increasing workpiece thickness in both dry and wet samples. For a given thickness,

slower speeds were required for wet than for dry wood. The magnitude of the difference increased as the thickness of the workpiece decreased. The authors have also compared the quality of the laser cut surface with the traditional bandsawing and circular saw techniques and found that kerf width was narrower with laser cutting than with the conventional saws. The kerf width was found to be unrelated to cutting direction, moisture content, and specific gravity, but increased with increasing workpiece thickness. SEM micrographs indicate smoother surface for laser cut wood than sawn wood.

Barnekov et al. (1986) have studied the factors influencing laser cutting of wood. According to the authors the quality of cut depends on:

1) Characteristics of the laser beam
2) Equipment and processing variables and
3) Properties of the wood.

Cutting wood with a laser generating Gaussian or near Gaussian energy distribution (TEM_{00}) generates a small focal point with high energy density thereby giving a better quality of the cut surface. The location of the focal point with respect to the wood sample also affects the cutting efficiency. If the focal point is above the work surface, the energy density is diminished, kerf width is increased, and the upper surface of the work is charred. If the focal point is on the workpiece surface, the energy decreases as the workpiece thickness increases. If the focal point is positioned at or slightly above the middle of the workpiece, the energy density is more uniform, the cut surface has less char and is smoother, and deeper cuts are possible. For solid wood, an assist gas pressure of approximately 60 psi is required. Compressed air or non reactive gas may be used. However the use of non-

reactive gases yields little improvement. When cutting particle and fiberboards, or other wood composites, an inert gas is essential. For laser beam at 10.6 μm the absorption coefficient of water is less than that of wood. Thus, absorption coefficient of green wood sample is less than that for dry wood sample. Hence more power is required for green wood than for dry wood.

2.3 Theoretical Work on Laser Drilling and Cutting

Theoretical efforts on modeling laser machining have centered on the solution to the classical heat conduction equation for a stationary or moving semi-infinite solid. Different cases have been studied with and without phase change for a variety of irradiation conditions. Since the pulse durations considered in this study are long ($\geq 20 \times 10^{-5}$ s) compared to the overall energy relaxation time of the molecular vibrations (10^{-13} s to 10^{-6} s), heat may be considered to be propagated according to Fourier's law.

The simplest situation from a modeling standpoint is that of laser drilling with a conduction model being used to identify a melt or an ablative isotherm. Ready (1965) was one of the earliest to present an analysis specifically for calculating hole depths for pulsed laser drilling of metals. He distinguished between moderate and high power (Q switched) pulses phenomenologically, and presented a simple one-dimensional transient model to predict hole depth. Paek and Gagliano (1972) developed an axisymmetric conduction heating model for laser drilling of alumina.

They used the calculated temperatures to calculate thermal stresses for this brittle ceramic material.

Yue et al. (1996) have developed a model to predict the profile of laser drilled hole based on the concept of threshold intensity and have extended the model to apply to deep penetration laser welding. The common ground for laser drilling and welding as well as their divergences are discussed in this paper: Brugger (1972), Maydan (1971), and Lax (1971) have solved the non-moving slab problem assuming that the intensity of the incident beam decays exponentially with distance into the material, i.e., volumetric absorption.

The modeling problem is more difficult when phase transition takes place. Dabby and Paek (1972) presented a one-dimensional transient conduction model while including the penetration of irradiation into the medium and vaporization. They found that it is possible for material removal to occur by the mechanism of sub-surface explosions.

While still using a one-dimensional model to describe laser drilling, Von Allmen's study (1976), also considered the expulsion of material. He assumed that a part of the liquid vaporizes according to the rate equation given by Batanov et al. (1973) and that if the pressure build-up due to the evaporation is strong enough, the liquid is forced out along the walls by laminar flow. Borsch-Supan et al. (1984) considered internal evaporation by including the fact that a change of state does not occur at a fixed temperature but rather according to a rate equation of the Arrhenius type. They assumed that any evaporated material can freely escape from the solid (making explosive removal of solid impossible).

Risch and Laub (1990) developed a model for one-dimensional ablation which includes translational non-equilibrium gas flow at the surface, thermochemistry and in-depth heat conduction. They found good agreement for carbon phenolic at radiances from 0.3 to 5 kW/cm^2. Wei and Ho (1990) studied quasi-steady drilling of metals and presented a model which identifies interfaces while including the effect of surface tension forces and vapor pressure. They found limited agreement with experimental results for copper by assuming complete absorption of laser energy.

The modeling problem becomes even more complicated (three rather than two-dimensional) if the laser is moved across the target (welding, cutting and scribing). Gonsalves and Duley (1972) used a moving point heat source solution from Carslaw and Jaeger (1959) to make comparisons with experimental data for CO_2 laser cutting of stainless steel. A general heat conduction solution was given by Modest and Abakians (1986), who studied a moving, semi-infinite body irradiated by a Gaussian laser source either uniformly in time or in pulsed mode.

The process of scribing with a moving laser was modeled by Modest and Abakians (1986) for irradiation by a CW laser with Gaussian energy distribution onto an opaque semi-infinite solid. They included the effect of angle of incidence of the laser beam with respect to the walls of the groove. They assumed one-step evaporation of the material (without beam interference), parallel laser beams, negligible reflection effects, and small heat losses. The conduction heat losses were calculated using simple integral method. The assumption of a parallel laser beam was later

relaxed by Biyikli and Modest (1988) who investigated the effects of beam focusing and focal plane position. In a follow up paper by Abakians and Modest (1988), semi-transparent bodies were considered; they showed that materials would have to display substantially different behavior as compared to surface absorption of laser energy.

Roy and Modest (1990) developed a model where one of the weakest assumptions made by Modest et al. (1990, 1991, 1992) was relaxed. Rather than treating conduction losses in a quasi-one-dimensional fashion, the full three-dimensional conduction was solved using the boundary element method. They reported that a more accurate treatment of heat conduction losses has a considerable effect on the depth of the groove, for small scanning speeds. They also found that the groove width is always predicted well by the quasi-one-dimensional model of Modest and Abakians (1988).

Bang and Modest (1991, 1992) included multiple reflection and polarization effects in deep grooves for materials of low absorptance. They conclusively showed that beam trapping (specular or diffuse) substantially reduces the taper of the groove and increases the material removal rate, particularly at low scanning speeds. They obtained good agreement with experimental data for silicon nitride considering the uncertainties in the knowledge of material and laser parameters.

Modest and Ramanathan (1994) have developed a three-dimensional model to predict the temperature distribution inside the solid, and the shape of one or several overlapping grooves formed by partial evaporation of a thick, rectangular body, when the body is irradiated by a moving laser

source. The governing equations are solved using a finite-difference method on a boundary fitted coordinate system. Results are presented for ablative groove development, including the effects of laser entry and exit, single and overlapped groove shapes and temperature distributions in the solid at different traverse speeds, pulsing conditions and power levels. Good qualitative agreement between the theoretical and experimental results were obtained by the authors.

Yilbas (1997) examined the heat transfer mechanism, including conduction, phase change and convection processes taking place during Nd-YAG laser irradiation of steel workpieces. To validate the theoretical predictions, optical methods and streak photography techniques were employed and they found that surface temperatures and evaporating front velocities obtained theoretically are in good agreement with the experimental results. Mazumder and Steen (1980) have also developed a three-dimensional heat transfer model for laser material processing with a moving Gaussian heat source. Sami and Yilbas (1996) have numerically solved the heat transfer mechanism relevant to pulsed laser heating using the kinetic theory approach for different types of laser pulses.

A number of researchers have investigated laser heating of metals with temperature-dependent material properties (absorptivity, thermal conductivity, and volume heat capacity). Dobrovol'skii and Uglov (1974) analyzed the effect of heating a semi-infinite slab with a Gaussian laser beam where the surface absorptivity varied linearly with temperature. They solved for the two-dimensional temperature distribution and compared the result of their theory to a one-dimensional model neglecting

radial effects. Nissim et al. (1980) treated the moving laser beam with elliptical beam profile, assuming conductivity to be temperature dependent. Rykalin et al. (1982) numerically solved the temperature distribution in a laser heated slab with absorptivity, thermal conductivity and volumetric heat capacity all varying with temperature. They showed that the combined effect of non-linearities gives substantially new results in a number of cases. Yilbas et al. (1997) proposed a heat transfer model that provides useful information on the laser induced interaction mechanism. Steady state and time dependent heating models are introduced and temperature profiles inside the materials were predicted.

The surfaces of most metals and some ceramics subjected to laser irradiation attain high temperatures and are oxidized. This in turn leads to very different absorptance values, particularly for metals. For example, pure aluminum has a reflectance of 98% at the CO_2 laser wavelength of 10.6 μm. However, oxidized aluminum, i.e., alumina (Al_2O_3), has a reflectance of only 2% at this wavelength. Thus, the effects of chemical reactions at the surface are important and have been studied by a number of authors. Uglov et al. (1983) calculated the effects of oxidation on metallic targets and concluded that the nonlinearity due to oxidation must be included in modeling. Kirichenko and Luk'yanchuk (1983) analyzed theoretically the kinetics of oxidation reactions for metal specimens in air during laser heating. They found that those points on the surface which are at a higher temperature oxidize faster and consequently absorb more energy resulting in thermal runaway. This results in much stronger temperature gradients in the material, than if the effects of oxidation are neglected. Roy et al. (1991) studied the effects of variable thermal properties on laser

scribing using a three dimensional conduction model. They found that the effect of variable properties can affect groove depths and material removal rates by 20%.

Engin and Kirby (1996) have recently developed a laser machining model for ceramics and glass ceramics from the analytical treatment of a one-dimensional vaporization problem with a distributed heat source. The developed solutions are used to predict the behavior of high intensity Nd-YAG laser pulses on a typical ceramic or glass ceramic material. Predictions include the critical intensity required for vaporization of material, material removal rate, thickness of the affected residual surface layer after a single laser pulse of given shape and intensity.

Borkin et al. (1985) studied the effects of self-focusing of radiation in the case of laser drilling of metals for different polarizations. They showed that beam guiding effects are very different in opaque metals as opposed to transparent insulators. They also found that in the case of metals most of the reflections are relatively tangential to the surface (whispering gallery modes) while in insulators the reflections are relatively normal to the surface (bouncing ball modes). They found that beam trapping effects in some materials can lead to a drop-shaped cavity.

A few theoretical models have been proposed in the recent past on laser cutting of glass and glass-ceramic matrix composite. Yakovlev (1996) has proposed a model for the structure of glass that makes it possible to analyze changes in its properties under various heating regimes. He has shown that the change in the properties of glass as temperature varies is

associated with the temperature dependence of the concentration of oxygen-atom vacancies. He has also proposed an analysis of the sharp change in the properties of glass upon heating using a modified model involving structural phase transitions. Atanasov and Gendjov (1987) have proposed a theoretical model for laser cutting of glass tubing. The thinning down of the wall of the glass tube has been taken into account in the model. The dependence of the duration of cutting upon absorbed laser power has been derived and compared with experimental data. This model gives a good physical comprehension of the laser cutting of glass tubing through melting.

2.4 In situ Measurements during Laser Processing

The measurement of material, process and laser parameters during laser processing is critical to enhance the understanding of the process. This information can be utilized to obtain better results from the process by using control and feedback loop. The measurements are also useful in providing new data on phenomena, which may be used to model the problem more accurately. Unfortunately, most of the literature is limited to presenting laser and process parameters which yield the best quality of cut. This information is often incomplete and is not of much use to others. Some of the measurements made during laser processing will now be reviewed, followed by a detailed review of the literature on measurement of temperature and reflectance during laser processing.

Arnot and Albright (1983) photographed the plasma plume during CO_2 laser spot welding of steel. They found that plasma plumes were

always larger in argon than in helium. They also found that the plasma of argon detached from the surface at high power densities preventing any further heat input to the target surface. Arata et al. (1984) photographed the plasma during CO_2 laser welding of steel using high speed photography and transmission X-ray methods. They found that reducing the ambient pressure to a few torr completely suppressed the plasma plume and yielded substantially higher penetration.

Ramanathan and Modest (1995) have used high speed photographic techniques to study plumes generated during drilling of ceramic and ceramic composites with a CO_2 laser. The principal objective of this study was to identify the mechanism of material removal (spattering, particulate and fiber debris, liquid droplets) and plume phenomena.High speed photographic visualization (1000 frames per second) was undertaken for two monolithic ceramics, sintered α-SiC and hot pressed silicon nitride. and two continuous fiber-ceramic matrix composites (C-SiC) and silicon carbide fibers in a silicon carbide matrix. This study has provided several valuable insights into material removal mechanisms and plume phenomena. It was observed that the plumes for ceramic based materials were not as luminous or dynamic as that observed for steel. The plumes were initially tall and columnar and rapidly diminish to an approximately Gaussian shape, after which the shape remain relatively unchanged. This observation has led the authors to believe that during the initial phase the material removal mechanism is vaporization for all the materials under study. Subsequently, the material removal mechanism is purely ablative for monolithic α-SiC and graphite, while the removal process is aided by periodic ejection of liquid silicon for silicon nitride and by fiber/particle

ejection in the case of continuous-fiber/ceramic-matrix composites viz. C-SiC and SiC-SiC. This macroscopic ejection of material in the composite materials is attributed to stress build-up and fracture in the voids of these materials, eventually resulting in the expulsion of matrix and fiber.

Grum and Zuljan (1996) have analyzed the heat effects in laser cutting of steels. They analyzed the emission of infrared rays from the cutting front with a photodiode, statistically analyzed the temperature signals and optimized the laser cutting process based on a critical cutting speed. The measured infrared radiation was converted into a temperature that was related to the formation of macro- and microstructures and to the change in the microhardness in the surface layer of the cut. On the basis of the experimental results it was proved by the authors that heat effects in the cutting front decisively influenced the quality of cut.

One of the problems in dealing with ceramics (as compared to pure metals) is that ceramics, upon heating, may decompose into a variety of compounds over a wide range of temperatures. Thus, in order to determine the decomposition reaction and the decomposition temperature, elaborate thermodynamic equilibrium calculations or accurate measurements of the reaction coefficients need to be undertaken. Kinetics and mechanisms for thermal decomposition of silicon nitride were calculated by Batha and Whitney (1973). They reported that their calculations agreed with other mass spectroscopic studies. Their calculations showed that silicon nitride decomposes into liquid silicon and nitrogen and provided equations for the rate constant of the reaction. Drowart et al. (1958) studied the thermal decomposition of silicon carbide using mass spectrometry and found that

the predominant vapor species are Si, SiC_2 and Si_2C. Scace and Slack (1960) found that SiC dissociates into carbon and a silicon rich liquid around 3100 K. Baird and Taylor (1958) reported that silicon carbide decomposes at temperatures between 2600-2750 K into carbon and a silicon rich vapor under high pressures. DeBastiani et al. (1990) performed some CO_2 laser scribing experiments and found no evidence of any liquid phase in the groove. They also found that during laser scribing, different dissociation products are obtained for single crystal silicon carbide and sintered silicon carbide, probably due to sintering additives. Singhal (1976) presented a thermodynamic analysis for silicon nitride and silicon carbide at high temperatures in an oxidizing atmosphere. He reported that the partial pressure of Si vapor at 2000 K is substantial and may limit its high temperature application. He also determined that the decomposition of silicon carbide is strongly dependent on the carbon potential and any carbon deposits on the surface will lower its volatilization.

Schenk et al. (1990) used emission spectroscopy and mass spectrometry to resolve spatial and temporal characteristics of laser induced plumes. Kunz et al. (1990) also performed spatially and temporally resolved emission and transmission measurements over a plume created over a carbon target irradiated with a CO_2 laser. The probe laser was a tunable dye laser operating in the range 300 to 700 nm. The motivation behind this experiment was to determine the dissociation products of carbon under different ambient pressures.

The focused spot size of the laser beam needs to be known for comparing any model with experimental results. Lim and Steen (1982)

developed an instrument that uses a rotating, reflective needle to measure the beam profile at the focal plane. This device has a spatial resolution of 20 μm and a temporal resolution of 0.1 ns. It can handle fluxes ranging from 50 W/cm^2 to 10^7 W/cm^2. The problem with this device is that the reflections of the laser beam from the needle return into the laser cavity, thereby affecting the mode of the laser beam. Herziger et al. (1987) presented another device to measure the two-dimensional laser beam intensity for a high power CO_2 laser. This device has a 10 μm resolution and operates through a rotating needle and pinhole arrangement. A review of the problems associated with beam quality measurements and definitions has been given by Hachfeld (1992). Even if the beam profile can be measured accurately before and after the process, it has been shown by Gregersen and Olsen (1990) that, for a strongly reflective material during welding, the back reflections into the laser significantly change the state of polarization of the laser beam and the output laser power. This makes it necessary to measure the beam profile during the process.

When a material is heated with a laser, the surface may oxidize, decompose with violent boiling, melt and vaporize. All of these may change the absorptance of the material from that of the original specimen. The incident energy which is not absorbed by the material is reflected. This energy may be reflected equally in all directions (diffuse) or otherwise. Knowledge of the value of the absorptance at the laser wavelength and at the material removal temperature is essential for the success of modeling efforts. The literature available on the measurement of absorptances is hence reviewed in the following section.

2.5 Absorptance Measurements

Chun and Rose (1970) were amongst the earliest to initiate reflectance measurements during the laser drilling process. They measured the energy reflected from a metal target, irradiated with a Nd-YAG laser, using an integrating sphere. They found that the absorptance increased rapidly for metals such as copper and molybdenum, once evaporation was initiated. They also postulated that in the first 50 to 100 μs the material was removed through vaporization. After this period, the combination of buildup of vapor pressure, heat diffusion and formation of melt results in the vapor pressure ejecting the molten material through the sides of the laser drilled cavity. Kocher et al. (1972) made measurements of laser transmission through sapphire using a Nd-YAG laser. They found that the absorption coefficient of sapphire increased by five orders of magnitude (10^{-2} to 10^{3} cm^{-1}) within 10^{-7} seconds. Sturmer and Von Allmen (1978) measured the time-resolved, specularly reflected CO_2 laser power from metallic targets in different ambient conditions. They found that target damage was strongly influenced by a laser supported detonation wave in the ambient gas.

Von Allmen et al. (1978) made measurements on Nd-YAG lasers irradiating metal targets (10^{7} to 10^{9} W/cm^2) using an elliptical reflector. They found that the unusually high absorptances were due to plasma above the material, which absorbed the incident laser energy and transferred it by heat conduction to the target. Schellhorn et al. (1986) measured the reflectance of metallic targets, subjected to CO_2 laser irradiation, and found that the reflectance decreases, as the intensity decreases, due to plasma

formation. The normal spectral reflectivity for silicon carbide and silicon nitride was measured by Roy et al. (1991). They measured the variation of reflectance between 9 and 11 μm, at temperatures up to 1273 K. Watanabe et al (1992) measured the reflectance of aluminum alloys during spot welding with a Nd-YAG laser beam. The reflectance was measured using an integrating sphere to determine which were the easiest alloys to weld.

Thus from the literature review carried out it can be observed that the insitu measurements adopted for the measurement of laser beam parameters involve expensive instrumentation. In the present investigation an alternate technique will be adopted, to obtain the beam parameters, with the same accuracy. A simple procedure is used for determining the material removal temperature for silicon nitride which may be extended to other ceramics and ceramic composites. In addition, the procedure also facilitates in understanding the mechanisms of laser material removal. Much of the existing literature on laser machining of silicon nitride, report that the material removal takes place via the decomposition of silicon nitride. The changes in the microstructure and the role of the sintering additives in the formation of compounds has not been reported. It will be shown in the present investigation that the sintering additives, form glassy silicates due to laser irradiation and the rate of formation of these glassy silicates is enhanced at high translation speeds. It will also be shown that the translation speeds influence the microstructure.

In the present investigation, a three-dimensional model has been developed which gives the temperature profile and shape of the drilled hole

resulting from the absorption of high intensity radiation. The model considers the effect of variable heat source intensity with the depth of hole, and can be applied for any material and for any type of laser. A distinct feature of this model would be the flexibility to change the boundary conditions, thus allowing simulation of actual drilling conditions.

Laser assisted machining has been investigated in the past with the intention of reducing cutting forces on the tool, increasing tool life and thus process difficult to machine materials using ordinary carbide tools. However not much work has been reported on an absorptive coating for metal specimen to increase the absorptivity to the CO_2 laser beam. In this investigation a parametric study would be conducted to establish optimal conditions for laser assisted machining of metals with special emphasis on selection of a suitable absorptive coating to increase absorptivity of metals to CO_2 laser beam (10.6 μm).

CHAPTER 3

PROBLEM STATEMENT

The rapid advances in material science and technology have provided innumerable opportunities for the development of new materials with advanced technological applications. Ceramics, composites, nickel- and cobalt-based superalloys etc. are candidate materials for high temperature applications such as heat exchangers, gas turbines, space applications etc. Ceramics are difficult to machine by conventional techniques. Lasers have emerged as an alternative machining technique for these advanced materials. Although laser processing of ceramics appears to be attractive and technically viable, there are certain limitations on its use for this application (Duley, 1983). To address the problems associated with laser machining, it is necessary to understand the material processing using lasers. A 1500 W CO_2 laser was used in the present investigation for this purpose.

The first task of this project was the setting up of the CO_2 laser machining center and its auxiliaries. Since it is necessary to conduct a variety of experiments to understand the laser machining process, the task was to build a setup which would give the researcher ease of operation and flexibility to conduct different experiments without modifying the setup every time.

The deterministic components of the laser machining process are phenomena such as heat conduction, evaporation, effect of spot size etc.

The successful modelling of these deterministic phenomena can be used substantially to reduce the number of trials required to optimally process a material.

The success of any modeling depends on several input parameters such as reflectance, latent heat of melting, thermal conductivity etc. Certain high temperature thermophysical properties such as material removal temperature, focused beam spot size and beam profile are difficult to determine and are assumed in most modeling. The results obtained thereof show large deviation from experimental results and the validity of such a model hence, becomes questionable.

Laser machining is a thermal process involving heating, melting and vaporization of the work material. Consequently a recast layer is formed on the machined surface. This can adversely affect the surface and is also responsible for the formation of cracks on the machined surface. The mechanism of material removal and the products of laser irradiation is an area which needs a thorough investigation to understand the laser machining process.

Laser assisted machining has been investigated in the past with the intention of reducing cutting forces on the tool, increasing tool life and thus process difficult to machine materials using ordinary carbide tools. However not much work has been reported on an absorptive coating for metal specimen to increase the absorptivity to the CO_2 laser beam.

The present investigation was aimed at addressing some of the problems associated with the laser processing of materials.

The specific problems that need to be addressed are as follows:

- Setting up of the CO_2 laser machining center to offer flexibility for carrying out a variety of experiments. This includes integrating the laser with a lathe and providing a beam delivery system for carrying out experiments on laser assisted machining, drilling and grooving tests.

- Development of a technique to determine the material removal temperature.

- Development of a technique to determine the focused beam spot size and beam profile.

- Development of a theoretical model for laser drilling process considering the effect of variable intensity with increasing hole depth.

- Drilling and grooving tests on metals, cemented carbides and ceramics.

- Study of material removal mechanism in silicon nitride.

- Study of the recast layer formation in cemented carbides and ceramics.

- Laser assisted machining and selection of proper absorptive coating to increase absorptivity of metals to CO_2 laser beam.

CHAPTER 4

EXPERIMENTAL SETUP

4.1 Description of the CO_2 Laser

The laser used in the present investigation is a MFKP series 1500 watt carbon dioxide (CO_2) laser manufactured by Laser Ecosse, Scotland. It utilizes liquid cooled discharge tubes in which the optical cavity is folded to produce a compact device. The schematic of the laser is shown in Figure 4.1.1. Each folded leg has two separate central anodes, each feeding one discharge tube. Each anode is fed through a separate ballast resistor from a single high voltage (H.V.) source. The H.V. may run continuously (CW mode) or be switched on and off rapidly by means of a triode valve (pulsed mode).

The laser output beam is deflected by a mirror to pass downwards through the output channel, emerging through the base of the laser head. The laser structure is itself suspended inside the base tray in such a way that it is decoupled from any twisting deformation of the base. However, since the base tray is mounted on a rigid structure, the beam delivery system mounted on the same structure retains its alignment with the laser head.

The output beam is intercepted by a mirror in the output channel which deflects it into a calorimeter, a water cooled absorber. The rise in temperature of the calorimeter cooling water is used as a measure of the

power of the laser beam. This deflecting mirror - the shutter mirror - is moved out of the path of the output beam when a solenoid is activated, allowing the laser beam to emerge from the laser head.

A steady flow of gas mixture is drawn through the discharge tubes by a vacuum pump. The exhaust gas from the pump is fed back to the laser after it passes through the gas recirculation and drying system mounted inside the control panel of the laser. Small losses of the gas mixture are compensated for by feeding in pulses of fresh gas mixture at automatically timed intervals.

The high voltage electrical supply for the discharge can operate from CW to 2500 Hz pulsed, with a number of options available for external control of the high voltage. The operating procedure is controlled by, and the protective interlocks monitored by, a programmable logic controller (PLC). The specifications of the CO_2 laser are given in Table 4.1.1:

Table 4.1.1 Specifications of CO_2 Laser

Laser output Power (CW,High Power mode)	1820 Watts
Laser output Power (CW, Low Power mode)	750 Watts
HT current at CW High power mode	0.85 mA
HT current at CW Low power mode	0.40 mA
Pressure inside system	22 mBar
CO_2	8.5 %
Helium	72 %
Nitrogen	19.5 %

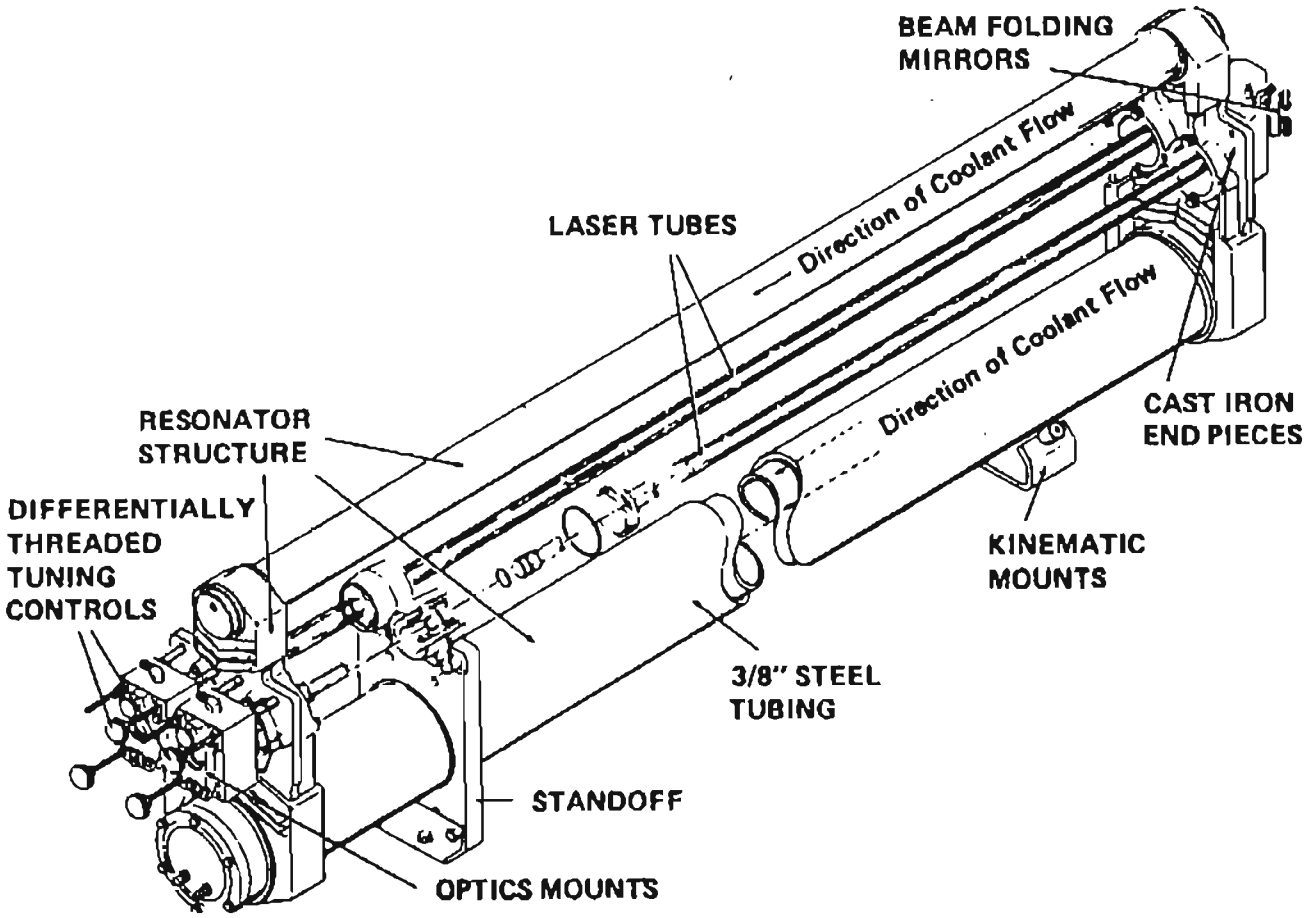

Figure 4.1.1 Schematic of the CO_2 Laser (after Duley, 1983)

4.2 Beam Delivery System

Preliminary tests were conducted with a beam delivery system, designed and fabricated indigenously in the lab. Figure 4.2.1 is a schematic of the original beam delivery system. Subsequently, it was replaced by an articulated arm, manufactured by Laser Mechanisms Inc. The articulated arm is a seven mirror module consisting of eight ball bearing rotary joints and seven pre-aligned right angle mirror joints. Figure 4.2.2 gives the schematic of the articulated arm. The beam from the laser head is totally contained within the aluminum tubing providing operator safety and a controlled atmosphere through which the beam can propagate. The laser beam travels a constant distance to the focussing lens, resulting in a fixed beam size at the lens. This produces a constant focal spot size and beam wavefront, which gives uniform kerf width throughout the full range of the arm motion. Relative motion between the laser arm combination and the beam motion system causes no change in the focal point position or loss of power. Specifications of the beam delivery system are given in Table 4.2.1:

Table 4.2.1 Specifications of the Articulated Arm

Clear aperture	35 mm
Mirror size	2.0" water cooled zero phase shift
Range of Movement	7 ft
Total Movement of the beam	±0.5 milliradian angular ±3 mm displacement
Focal spot accuracy	Spot stays within 0.005 inch circle over full range of arm travel

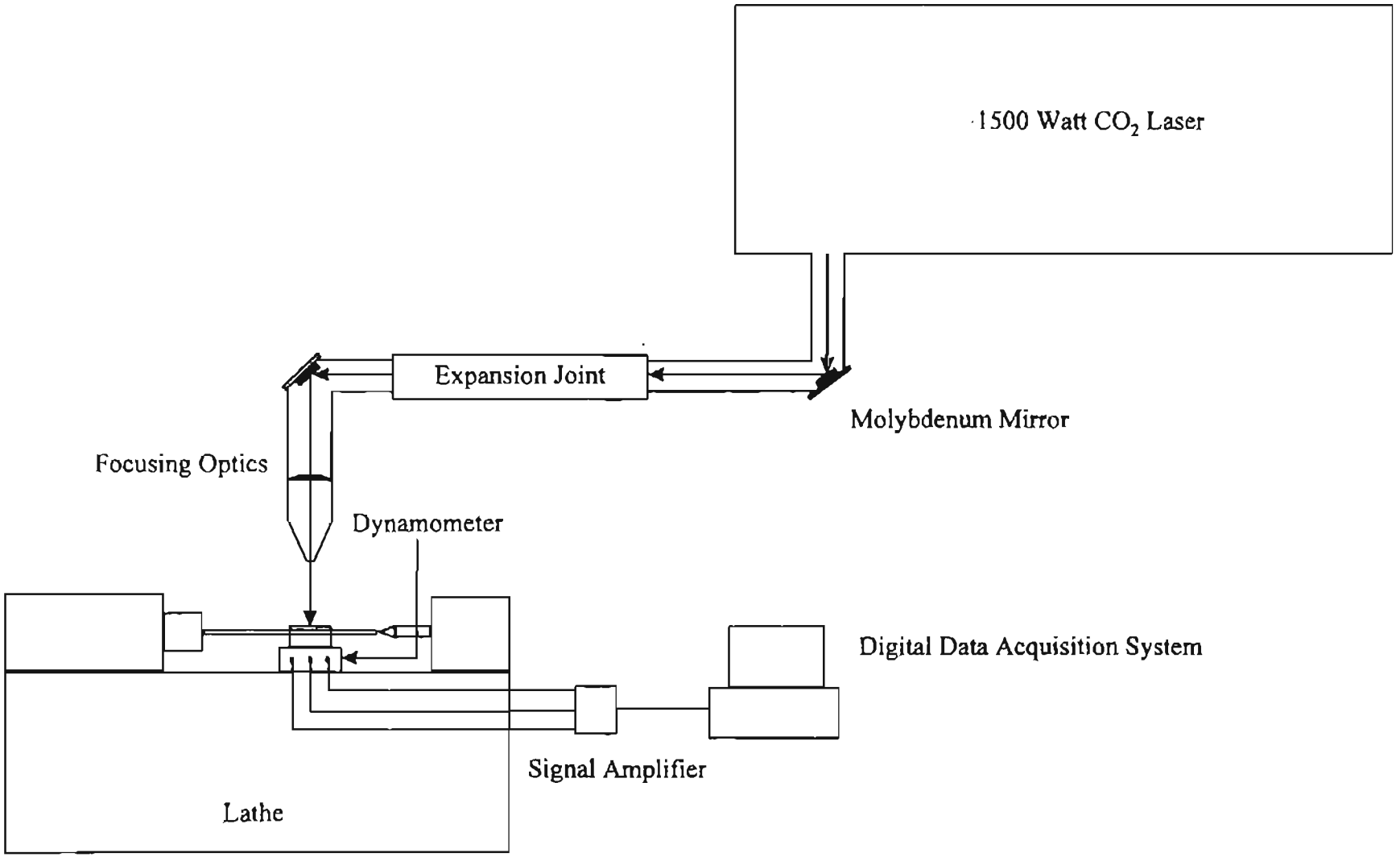

Figure 4.2.1 Schematic of the Original Beam Delivery System

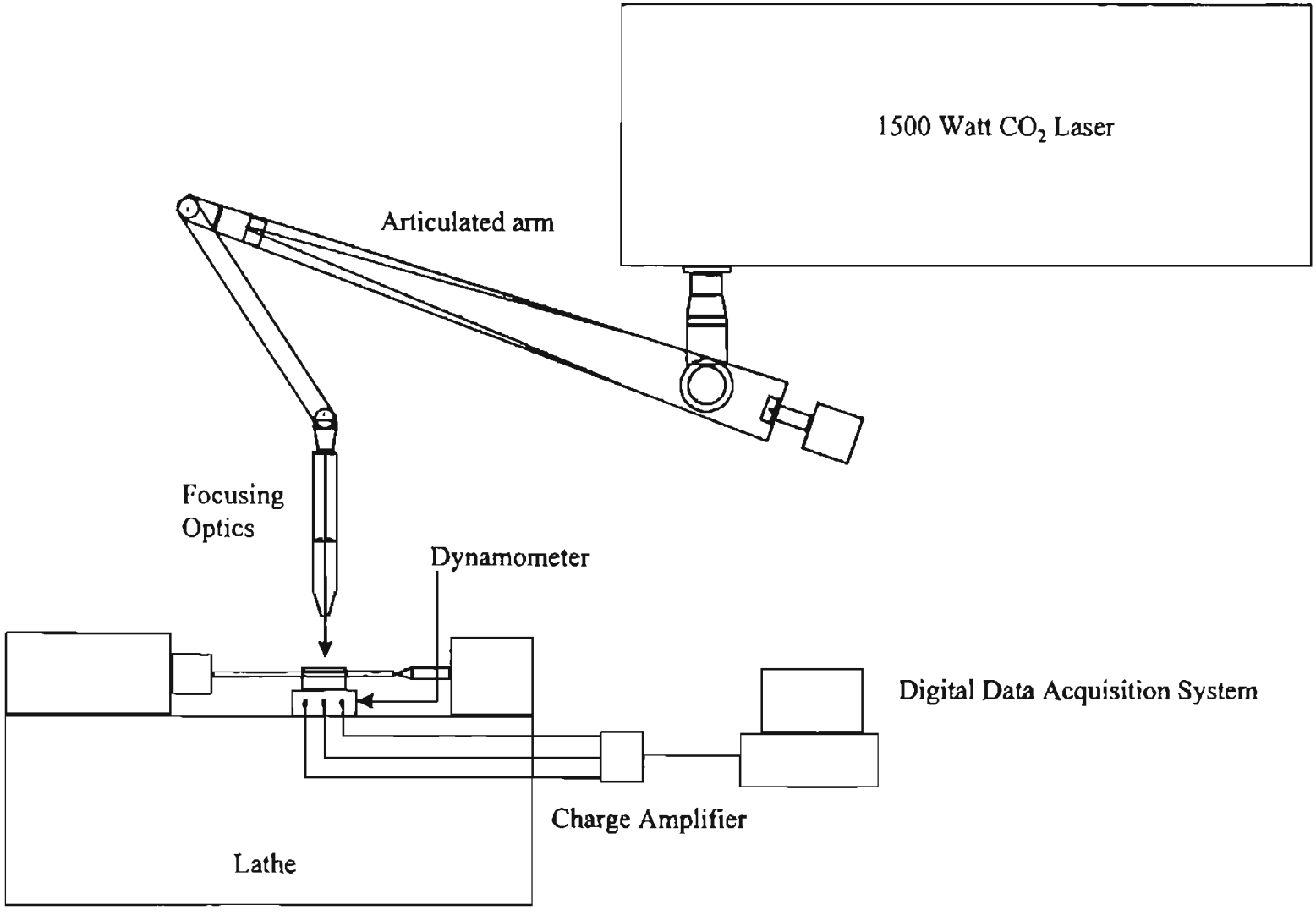

Figure 4.4.2 **Schematic of the Laser Machining Center with the Articulated Arm**

4.3 Focussing Optics:

The focussing optics is attached to the articulated arm and is supported by a fixture attached to the tool carriage of the lathe. The schematic of the focussing optics is shown in Figure 4.3.1. The fixture permits the focussing head to be moved in the x-, y-, and z-directions. Angular movements can also be imparted to the focussing head using this fixture. The focussing optics consists of a water cooled plano-convex lens of 5" focal length. The focussing head also has a gas jet assist manifold which provides a means to introduce various gases coaxially through and around the tip for both material processing and lens protection. The focussing optics has a precision vernier slide which provides vertical motion of the lens mounts and gas jet. The telescoping tube design keeps the beam path totally enclosed.

4.4 Vinyl Radiation Protection Screen

The working space around the laser is shielded by fire resistant, self extinguishing, infra red protective PVC screen supported on steel frames. The individual PVC strips are 6" x 0.06" x 6'. The strips being flexible, offer easy access to the laser focussing head and workpiece while setting up the experiment. The PVC strip is transparent and hence the operator can view through the screen during the experiments.

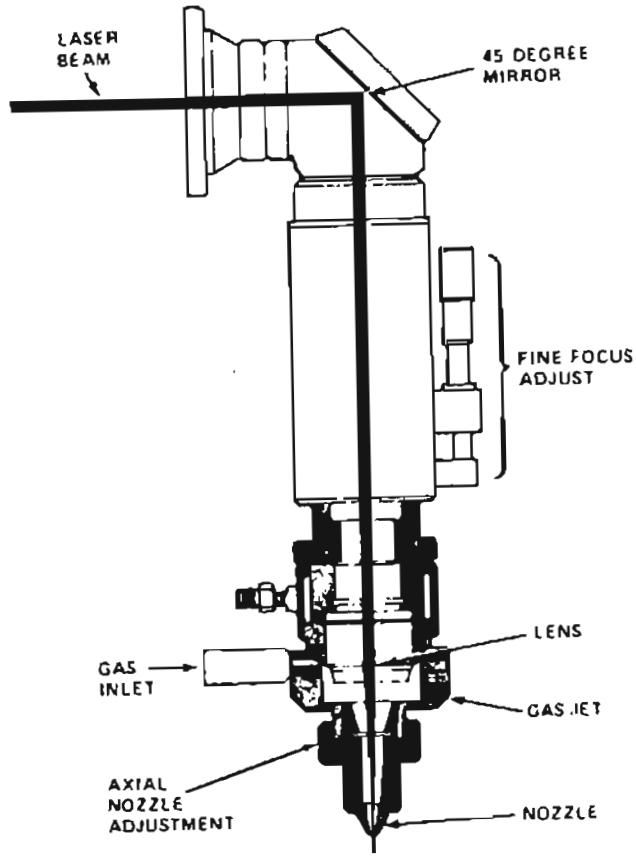

Figure 4.3.1 Schematic of the Focussing Head (after Duley, 1983).

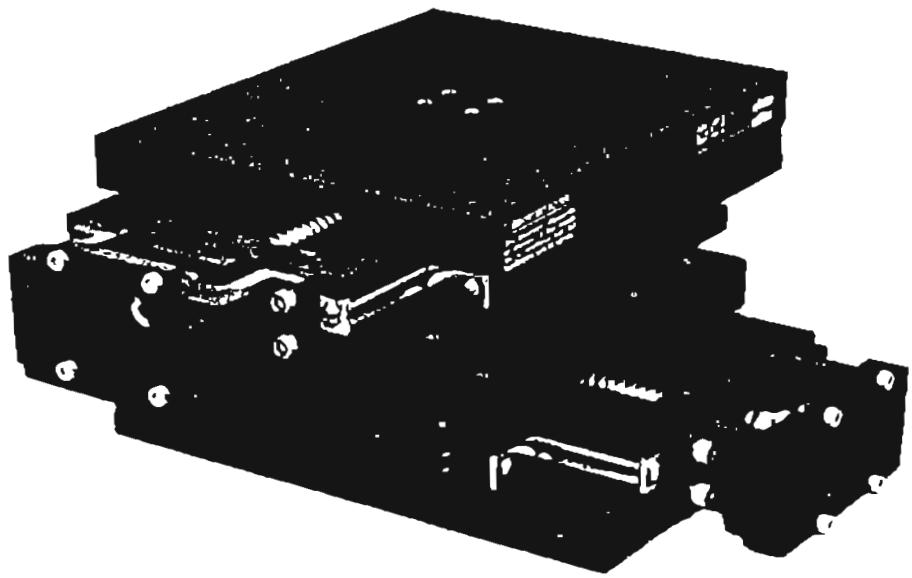

Figure 4.6.1 Schematic of the X-Y Stage

4.5 Exhaust System

The work space is provided with an exhaust duct to evacuate any gases formed due to laser machining. The duct is flexible and is connected to the tool carriage of the lathe. Hence, it can be moved along with the tool and focussing head during laser assisted machining tests. The other end of the duct is connected to an exhaust fan which takes the gases/fumes to the main exhaust duct.

4.6 X-Y Table

A two axis stage (Fig 4.6.1) is used for positioning the workpiece with respect to the laser focussing head. This X-Y stage moves on 2 lead screws which have 10 threads/inch pitch and offer an accuracy of ±0.00005 in/in bidirectionally. This precise movement helps in positioning the workpiece accurately for grooving tests.

4.7 Lathe

A Harrison lathe with 11 inches swing is used for the laser assisted machining tests. The lathe is driven by a 10 hp motor and has a rpm in the range of 34-1500. The lathe has feedrates in the range of 0.001-0.0087 in/rev.

The CO_2 laser was integrated with the lathe, using the beam delivery system. Figure 4.7.1 shows the CO_2 laser machining center.

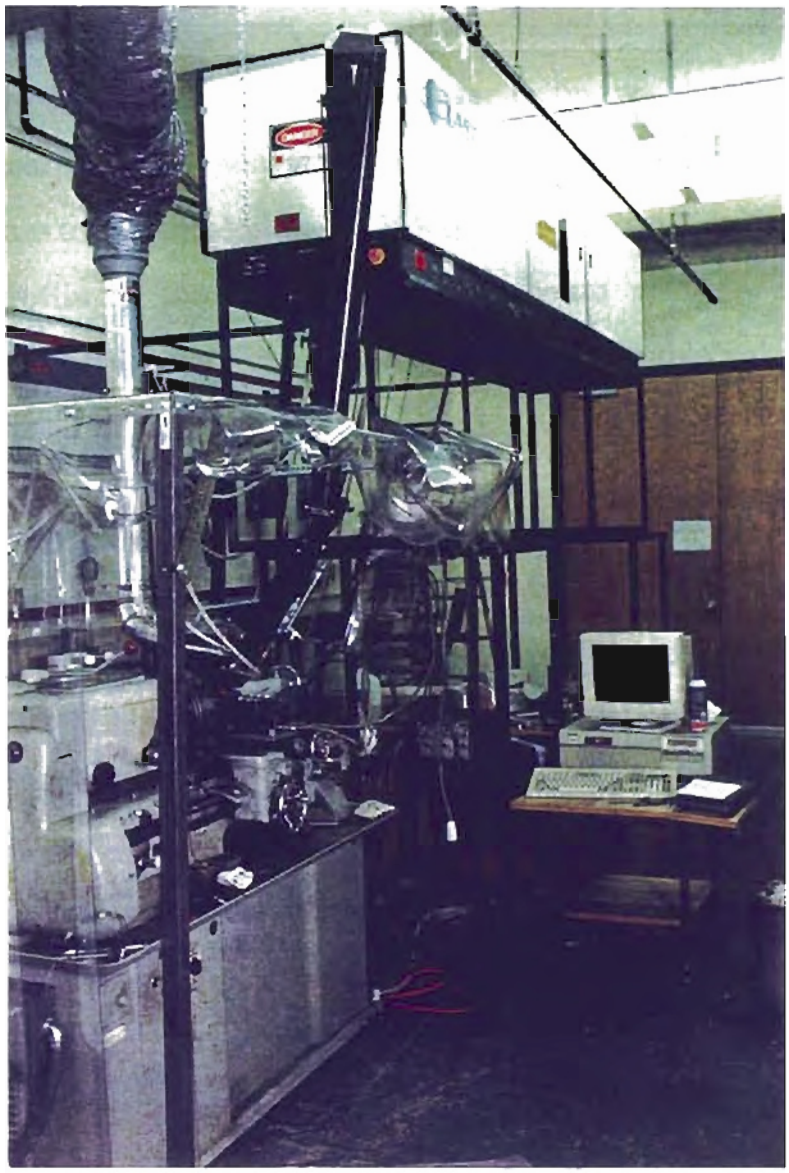

Figure 4.7.1 Photograph of the Laser Machining Center

CHAPTER 5

DETERMINATION OF THE BEAM PROFILE AND SPOT SIZE

The spot size of the focused laser beam, w_0, determines the intensity of the laser beam at the workpiece. The extremely high power density of the laser beam at the focal plane ($\approx 10^6$ W/cm^2) makes it difficult to measure the beam profile at that location. Laser beam profilers are commercially available, but are very expensive and of questionable value. An alternative method used in this study is presented in this chapter.

Consider a spherical, thermocouple bead placed in the path of the laser beam. Assuming that the temperature of the thermocouple is steady and considering negligible lead losses, performing an energy balance on the surface of the thermocouple yields (Chryssolouris, 1991)

$$\varepsilon I \pi r_t^2 = h 4\pi r_t^2 (T-T_\infty) + \bar{\varepsilon}\sigma 4\pi r_t^2 (T^4-T_s^4) \qquad (1)$$

where I is the intensity of the laser beam, ε is the spectral absorptance of the thermocouple bead at the laser wavelength, $\bar{\varepsilon}$ is the total emittance of the thermocouple bead, r_t is the radius of the bead, h is the convective heat transfer coefficient at the surface of the beam and σ is the Stefan-Boltzmann constant. The temperature of the surface of the bead is T (K), the temperature of the surrounding air is T_∞ and the temperature of the surroundings for radiant exchange is T_s. Assuming that convective heat transfer occurs only through natural convection and that the radius of the

thermocouple bead is small, yields the heat transfer coefficient h to be (Chryssolouris, 1991)

$$h = k_f / r_t \tag{2}$$

where k_f is the thermal conductivity of air. Substituting Eq. (2) into Eq. (1) yields

$$\varepsilon I = 4\frac{k_f}{r_t}(T - T_\infty) + \bar{\varepsilon}\sigma 4(T^4 - T_s^4) \tag{3}$$

Now, assuming that radiation heat losses are negligible ($T \leq 500$ K), we have

$$I \alpha (T - T_\infty) \tag{4}$$

Thus, the intensity of the laser beam is proportional to the temperature rise of a thermocouple bead placed in its path.

However, a thermocouple bead cannot be used to measure the beam profile at the focal plane for two reasons. 1) the diameter of the smallest available thermocouple is comparable to the focused spot diameter of the laser beam (≈ 300 μm), and 2) the intensity at the focal plane is so large that any thermocouple would melt or vaporize.

The change in the spot size of the laser beam can be approximated to (Chryssolouris, 1991)

$$w^2(z) = w_0^2\left[1 + \left(\frac{M^2(W + z)}{\pi w_0^2/\lambda}\right)^2\right] \tag{5}$$

where W is the distance between the focal plane and the location of interest (positive for a focal plane above the surface); M^2 is the beam propagation factor which is a measure of how close the actual beam is compared to an

ideal Gaussian laser beam. Eq. (5) implies that the spot size increases symmetrically above and below the focal plane. In reality, this is often not true due to diffraction effects from the output aperture of the laser (Duley, 1983). The beam quality factor (M^2) of this laser was specified by the manufacturer (Laser Ecosse Inc.) to range from 2.7 to 3.5. The M^2 value depends on a number of factors such as the quality of optics, purity of gases used in the laser, output power of the laser etc. Assuming that the M^2 of the laser is known and if the beam profile is measured at a given distance from the beam waist, it is possible to calculate the spot size from Eq. (5).

Figure 5.1 is a schematic of the setup used to measure the beam profile. Preliminary tests showed that the thermocouple bead melts even when it was placed far away (25 cm) from the focal plane of the f/5 lens. Hence the laser was operated on pulsed mode at 10% duty cycle on low power mode. This reduced the intensity of the laser beam at the thermocouple by a factor of 10.

A chromel-alumel (K-type) thermocouple 0.8 mm in diameter was used for measurements. The 95% response time of this thermocouple was measured to be 4 seconds and consequently does not respond to the temporal variations (200 Hz). The output voltage from the thermocouple was compared to the value obtained using a power meter and were observed to be linearly correlated. The beam profile was measured 11 cm below the focal plane of the 5 inch focal length lens at 600 W laser power, by traversing along two perpendicular directions at a speed of ~ 1 mm/sec.

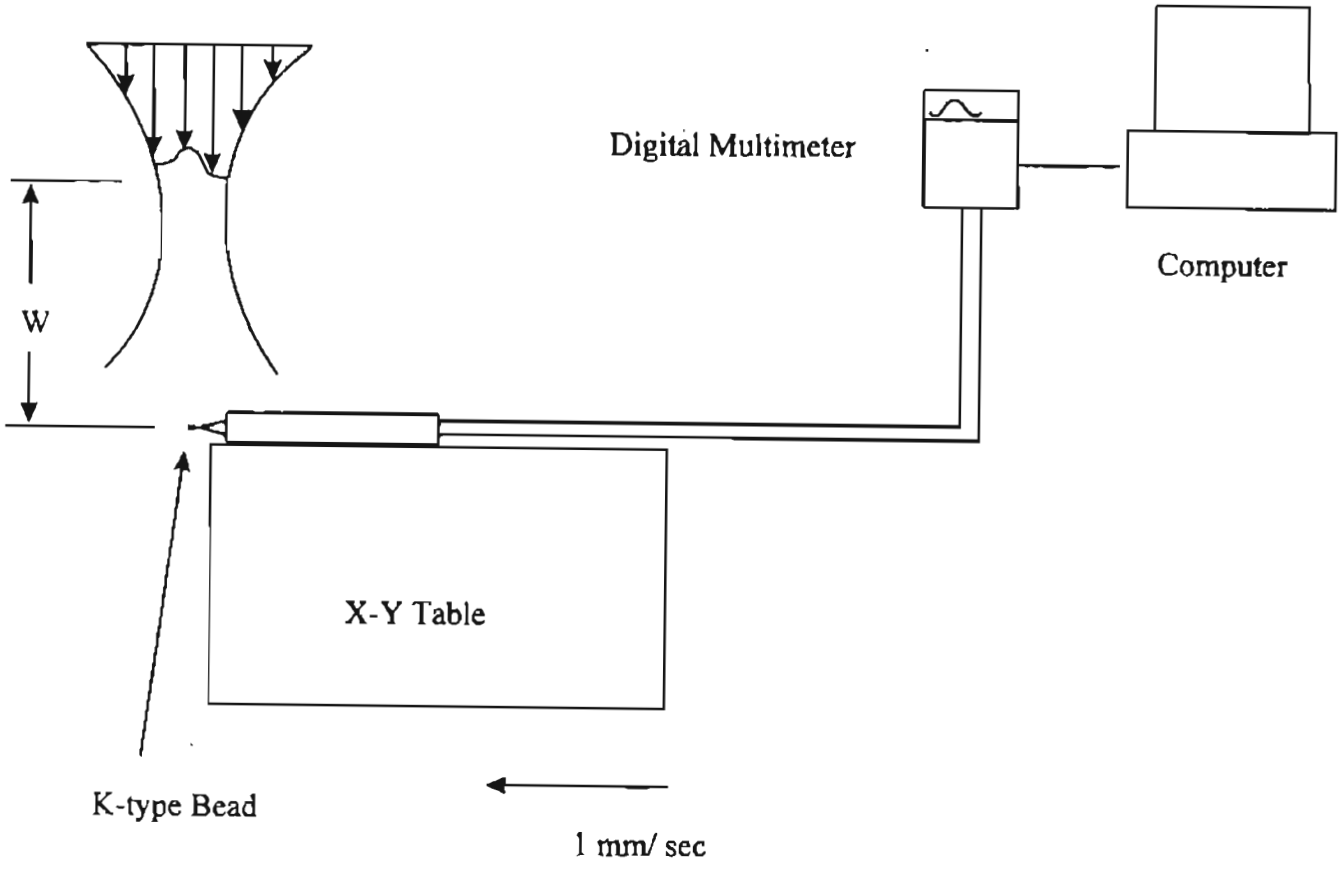

Figure 5.1 Schematic of the Setup for Measuring Beam Profile and Spot Size

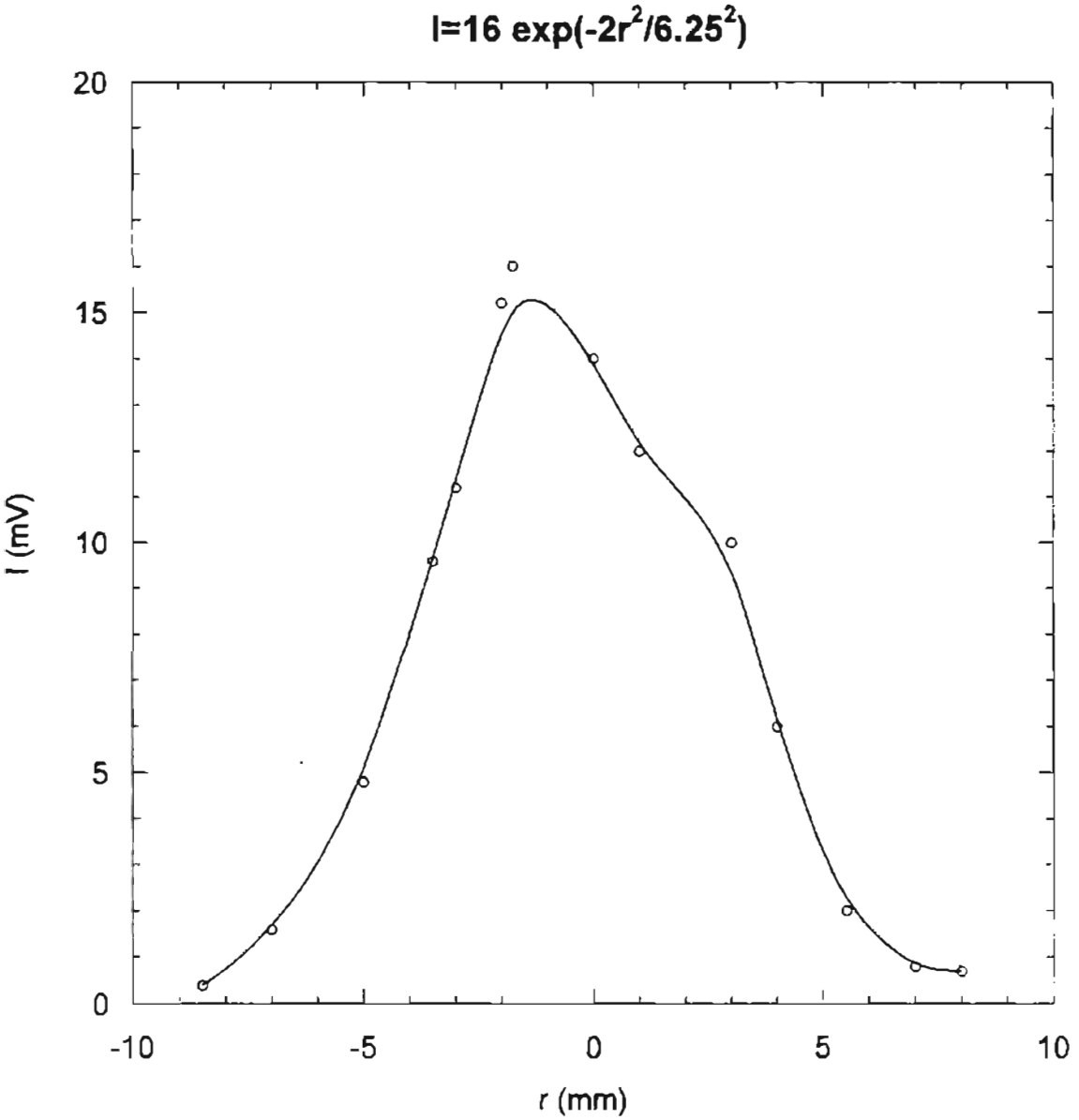

Figure 5.2 Laser Beam Profile Measured 11 cm from the Focal Plane at 600 W

The resulting thermocouple voltage was recorded using a multimeter interfaced to a PC. The voltage readings were curve fitted to a Gaussian intensity profile

$$I = I_0 e^{-2r^2/w^2} \tag{6}$$

The results obtained from the measurements are tabulated in Table 5.1.

Table 5.1 Beam Profile and Focused Beam Spot Size

Beam Profile	Elliptical Major axis : 7.4 mm Minor axis : 6.25 mm
Beam Diameter at the Focal Plane	150 μm

Thus the beam profile was found to be elliptical with 6.25 mm minor axis and 7.4 mm major axis. One such measured beam profile and the resulting curve-fit are shown in Figure 5.2. This yielded the average spot size below the 5 inch lens, 11 cm from the focal plane, to be 6.80 mm. Using the average spot size from the elliptical laser beam and assuming $M^2 = 2.7$, the spot size at the focal plane was obtained to be (from Eq.(5)) 150 μm. The value of the focused spot size depends considerably on the beam propagation factor (M^2). As long as the value of M^2 remains constant, the beam profile or the spot size would remain constant. For all practical purposes, this value was assumed to remain constant throughout the course of the experimental work in this project.

CHAPTER 6

MEASUREMENT OF MATERIAL REMOVAL TEMPERATURE

6.1 Introduction

The measurement of the material removal temperature (T_{rem}) is a very useful input for any laser processing model. It determines the amount of heat that has to be supplied to the material before the ablation process can begin. In the case of ceramics, the material removal temperature is equivalent to the decomposition temperature. Most of the data available on the decomposition temperature of ceramics is available mainly for single crystals. The effect of sintering, hot pressing, sintering additives etc. is not considered in these assumptions (Grigoryants, 1994). This chapter discusses a simple procedure for determining the material removal temperature for silicon nitride which may be extended to other ceramics and ceramic composites. In addition, the procedure also facilitates in understanding the mechanism of laser material removal.

In the case of ceramics, temperatures in the range of 1500 K to 4500 K are usually experienced during laser processing (Grigoryants, 1994). Optical pyrometry is a good technique to measure temperatures below 5000 K. Optical pyrometry works on the principle that the electromagnetic energy emitted by a hot body at a given wavelength depends on the temperature and surface emittance of the body. Hence, if the emittance is known, the temperature of the body can be determined. However, the

spectral emittance of the material, at the wavelength of operation of the pyrometer, is often unknown. The spectral emittance may vary with temperature. The temperature corresponding to maximum emittance value of unity is called radiance temperature, T_{rad} (Chryssolouris, 1991). The actual surface temperature of a hot body is more than the radiance temperature. In order to minimize the errors due to unknown emittance in optical temperature measurements, multi-color pyrometers are often used. In multi-color pyrometers, radiance temperature is measured at different wavelengths and the variation of emittance with wavelength must be known or assumed.

6.2 Experimental procedure

In this investigation, a Williamson Tempmatic 8000 series pyrometer was used. This is a dual wavelength pyrometer capable of measuring temperatures in the range of 300° to 4000° F (150°-2200° C). It uses a silicon detector with operating wavelength of 0.8 to 1.0 μm and views an area of 400 μm^2. It has a 95% response time of 0.2 secs. The pyrometer is set at a distance of 6 inches from the target.

The dual wavelength pyrometer features a rotating chopper carrying four narrow band pairs of spectral filters of different wavelengths and determines temperatures by computing the ratio of the radiance energies emitted by the target in these wavelengths. Since this ratio is a function of temperature only, it remains constant under changing target and operating conditions thereby eliminating many application errors.

The pyrometer is mounted on a tripod with the pyrometer at an angle of ~ 45^0 from the vertical aimed on the sample. The sample was kept at the focal point of the laser beam. Nitrogen was used as coaxial assist gas. The output of the pyrometer was recorded on a digital temperature indicator. The schematic of the experimental setup is shown in Figure 6.2.1.

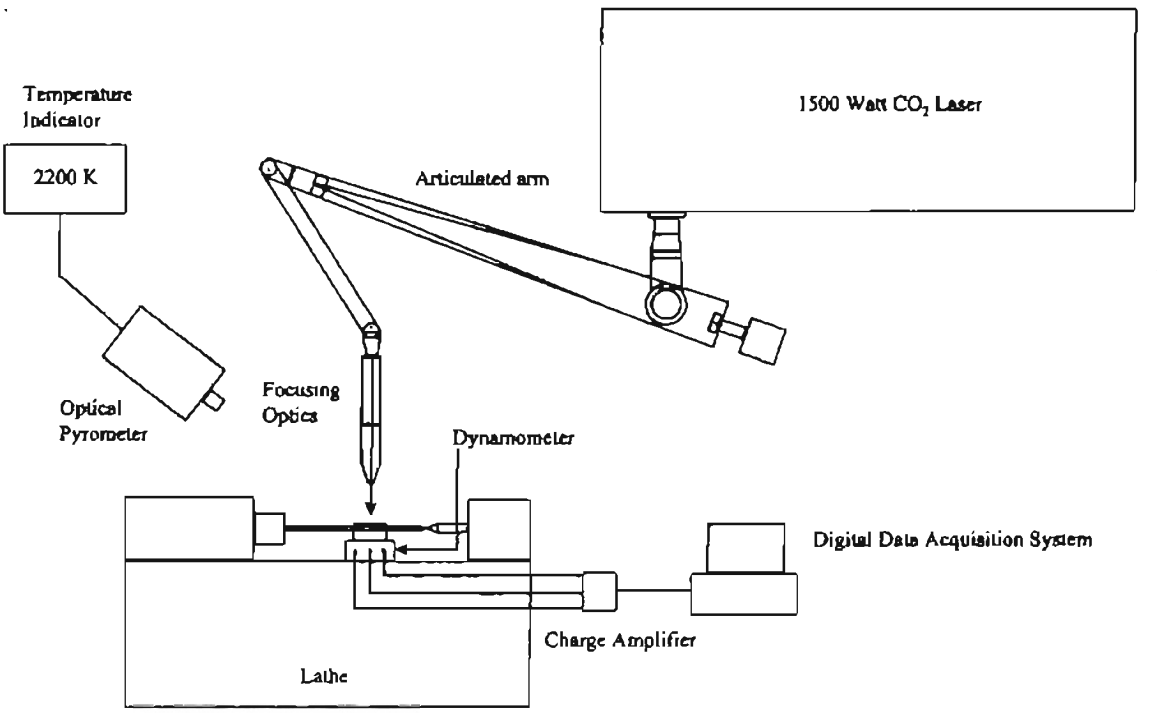

Figure 6.2.1 Schematic of the Setup for the Measurement of Material Removal Temperature

6.3 Results

Results obtained from several experiments are tabulated in Table 6.3.1. In all these experiments, the surface emittance was set at unity in the pyrometer. Hence the temperature recorded is the radiance temperature T_{rad} which is less than the actual surface temperature. The laser was kept on for 5 seconds during each of these experiments. The criterion used for identifying material removal was the presence of solidified droplets on the surface of the material near the laser irradiated spot at the conclusion of the experiment.

Table 6.3.1 Results of Temperature Measurement Experiments

Expt. No	Laser Power (W)	Duration (sec)	T_{rad} (K)
1	400	5	2190
2	450	5	2147
3	500	5	2120
4	550	5	2117
5	600	5	2110
6	650	5	2087
7	700	5	2085
8	750	5	2082
9	800	5	2075
10	850	5	2065

Material removal was observed in all the above experiments. It can be seen that the radiance temperature from Table 6.3.1 is in the range from 2065 K to 2190 K. This temperature decreases with increasing laser power. The reason for this stems from the fact that as the laser power increases, more

of the target surface is covered by liquid silicon from the decomposition of silicon nitride (Solomah,1991).

$$Si_3N_4 \dashrightarrow 3Si\ (l) + 2N_2\ (g).$$

The emittance of liquid silicon is 0.3 and that of silicon nitride is 0.9 (Schenk et al., 1990). Thus the decrease in radiance temperature with increasing laser power is due to the decrease in the emittance owing to the large fraction of the target material being covered with liquid silicon.

Assuming a surface emittance of 0.6 (average emittance of liquid and solid phase of the target material), the experiments were carried again with corrective settings in the pyrometer. This time it was found that the material removal temperature T_{rem} was in the range between 2227 to 2345 K. Again, if the surface emittance is assumed to be that of liquid silicon (when the target surface is covered with liquid silicon) i.e 0.3, the temperatures were recorded in the range between 2410 K to 2620 K. Thus from these experiments one can conclude that the decomposition temperature for silicon nitride ranges from approximately 2200 to 2600 K.

CHAPTER 7

LASER DRILLING

7.1 Introduction

Laser drilling involves a stationary laser beam which uses its high power density to melt and/or vaporize the material from the workpiece. It is often called percussion or on center drilling (Chryssolouris, 1991). As shown in Figure 7.1.1, laser drilling is governed by the energy balance between the irradiating energy from the laser beam and conduction heat into the workpiece, the energy losses to the surroundings, and the energy required for phase transformation in the workpiece. The incident beam energy has a spatial intensity distribution which in laser drilling is usually a Gaussian distribution produced by the laser operating in TEM_{00} mode.

The focussed beam radius is usually specified as the distance between the beam center and a point where the intensity is reduced from its maximum value at the beam center by a factor of e^2 as shown in Figure 7.1.2. The average diameter of the drilled hole may be less than the beam diameter due to various heat loss effects. These heat losses, primarily conduction to the interior of the workpiece and losses to the environment, divert beam energy away from the actual hole drilling process.

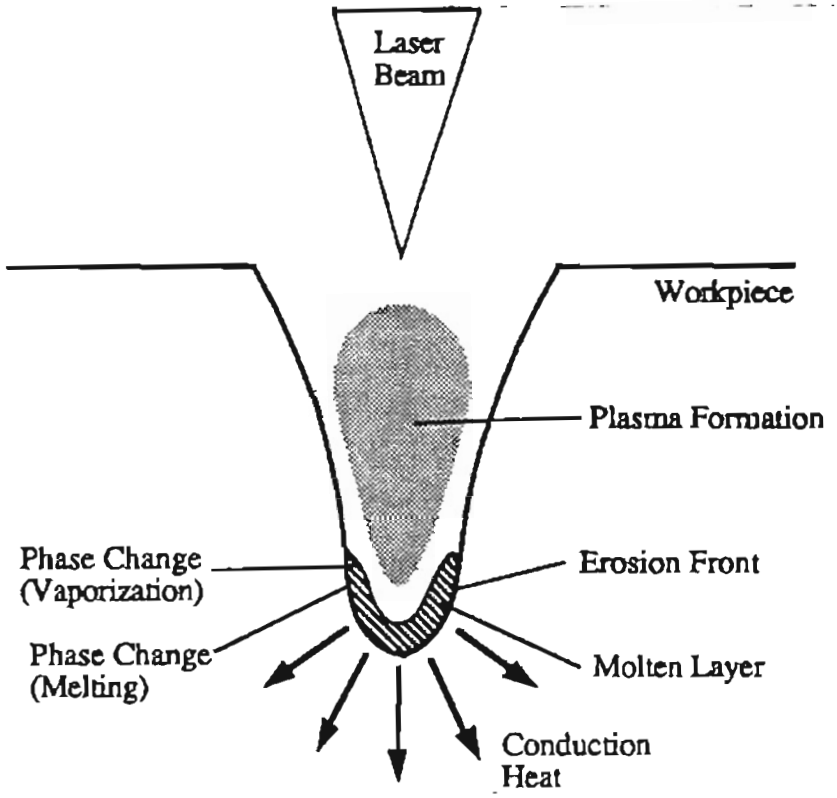

Figure 7.1.1 Laser Drilling (after Chryssolouris, 1991).

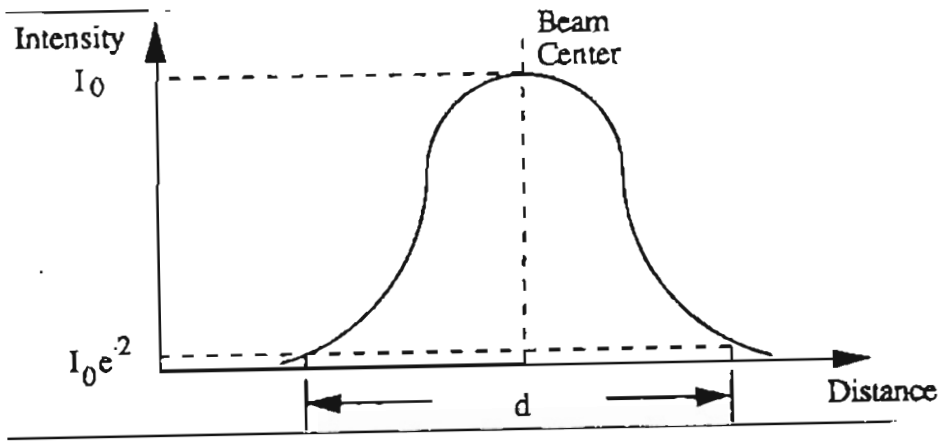

Figure 7.1.2 Spatial Intensity Distribution for TEM_{00} Laser Beam(after Chryssolouris, 1991)

Conduction heat, which is a result of the temperature difference between the hole surface and the interior of the workpiece depends on the thermal diffusivity α of the material and the interaction time t_i. The thermal penetration depth is defined (Chryssolouris, 1991) as :

$$\delta = \sqrt{\alpha t_i}$$

Energy losses during laser drilling can be summarized as follows (Duley, 1983):

- If there is melting of the material due to laser interaction, the molten material accumulates along the side and bottom of the hole, thereby causing the laser beam energy to be lost in two ways. First, energy is used up in superheating the molten material in the hole to a temperature above its melting point. Secondly, in case of percussion drilling, where a sequence of holes is used to drill a hole, the molten material may resolidify between successive pulses. This causes a portion of the beam energy during each pulse to remelt the resolidified material.

- Plasma formation occurs when a material is vaporized. An opaque cloud of the vaporized material often forms above the interaction zone. This cloud absorbs part of the incoming beam energy and increases its temperature until a plasma is formed. The heated plasma may act as a secondary heat source and may improve the drilling process. However it is very difficult to control the directionality of this plasma which often causes dimensional

accuracy problems. The plasma formation can be reduced by using an inert assist gas which removes the vaporized debris from the path of the laser beam.

- The absorption of the laser beam depends on the wavelength of the laser radiation as well as the spectral absorptivity of the processed material. Metals, such as aluminum and copper exhibit high reflectivity (~ 97 %) for CO_2 laser radiation(10.6 μm wavelength). Besides, the presence of a molten layer formed during the laser interaction with metals or ceramics, also changes the absorptivity. Absorptivity of the laser beam also depends on the angle of orientation of the workpiece surface with respect to the laser beam. Incidence angles of more than 80^0 increases absorptivity (Chryssolouris, 1991). For deep holes, multiple reflection may take place along the wall of the hole (light pipe effect), thereby decreasing the availability of beam energy for material removal.

- The use of coaxial assist gas during laser drilling cools the erosion front through convective heat transfer. With an increase in thermal dissipation with the use of high pressure gas jet, more beam energy is required to maintain melting/vaporization temperature at the erosion front.

The advantages of laser drilling over conventional methods (Chryssolouris, 1991) are :

- Holes can be made in difficult-to-machine materials, such as ceramics, composites and hardened metals.

- Higher accuracies and and smaller dimensions can be achieved with laser drilling than with conventional drilling methods. Desired hole geometry can be obtained with a proper selection of beam power, pulse characteristics, focussing lens and interaction time.

- High drilling rates can be achieved in production environment using a pulsed beam source. Hole diameters and shapes can be changed rapidly by changing the process variables rather than by changing tools as in the conventional drilling process.

However, some limitations to the laser drilling process are (Chryssolouris,1991):

- Holes with stepped diameter cannot be drilled using a laser.

- Difficult to control the depth in blind hole drilling.

- During deep hole drilling, beam divergence may become unacceptable. This problem can however be resolved to some extent by using a longer focal length or by continuously moving the focal point along with the advancement of the hole in the workpiece using programmed motion controllers.

7.2 Experimental Procedure

In the present investigation, the following work materials were used for laser drilling:

- Cemented tungsten carbide (containing 6% Cobalt).
- Titanium Carbide coated cemented WC.

- SiAlON.
- Silicon nitride.
- Aluminum Oxide.
- Multi coated tool (Al_2O_3 + TiC +TiCN) on cemented WC.

The materials used for laser drilling were in the form of square tool inserts. These inserts were ultrasonically cleaned in a solution of acetone before carrying out the drilling tests. In order to study the profile of the hole drilled by the laser on a particular material, it is necessary to study the cross-section of the hole. The conventional technique involves the sectioning of the hole after drilling with a laser. In this study, a simpler approach was adopted. Two square inserts were held against each other in a vice. The laser was then operated on single pulse mode with the beam striking the inserts at the point where they butt against each other. Thus, without actually sectioning the material, a cross section of the hole profile could be obtained. This process is illustrated in Figure 7.2.1. The limitation of this technique is that, the parting plane is actually two surfaces instead of a solid material.

The materials under study were irradiated by a single pulse at different power levels. Nitrogen was used as coaxial assist gas. The gas pressure was maintained at 30 psig. Laser powers employed were 0.87, 1.75, 3.5, 5.25 and 7 W. Hole characteristics were quantitatively measured using a stereomicroscope and an x-y table, that can be moved with micrometer accuracy. Qualitative examination of the hole was done using an ABT 32 scanning electron microscope. The results of the drilling tests for different work materials are discussed in the following section.

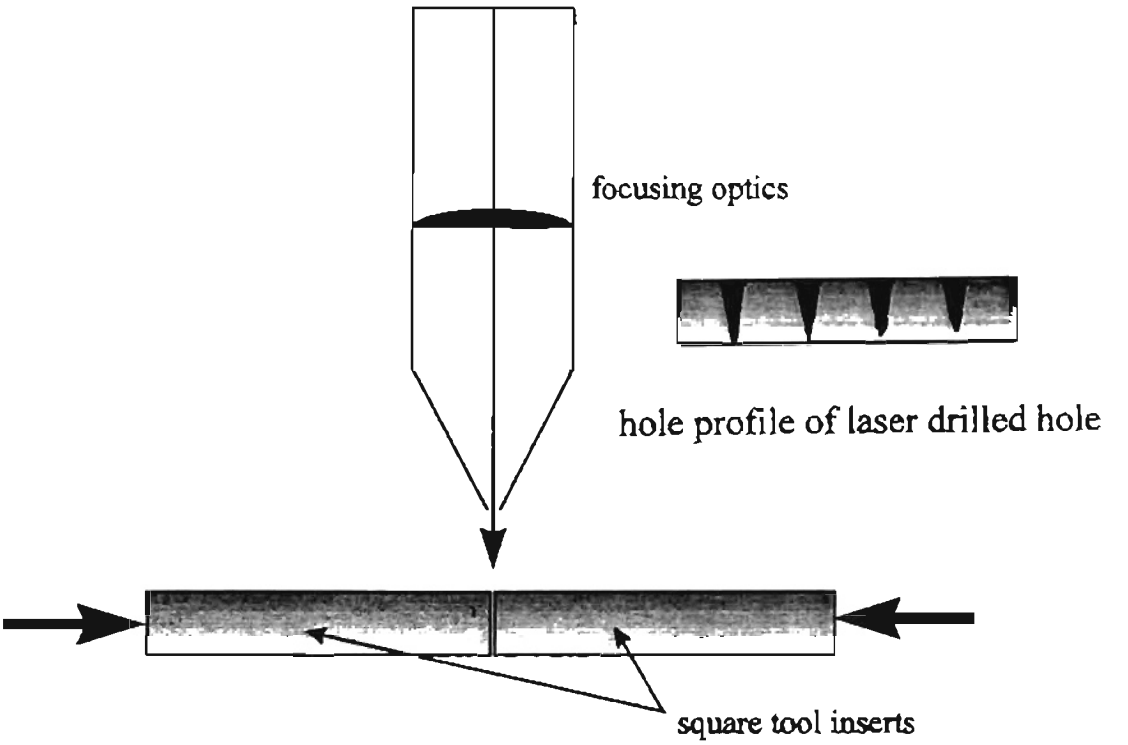

Figure 7.2.1 Schematic Showing the Laser Drilling Process.

7.3 Results and Discussion

7.3.1 Titanium Carbide coated Cemented Tungsten Carbide:

Figure 7.3.1.1 shows a SEM micrograph of the hole profiles for different power levels. Figure 7.3.1.2 shows the relation between the hole dimensions (diameter and depth) and the beam power. From the plot, it can be observed that the hole diameter does not vary significantly (0.4 to 0.5

mm) with power. However, hole depth increases with beam power. At high power (7 W), thermal cracking of the specimen was observed (Fig 7.3.1.3). The recast layer increases at the entrance of the hole with increase in beam power. Figure 7.3.1.4 is a micrograph of the hole entrance at high beam power. Energy dispersive X-ray analysis was conducted to analyze the elements present in the drilled hole and in the recast layer. Figure 7.3.1.5 is the EDXA map at the hole entrance, indicating the presence of both W and Ti. However the recast layer is found to be comprised of only W. No trace of titanium was found in the recast layer (Figure 7.3.1.6).

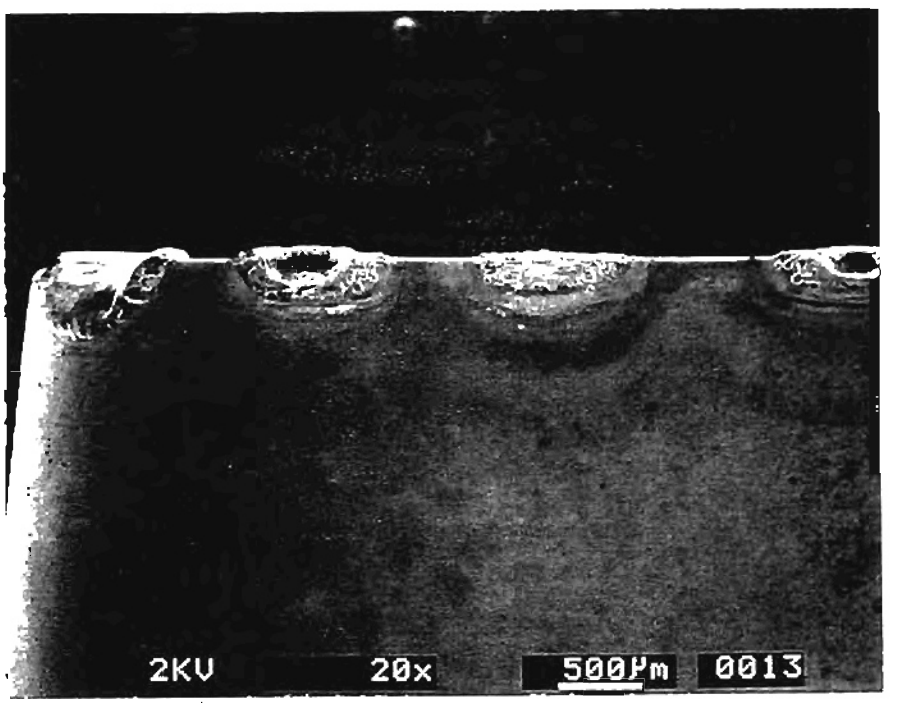

Figure 7.3.1.1 SEM Micrograph Showing the Hole Profiles in TiC Coated Cemented WC at Different Beam Powers

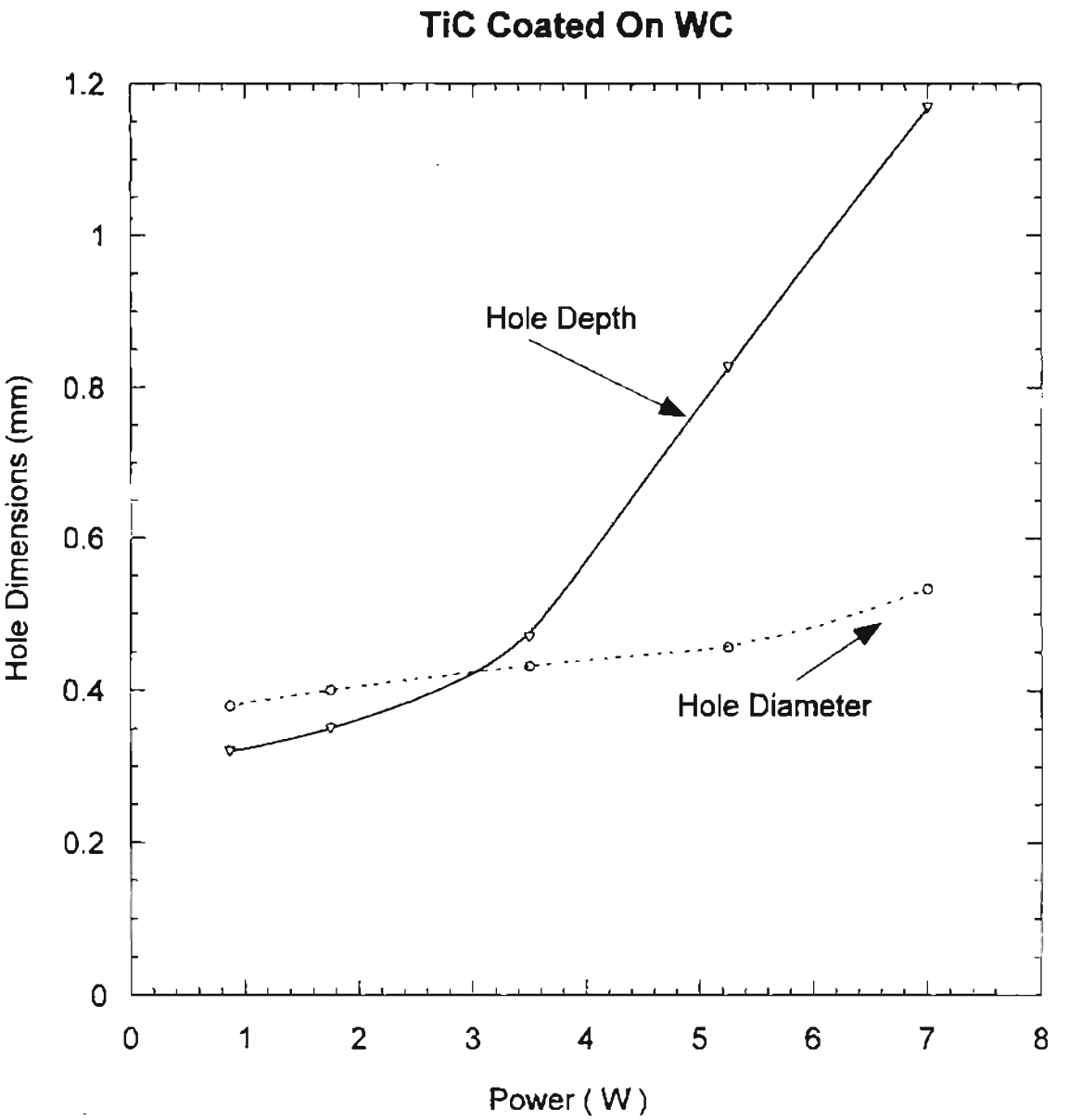

Figure 7.3.1.2 Plot Showing Hole Dimensions Vs Laser Power for TiC Coated Cemented WC

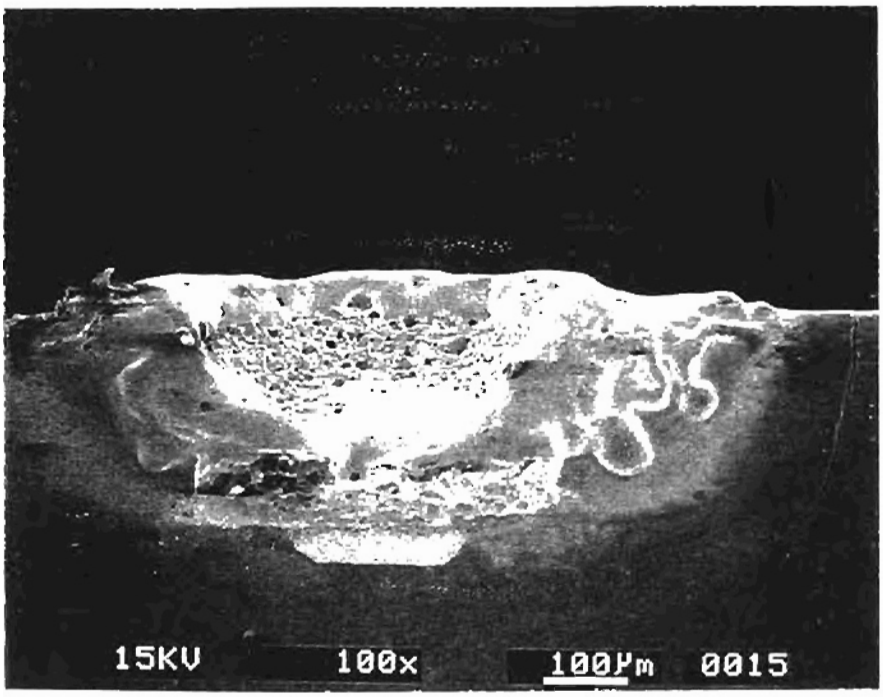

Figure 7.3.1.3 SEM Micrograph Showing Thermal Cracking at 7 W Power in TiC Coated Cemented WC

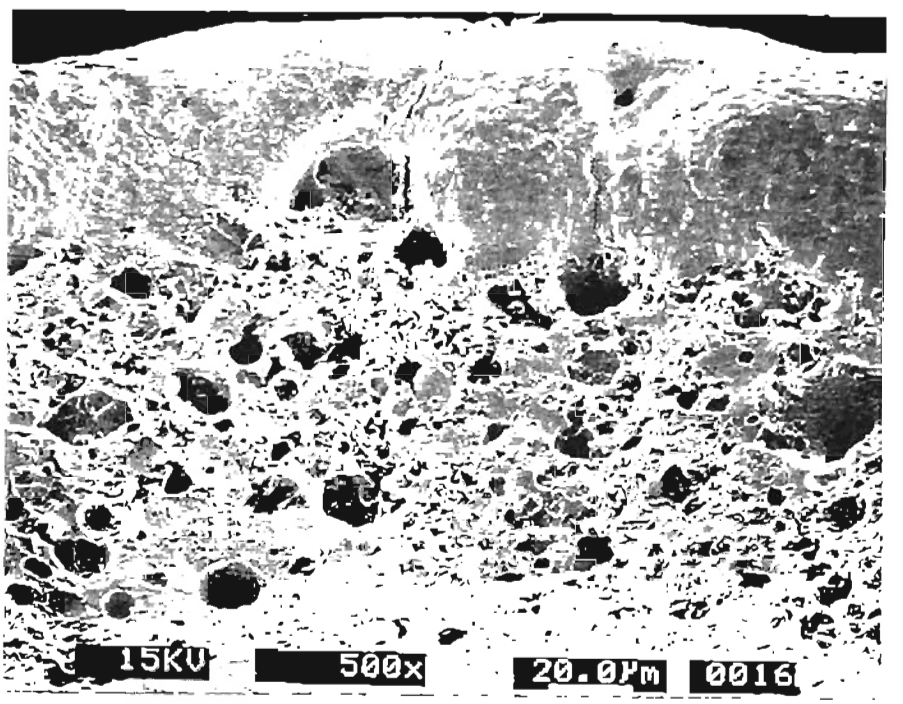

Figure 7.3.1.4 SEM Micrograph Showing the Hole Entrance at High Power in TiC Coated Cemented WC

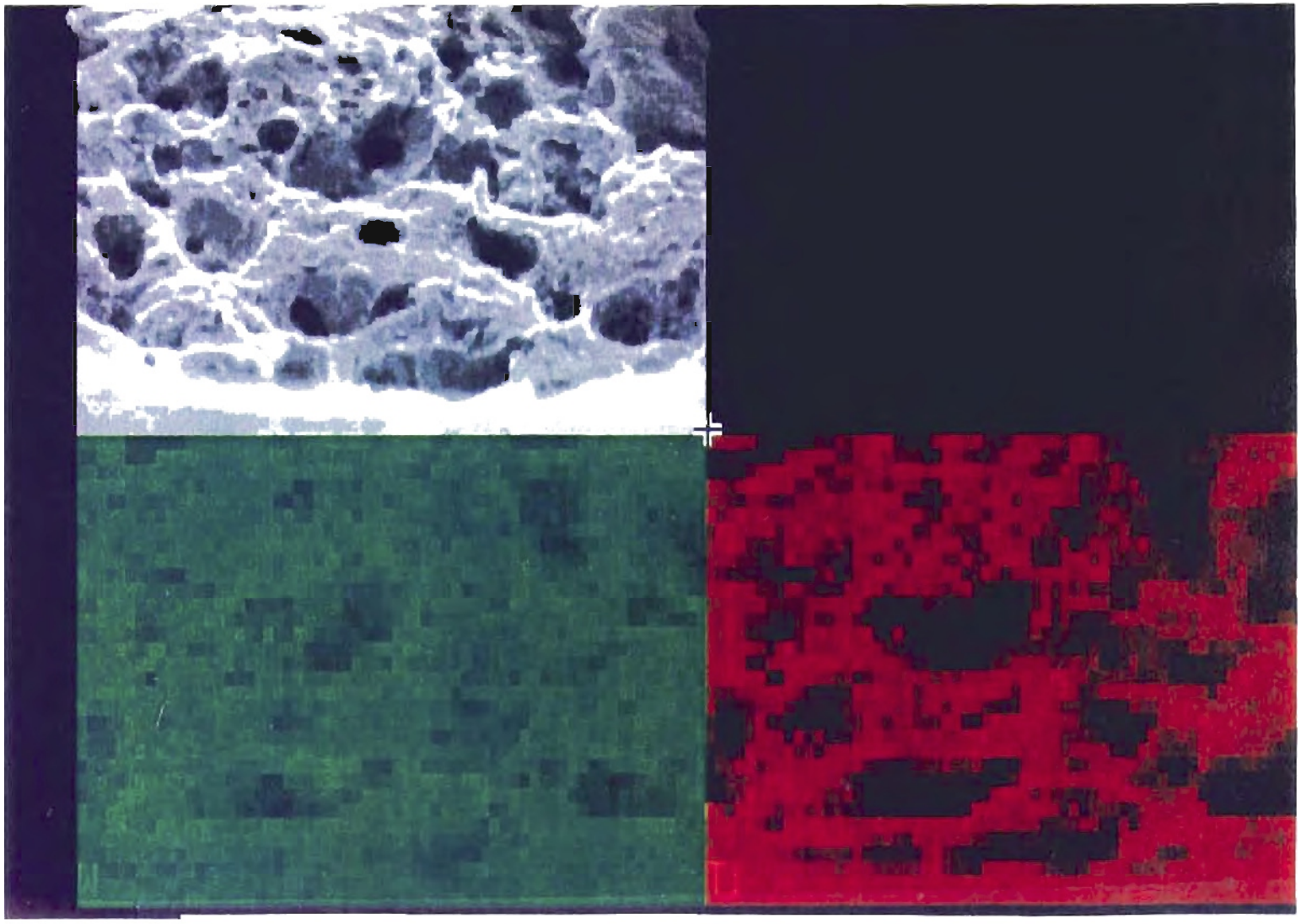

Figure 7.3.1.5 EDXA Map at Hole Entrance Indicating Presence of W and Ti in TiC Coated Cemented WC

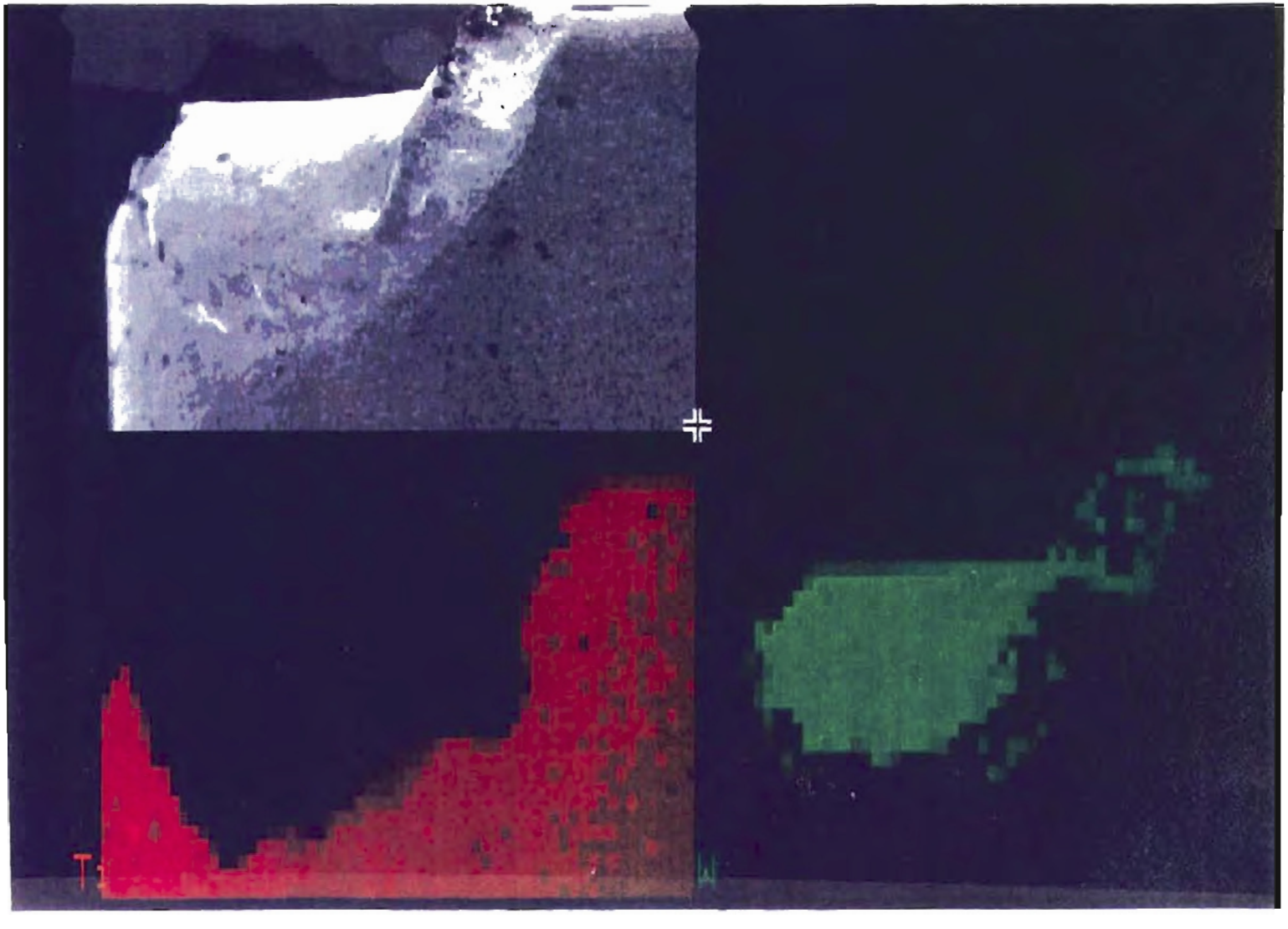

Figure 7.3.1.6 EDXA Map of the Recast Layer in TiC Coated Cemented WC
Showing only W

7.3.2 Cemented Tungsten Carbide (6% Cobalt)

Figure 7.3.2.1 is a SEM micrograph of the hole profiles at different powers. Fig 7.3.2.2 is a plot of the variation of hole dimensions (diameter and depth) at different laser powers for cemented tungsten carbide. It is evident from the plot that the beam diameter remains essentially constant at ~ 0.5 mm at all laser powers while the hole depth increases with beam power. Figure 7.3.2.3 is the micrograph of a hole at low beam power. It can be observed that there is a change in the microstructure in the heat affected zone. Also, there is no thermal cracking at low power. Figure 7.3.2.4 is the micrograph of the hole drilled at high power. At this power it can be observed that there is a thermal crack originating from the recast layer. Figures 7.3.2.5 and 7.3.2.6 show the EDXA maps of the laser drilled holes. The molten layer reveals the presence of tungsten in major amounts. However in the heat affected zone, cobalt is detected along with tungsten. The recast layer is less compared to the TiC coated tool.

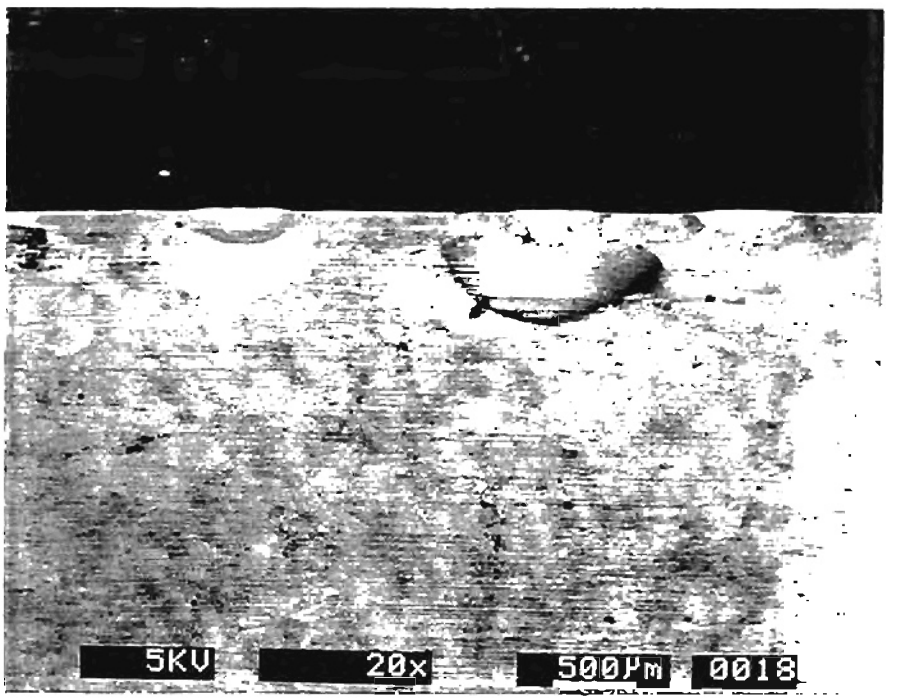

Figure 7.3.2.1 SEM Micrograph Showing the Hole Profiles in Cemented WC (6% Cobalt) at Different Beam Powers

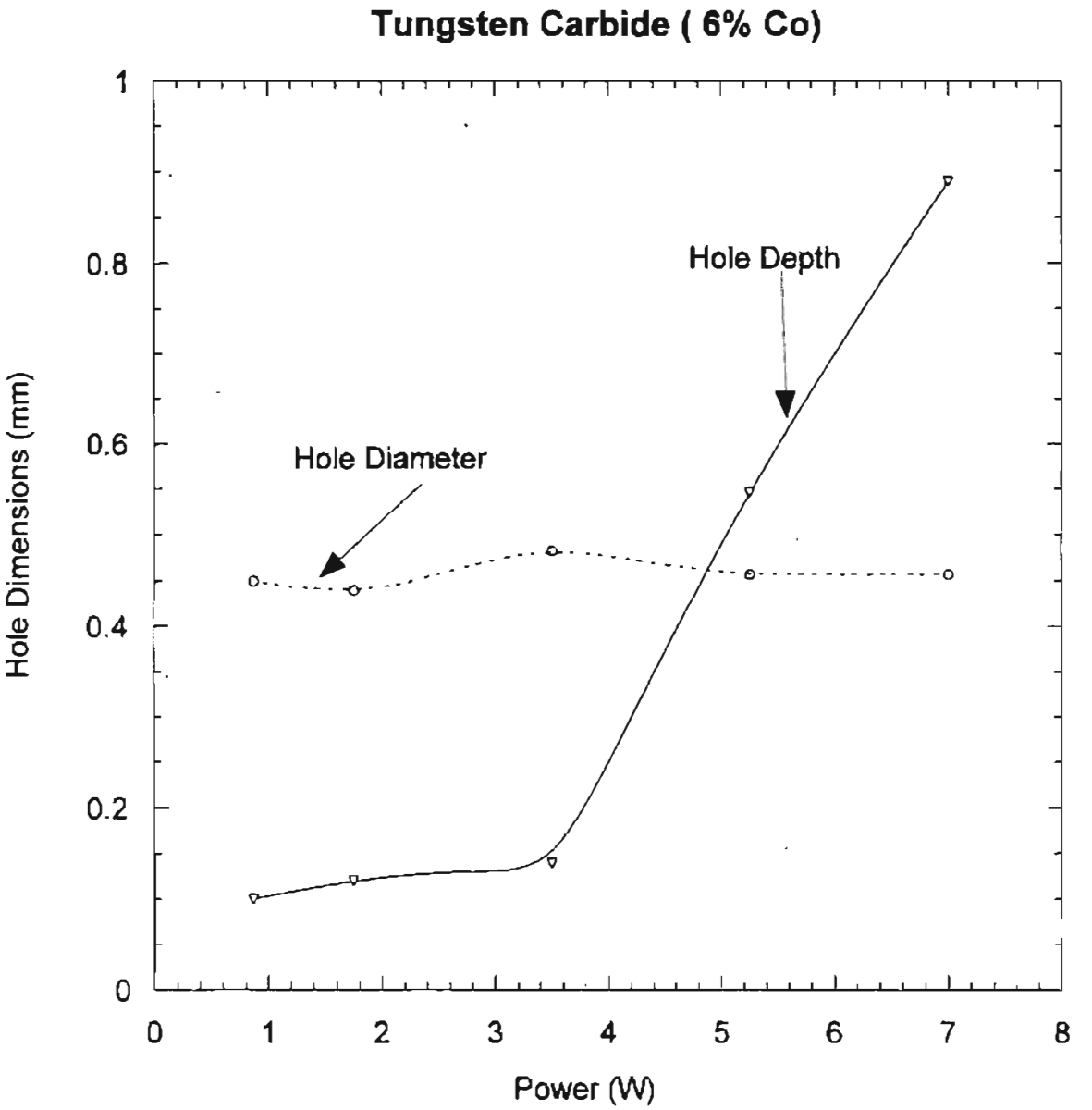

Figure 7.3.2.2 Plot Showing Hole Dimensions Vs Laser Power for Cemented WC (6 % Cobalt)

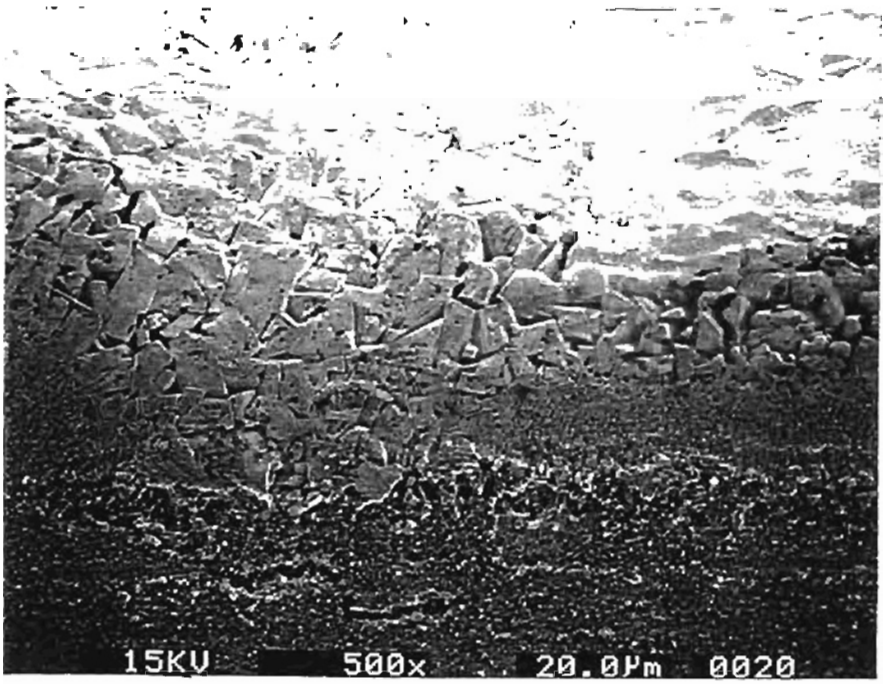

Figure7.3.2.3 SEM Micrograph Showing the Change in Microstructure in the Heat affected Zone in Cemented WC (6% Cobalt)

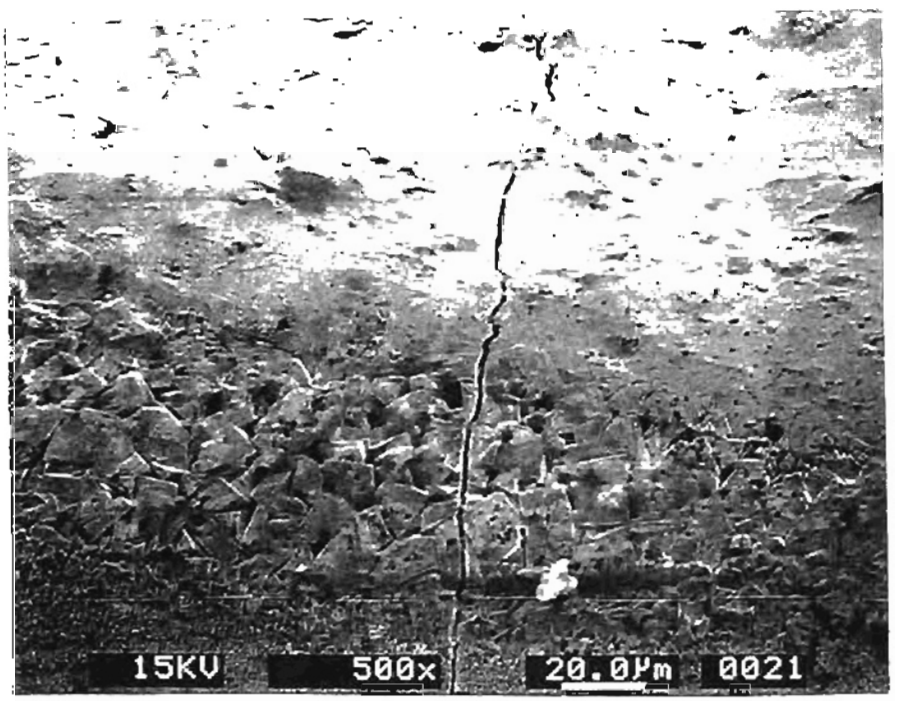

Figure 7.3.2.4 SEM Micrograph Showing Thermal Cracking in Cemented WC (6% Cobalt) at High Power in the Recast Layer

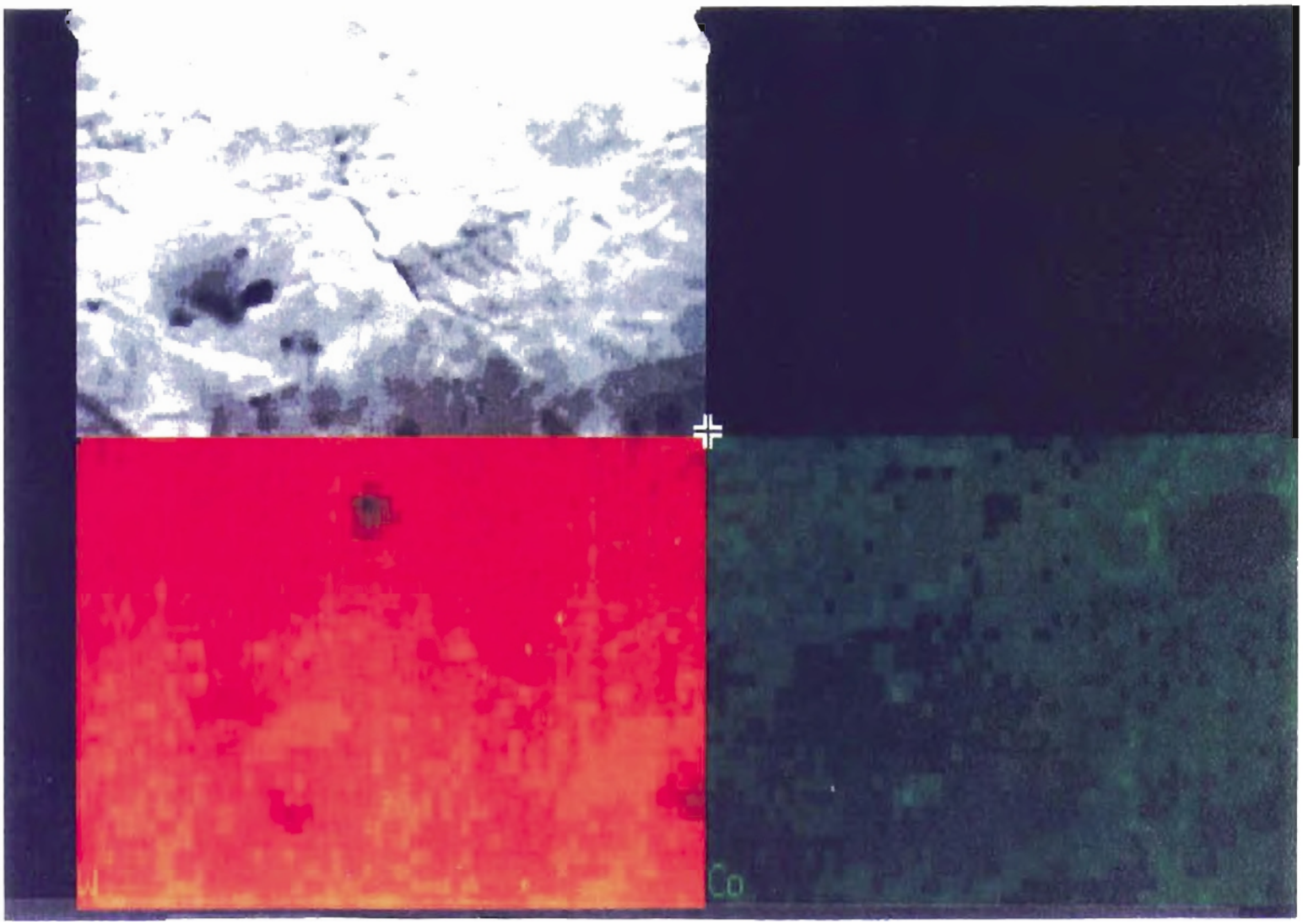

Figure 7.3.2.5 EDXA Map of the Laser Drilled Hole in Cemented WC (6% Cobalt) Revealing Major Amounts of W in the Molten Layer

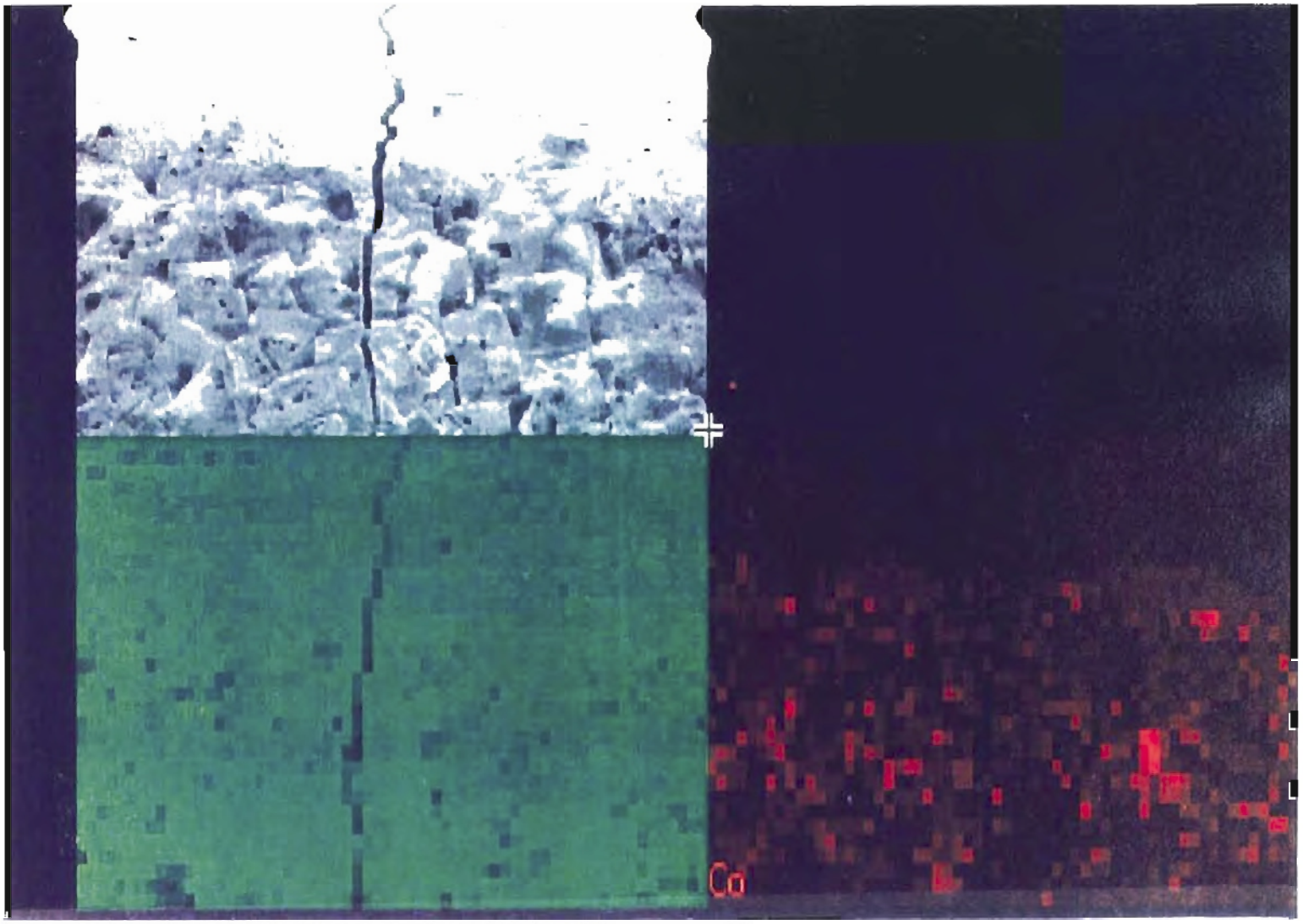

Figure7.3.2.6 EDXA Map of the Heat Affected Zone in Cemented WC (6 % Cobalt) Indicating the Presence of Cobalt and W

7.3.3 SiAlON

Figure 7.3.3.1 is a SEM micrograph of the hole profiles at different powers. From the micrograph it can be observed that high aspect ratios are obtained. Figure 7.3.3.2 gives the hole characteristics for SiAlON at different laser powers. Hole diameter at the hole entrance is constant at roughly 0.5 mm at all power levels. Hole depth of approximately 7.5 mm was observed at 7 W beam power. Figures 7.3.3.3 and 7.3.3.4 show the micrographs of the cross-section of the holes at low (0.87 W) and high (7 W) power respectively. Thermal cracks are observed at both powers. It can also be observed that the amount of recast layer increases with increase in power. Thermal cracks seem to propagate radially as compared to the axial crack propagation in cemented carbides.

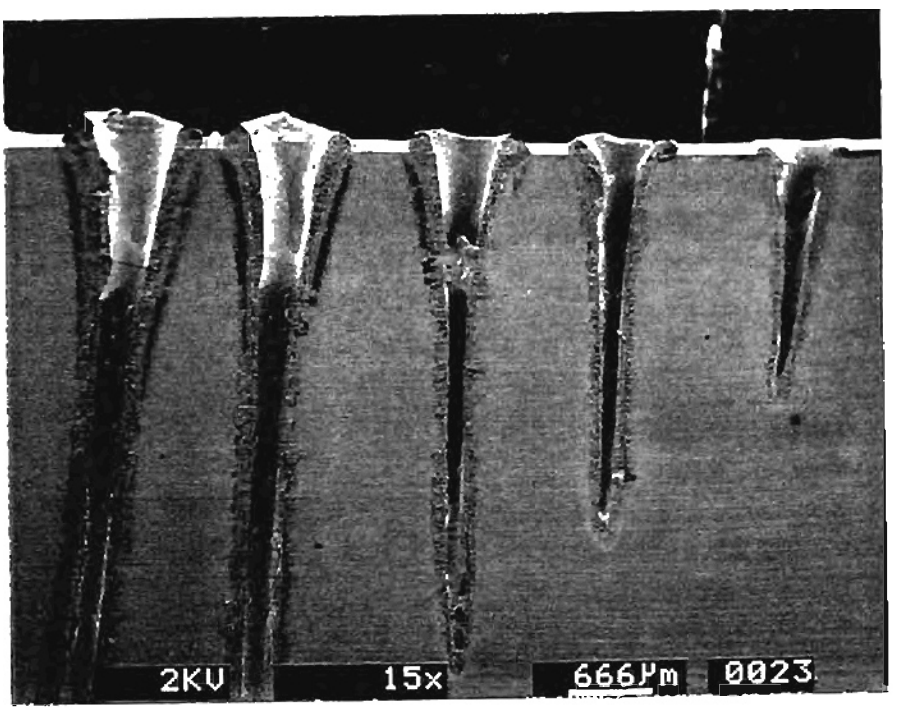

Figure 7.3.3.1 SEM Micrograph Showing the Hole Profiles in SiAlON at Different Beam Powers

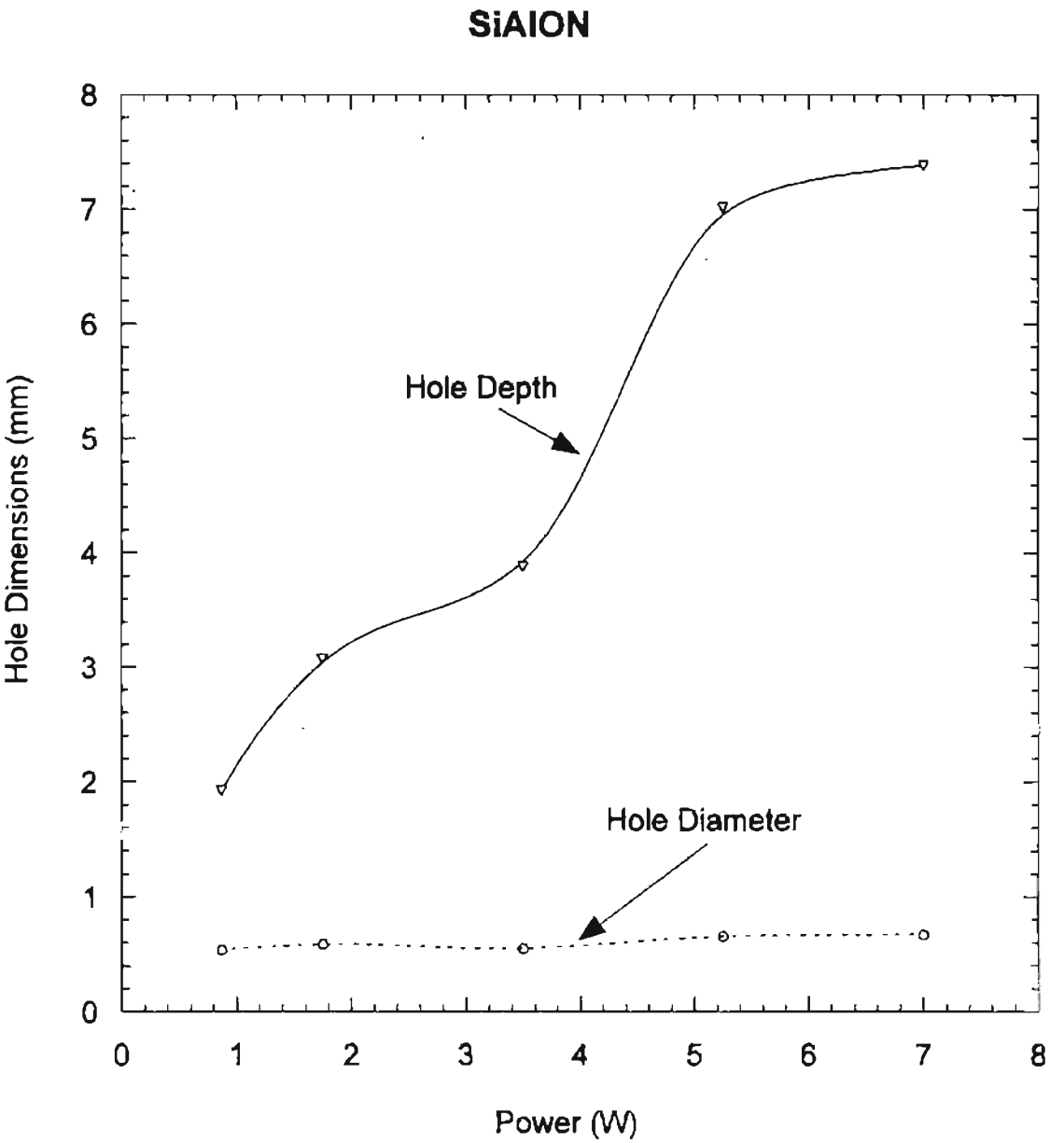

Figure 7.3.3.2 Plot Showing Hole Dimensions Vs Laser Power for SiAlON

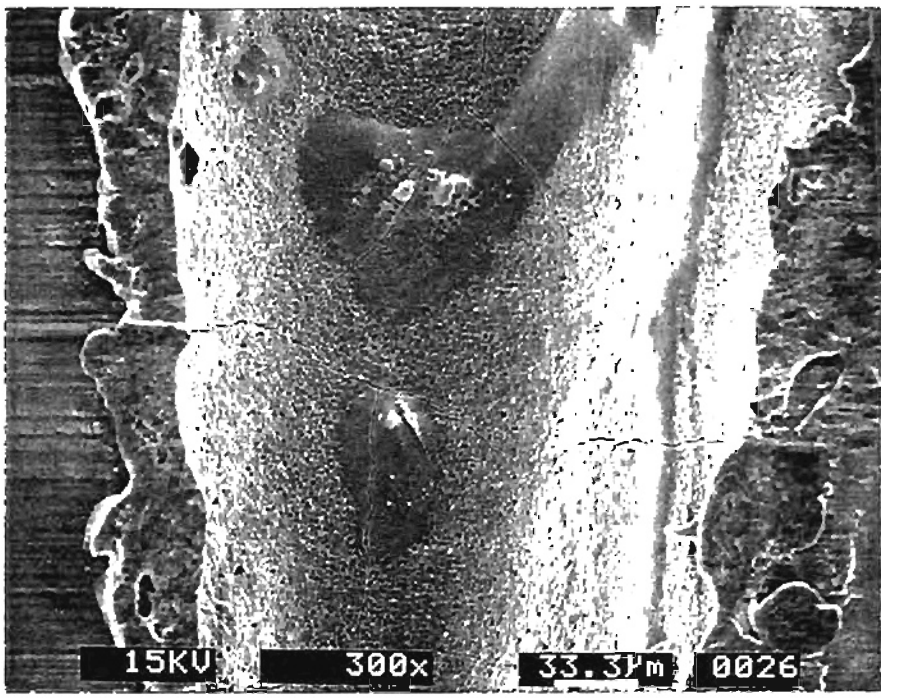

Figure 7.3.3.4 SEM Micrograph ShowingThermal Cracking in SiAlON at Low Power

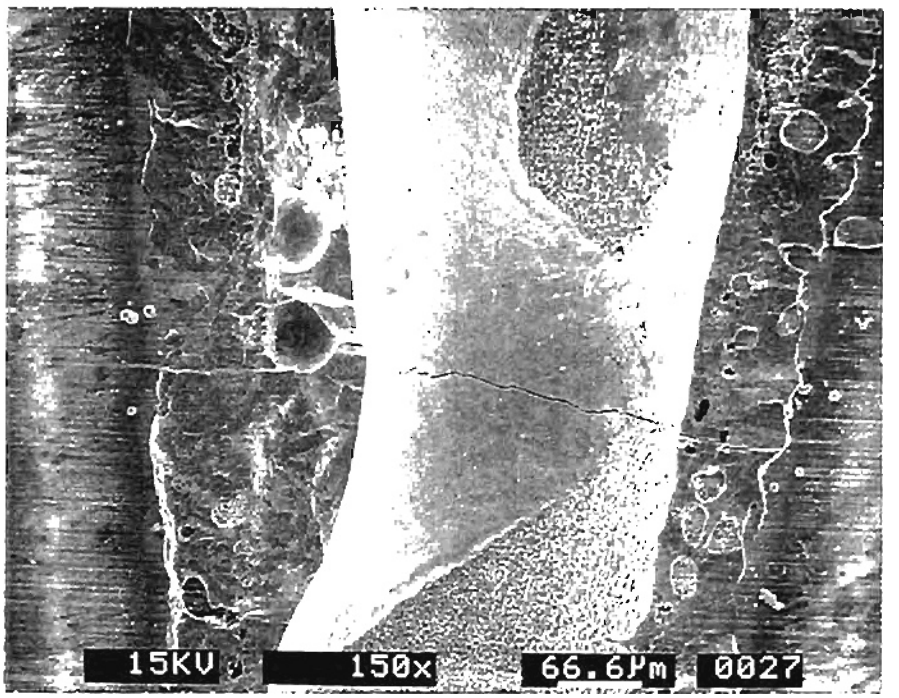

Figure 7.3.3.5 SEM Micrograph Showing Thermal Cracking in SiAlON at High Power

7.3.4 Aluminum Oxide

At high power levels aluminum oxide tends to shatter. Hence, drilling tests were restricted to power levels below 1 W. The SEM micrograph of the hole profiles at different powers is shown in Figure 7.3.4.1. The figure clearly shows the fractured surface at the hole entrance. Figure 7.3.4.2 is the plot of the relation between the hole dimensions and beam power. Hole diameter is essentially constant at ~ 0.5 mm at all power levels. Figures 7.3.4.3 and 7.3.4.4 are the micrographs of the hole cross-section at low and high power respectively. Thermal cracking is observed at all power levels. Recast layer has also been observed at the hole entrance.

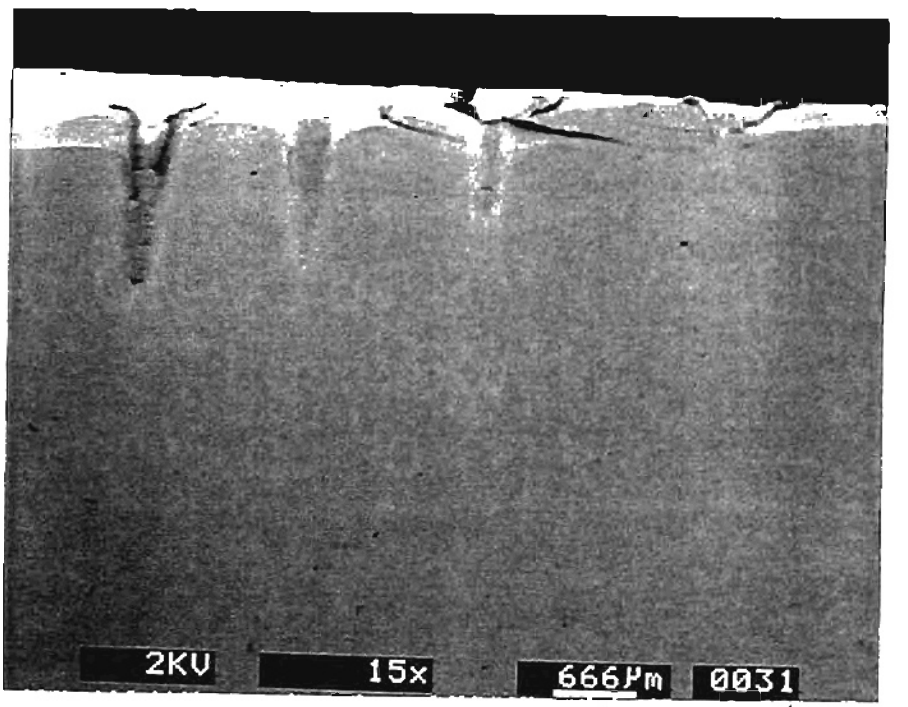

Figure 7.3.4.1 SEM Micrograph Showing the Hole Profiles in Al_2O_3 at Different Beam Powers

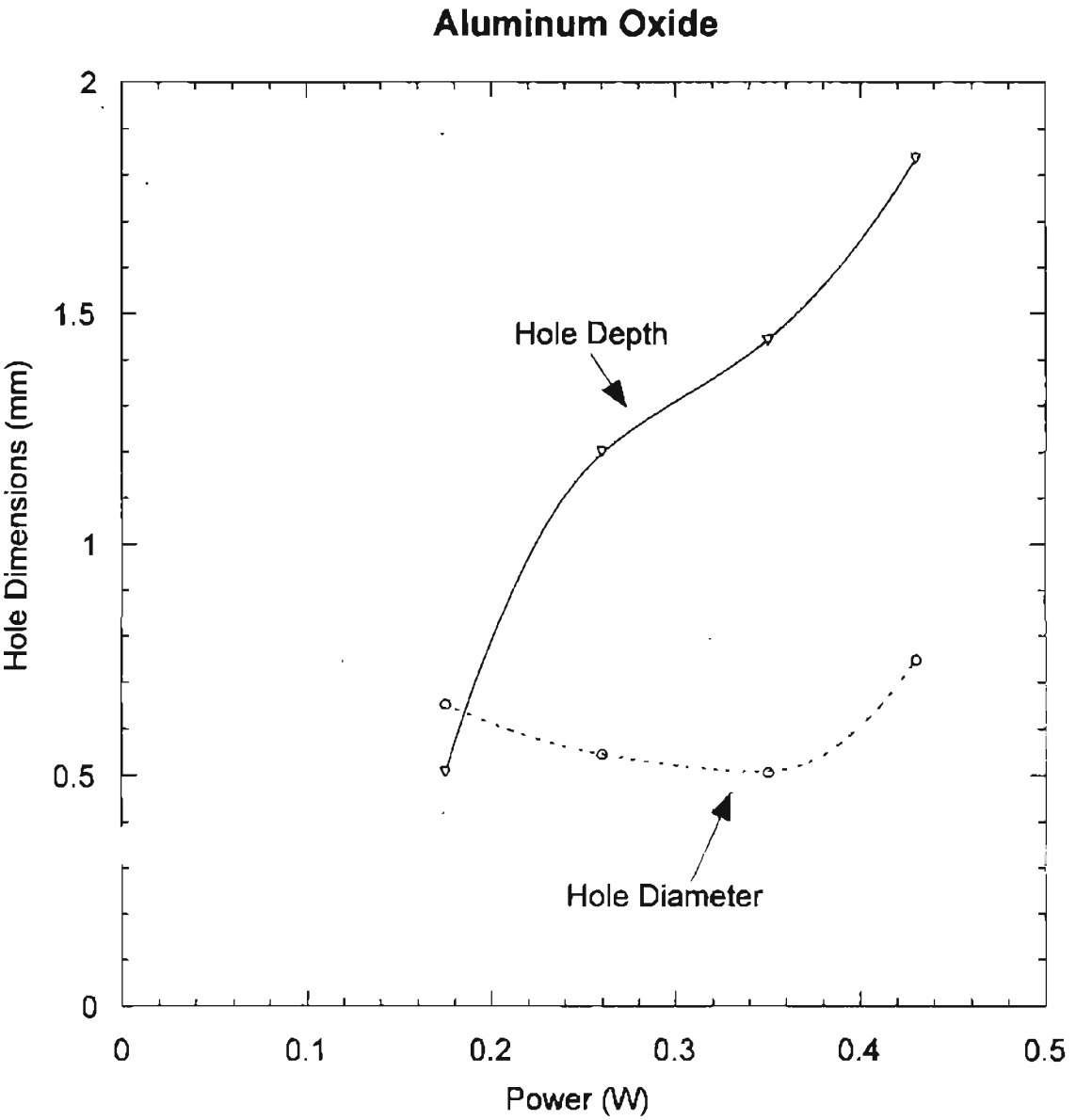

Figure 7.3.4.2 Plot Showing Hole Dimensions Vs Laser Power for Al_2O_3

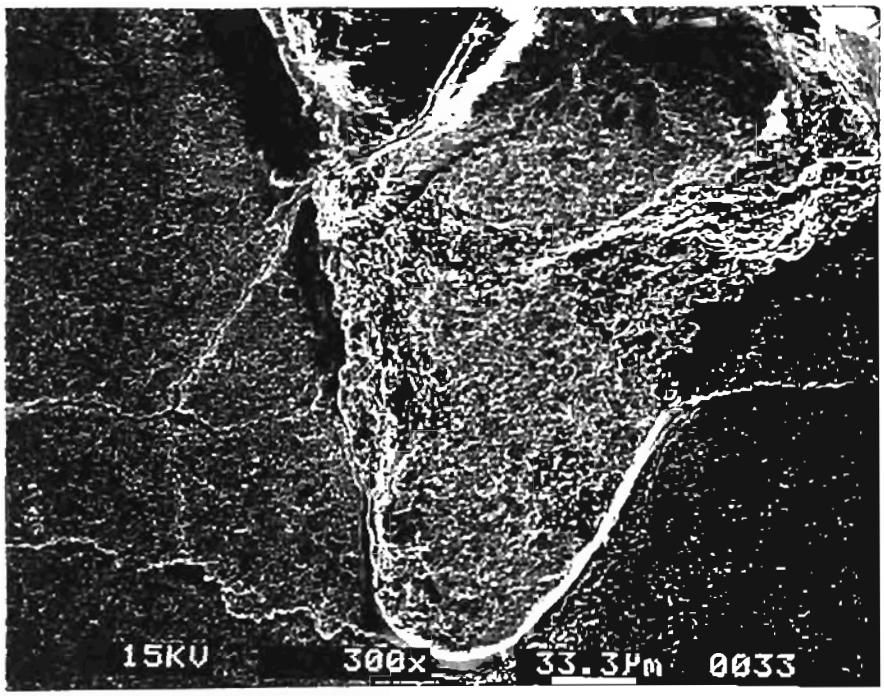

Figure 7.3.4.3 SEM Micrograph Showing Thermal Cracking in Al_2O_3 at Low power

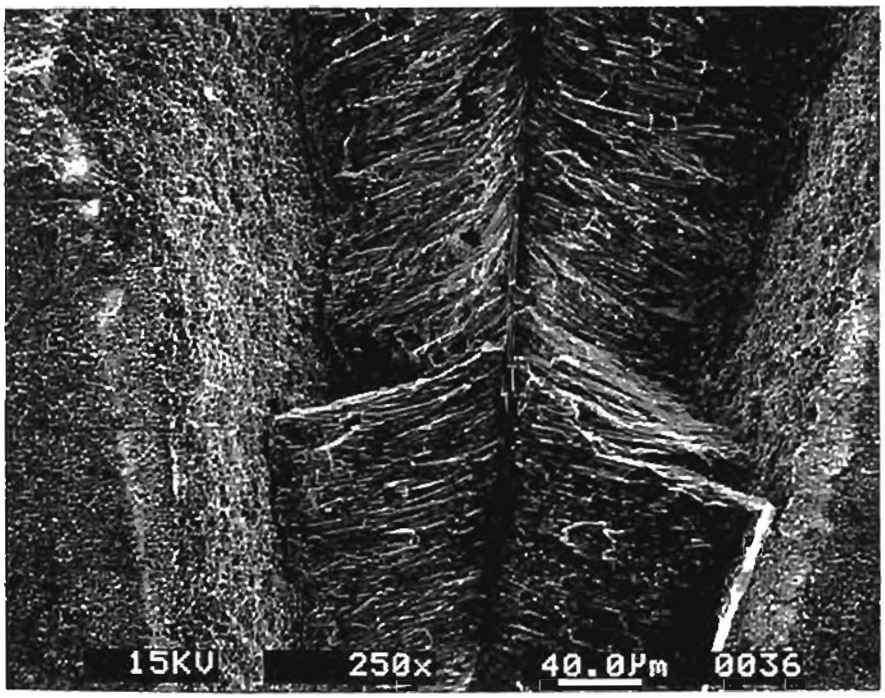

Figure 7.3.4.4 SEM Micrograph Showing Thermal Cracking in Al_2O_3 at High power

7.3.5 Multi layer (Al_2O_3 + TiC + TiCN) coated cemented WC tool

Figure 7.3.5.1 is the micrograph showing the hole profiles at different powers. Figure 7.3.5.2 is the plot showing hole dimensions at different laser powers. The hole diameter at the entrance remains constant at 0.1 mm at all power levels. Hole depth is found to remain constant at low power levels but increases linearly over 4 W power. Figures 7.3.5.3 and 7.3.5.4 are the micrographs of the cross-section of the holes at low and high power respectively. No thermal cracking was observed in the specimen surface at low power level. However, thermal cracking and recast layer was observed at 7 W power. The crack seems to have propagated axially in this case. Laser heating might be causing a change in the microstructure of the specimen.

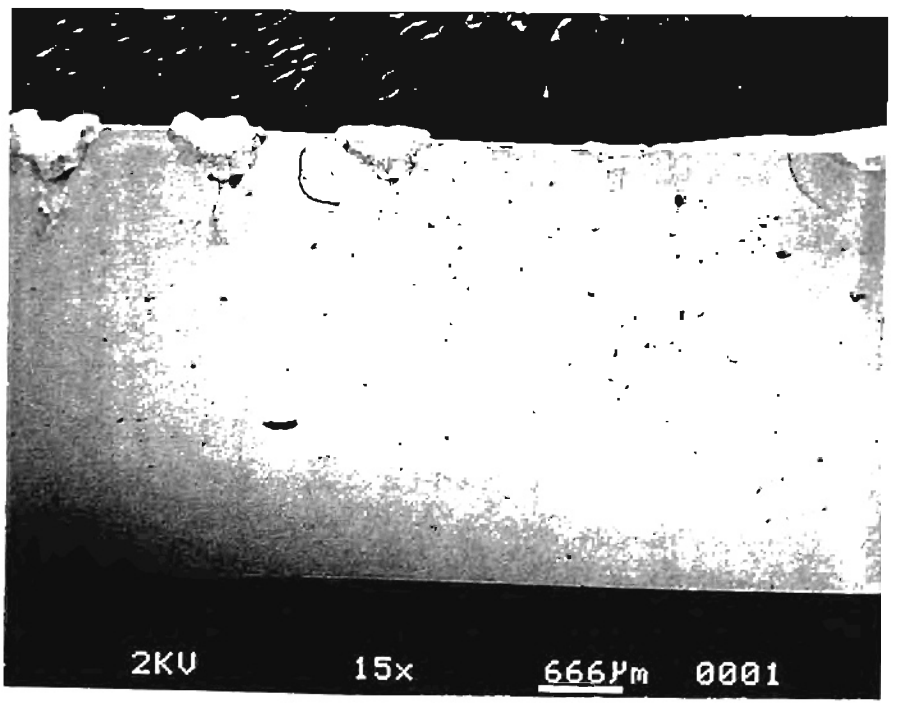

Figure 7.3.5.1 SEM Micrograph Showing the Hole Profiles in Multi Coated Tool at Different Beam Powers

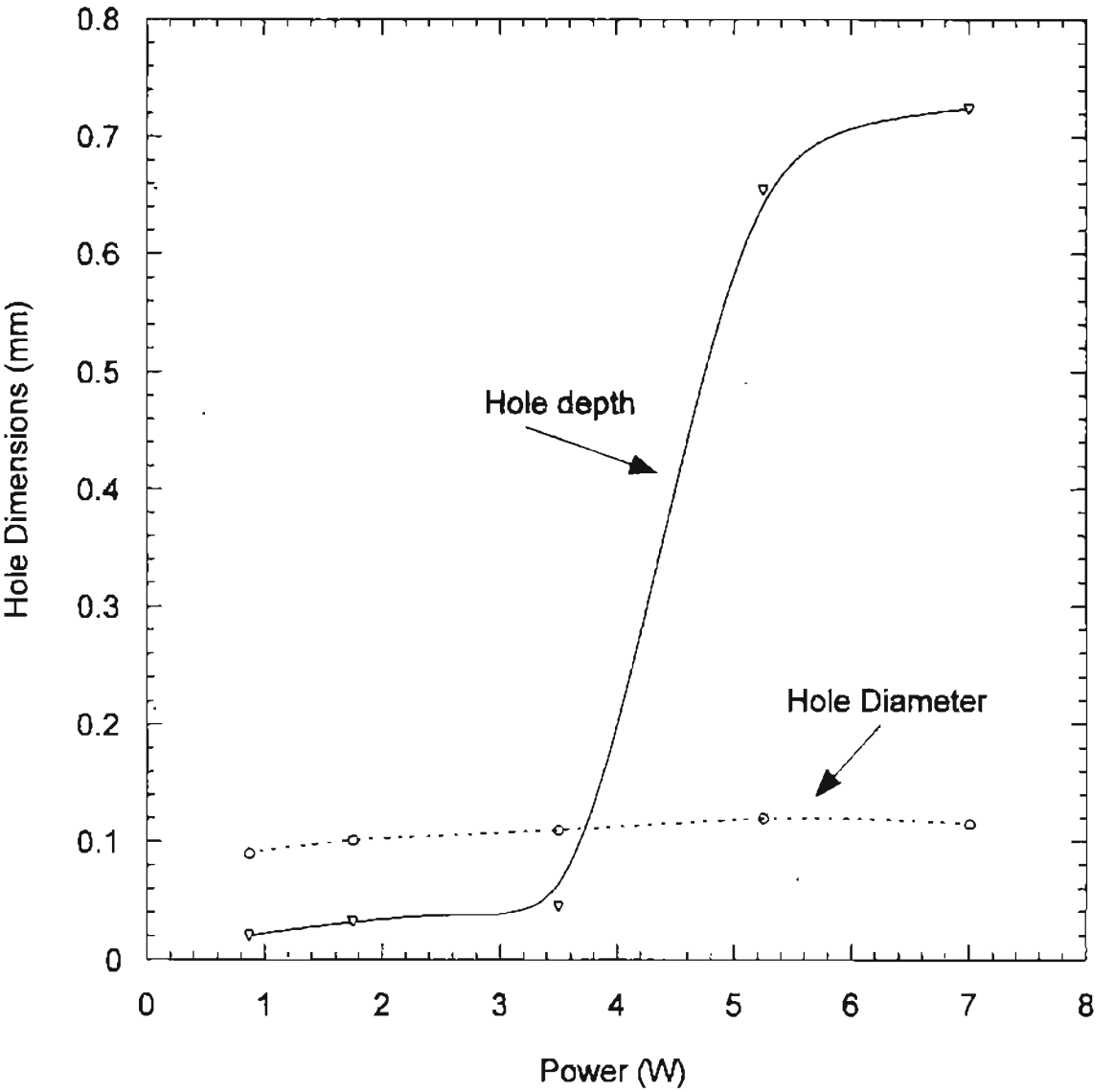

Figure 7.3.5.2 Plot Showing Hole Dimensions Vs Laser Power for Multi Coated Tool

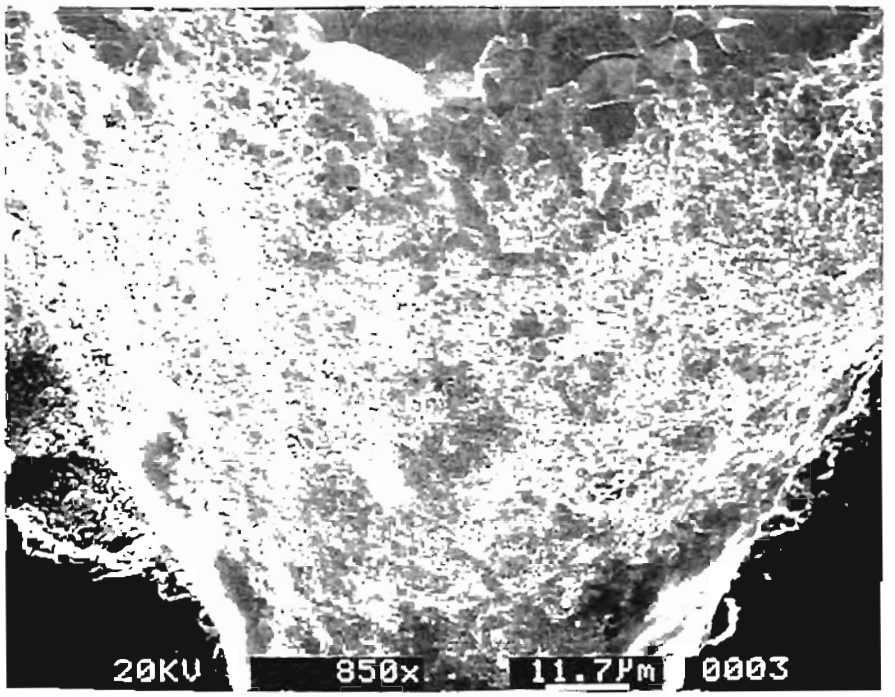

Figure 7.3.5.3 SEM Micrograph Showing no Thermal Cracks at Low Power

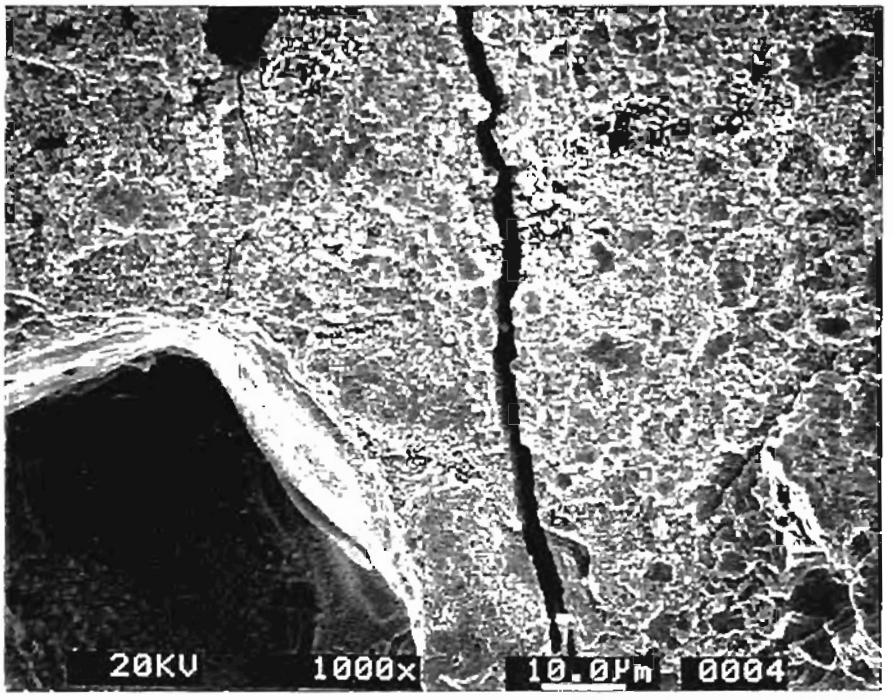

Figure 7.3.5.4 SEM Micrograph Showing Thermal Cracks at High Power

7.3.6 Silicon nitride

Figure 7.3.6.1 shows the variation of the hole dimensions with beam power for silicon nitride. It can be seen that the entrance hole diameter of ~ 0.5 mm is observed at all power levels. Hole depth was found to increase linearly with beam power. As seen from Figure 7.3.6.2, high aspect ratios are observed at power levels over 4 W. Figure 7.3.6.3 shows the cross-section of the laser drilled hole in silicon nitride. It reveals β-silicon nitride surrounded by the glassy phase of magnesium oxide. On laser irradiation, Si_3N_4 evaporates and decomposes above 1900°C (Solomah, 1991). It can be seen from Figures 7.3.6.4 and 7.3.6.5 that liquid silicon interacts with the molten oxides of the glassy phase, leading to the formation of compounds of silicon oxide. After the action of the laser pulse, the melt solidifies rapidly by quenching, leading to dendritic crystallization, as seen in Figure 7.3.6.6. It can be seen from Figure 7.3.6.7 that crack formation is observed at all power levels induced by tensile stresses due to thermal contraction during cooling. The cracks seem to propagate radially, similar to those in SiAlON.

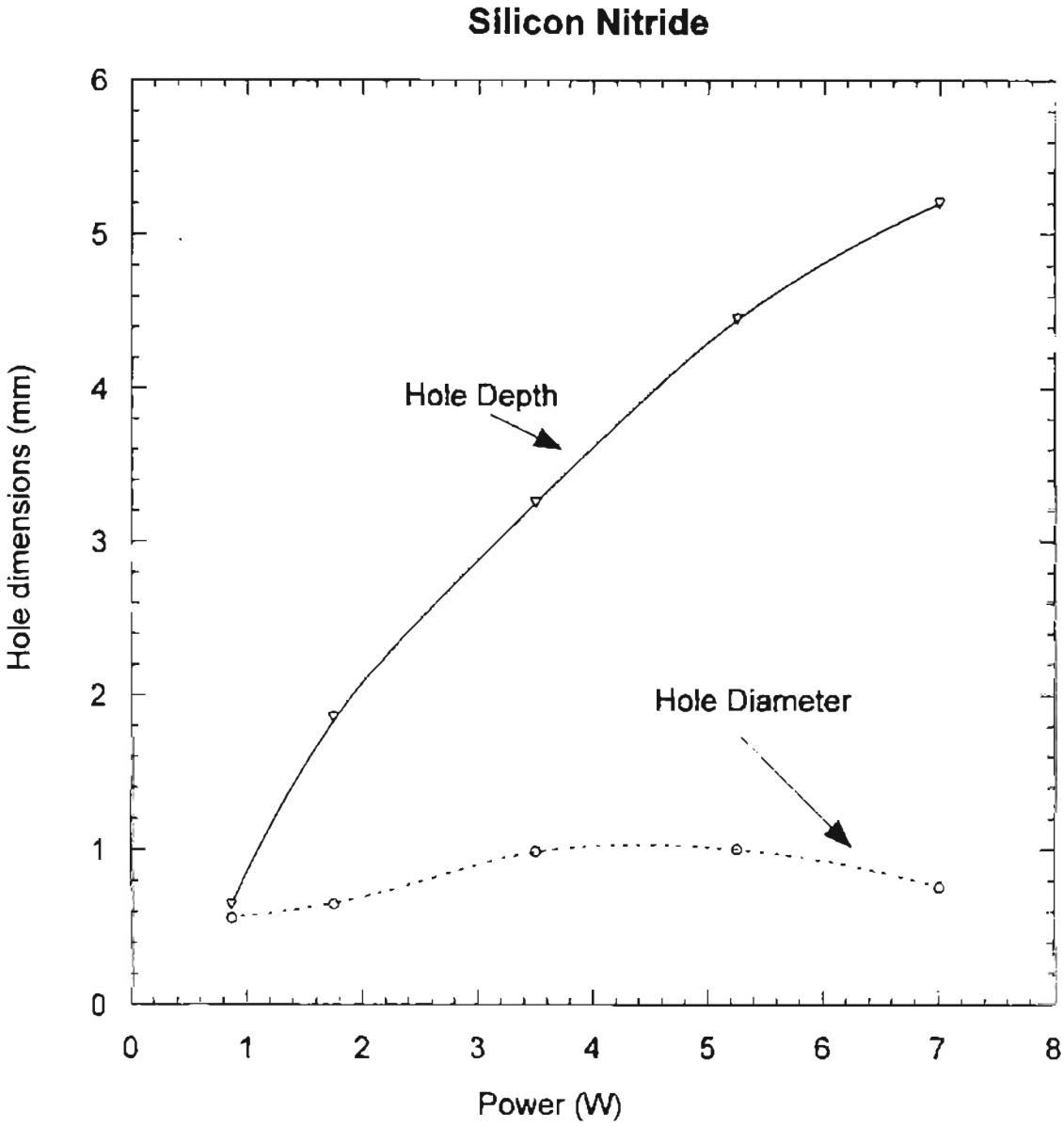

Figure 7.3.6.1 Plot Showing Hole Dimensions Vs Laser Power for Si_3N_4

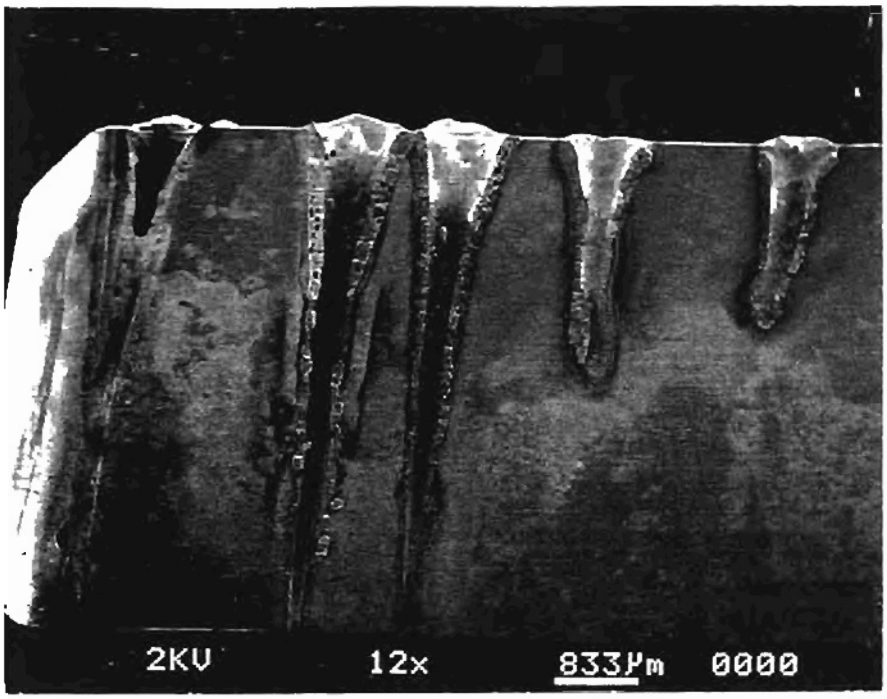

Figure 7.3.6.2 SEM Micrograph Showing the Hole Profiles in Silicon Nitride

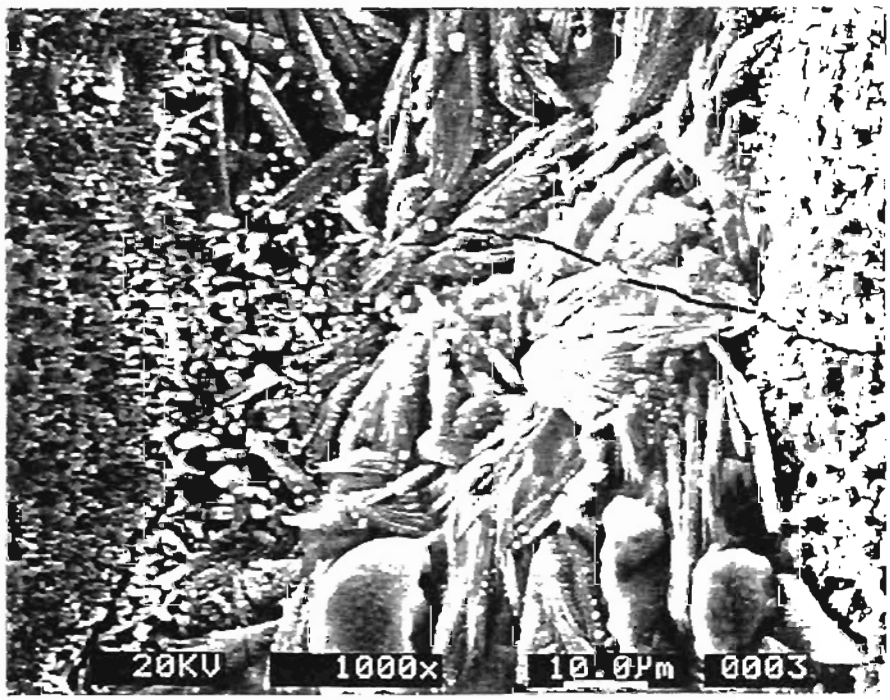

Figure 7.3.6.3 SEM Micrograph Revealing β-Si_3N_4 surrounded by Glassy Phase

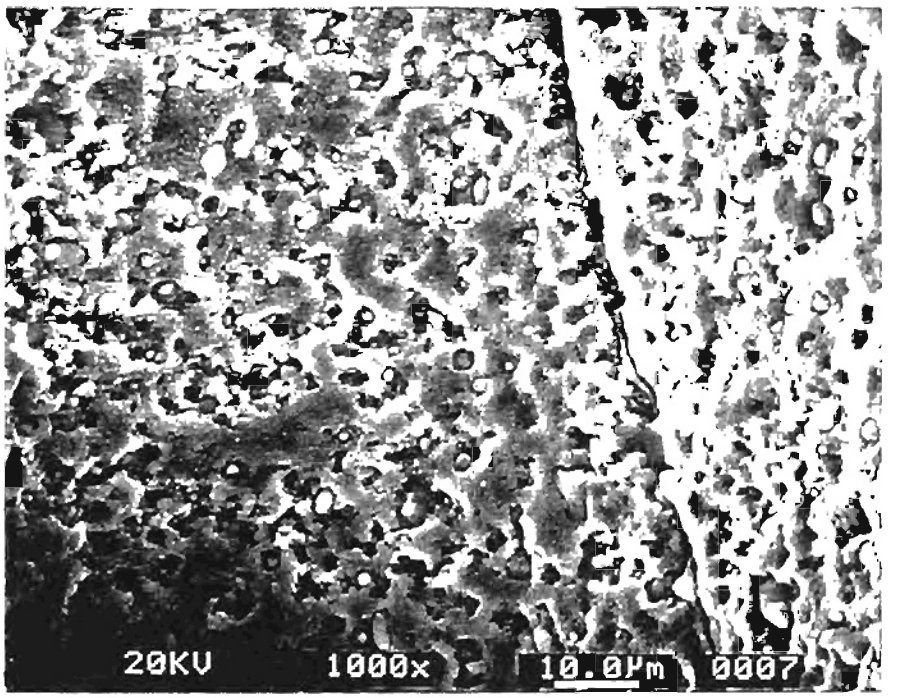

Figure 7.3.6.4 SEM Micrograph Showing Molten Silicon

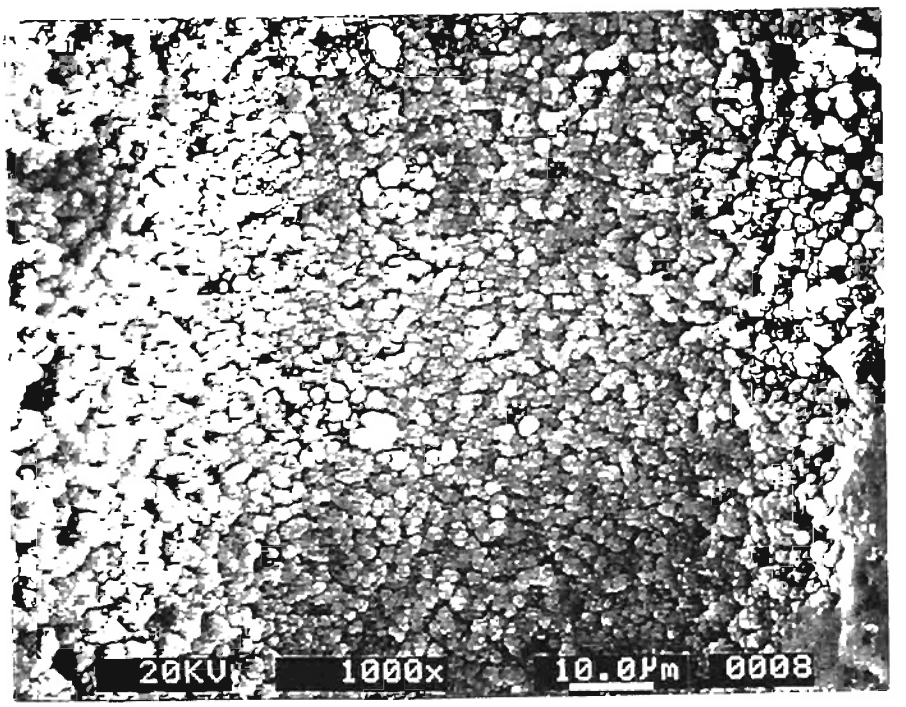

Figure 7.3.6.5 SEM Micrograph Showing Molten Silicon Coalescing to Form Large Droplets

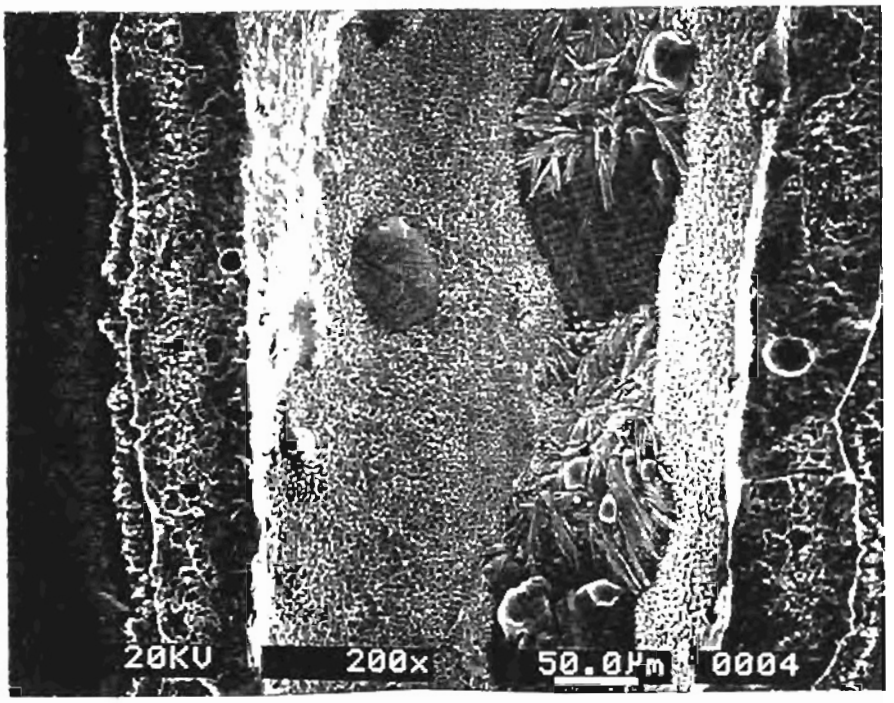

Figure 7.3.6.6 SEM Micrograph Showing Dendritic Structures in Silicon Nitride

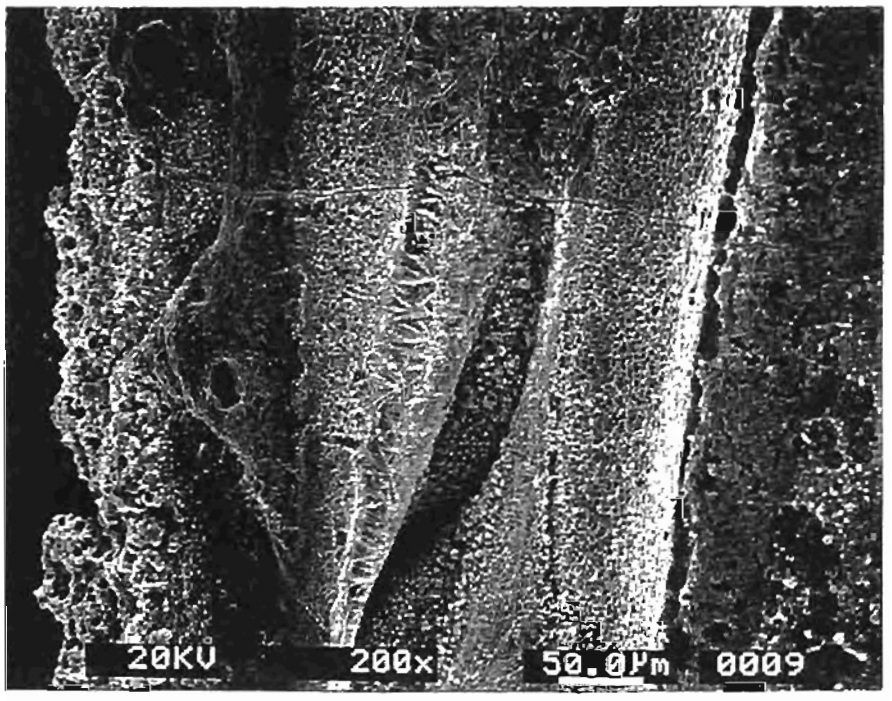

Figure 7.3.6.7 SEM Micrograph Showing Thermal Cracks in Silicon Nitride

7.4 Conclusions

The following conclusions can be drawn from the results.

- Silicon nitride and SiAlON have better hole profiles with larger aspect ratios due to their low thermal conductivity compared to cemented carbides having high thermal conductivity to the CO_2 laser beam.

- Cracking at the hole entrance observed in aluminum oxide can be attributed to low thermal conductivity (~ 5.8 W/m-K) at high temperature compared to Si_3N_4 and SiAlON (λ=10 W/m-K).

- Thermal cracking is observed in all specimen because of high thermal gradients observed in the laser ablation process.

- The amount of recast layer at the hole entrance increases with the beam power. The origin of the crack in the specimen seems to originate at the recast layer and propagate in the radial direction in the case of ceramics. However in the case of multi Al_2O_3 coated specimen and in cemented carbides, the crack propagates in the axial direction.

- Hole diameter at the entrance is essentially constant at approximately 0.5 mm in all the specimen. Hole depth increases linearly with beam power.

CHAPTER 8

THERMAL ANALYSIS OF LASER DRILLING

8.1 Introduction

Heat flow in the material has been treated in the past for the case of electromagnetic radiation from a high intensity source impinging on and being absorbed by a surface, and effecting a phase transformation within the surface layer (Gagliano et al., 1972). Solutions to this problem are given as temperature profiles for a one-dimensional heat conduction model. In the present work, a three-dimensional model has been developed which gives the temperature profile and shape of the drilled hole resulting from the absorption of high intensity radiation. This model can be applied for any material and for any type of laser.

As shown in Figure 8.1, a focused beam is used for the hole drilling process in an isotropic material. The focused beam is considered as a continuous, distributed and moving heat source in the beam axis (Z) direction. During laser drilling, a very large amount of energy is transferred to the material during a single pulse. The amount of energy in a single pulse can range between 1 mJ to even 100 J, with pulse duration ranging between 1 - 100 ms. Since ceramics are hard and brittle with low thermal conductivity, they tend to fracture because of the thermal stresses induced during the drilling process. Choice of proper drilling parameters is very critical for the processing of ceramics with a laser. Hence, one of the most significant contributions to be offered from the model is the

determination of the drilling parameters of a laser, which would enable crack free processing of ceramics.

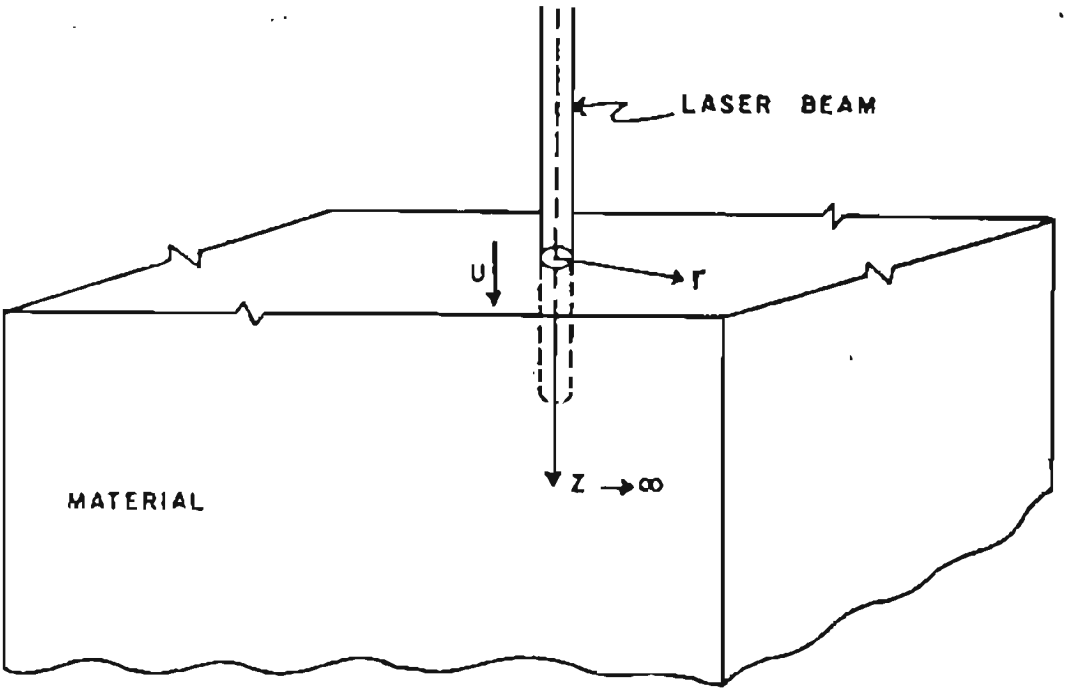

Figure 8.1 Physical Model of the Laser Drilling for a Semi-Infinite Body

8.2 Mathematical Model

The following assumptions were made in the development of a thermal model for a semi-infinite body:

- The thermal and mechanical properties of the work material are independent of temperature and remain constant during the laser drilling process
- There are no heat losses through the bounding surface
- Reflection losses are neglected so that the total power of the laser output is absorbed by the material.
- Effect of latent heat is not considered.
- It is assumed that only the vaporized material is removed during the drilling process. Ejection of material in molten state is not considered. Heat loss due to removal of material in vaporized state is not considered.
- Uniform energy distribution is assumed after the formation of plasma during the drilling process.
- The velocity of the heat source is assumed constant.

The model developed is based on the moving heat source theory. Hence, the velocity of the heat source should be known or assumed to determine the temperature field in the material. In the present analysis, this velocity is initially assumed to determine the temperature profile and the penetration depth for a given pulse duration. The theoretical velocity is then obtained by differentiating the depth of penetration z with respect to the time t. The assumed velocity is matched to the theoretical velocity, by iterations.

8.3 Temperature Distribution

As shown in Figure 8.1, the laser beam impinges on a circular area in the plane z=0, and its center is located at the origin O. With passage of time, the laser beam front, i.e., the heat source, moves down along the z-axis from the origin. This is an approximate physical description of the laser drilling process. The sequence of events that take place when a pulsed laser is used to drill a hole in alumina substrate has been determined using high speed photography (Gagliano et al., 1983) and are listed below as a proposed mechanism.

- Initial absorption of energy into the surface, which greatly increases the vibrational and electronic energy contents of the molecular structure beyond their equilibrium values.
- Subsurface (50-500 Å) vaporization of the localized areas.
- Explosive expansion of these areas with subsequent removal of particulate matter.
- Rapid rise of temperature with heating to melting and vaporization of adjacent areas within the focused beam spot.
- Steps 2, 3, and 4 may be repeated several times for the duration of the laser pulse.

In the present model the material is considered to be a half space, and its bounding plane is assumed to be insulated i.e.

$$\partial T/\partial z = 0 \text{ at } z = 0$$

This will have only one image of the moving heat source with respect to the bounding plane. The source is located at $z' = f'(t)$ along the z-axis and its

image is at z' = - f(t), which moves in the opposite direction to the heat source.

The moving heat source for laser drilling in the present model is considered to comprise of two parts:

a) A moving disc heat source with variable intensity.
b) A continuous cylindrical heat source with variable length and variable intensity.

The temperature rise at any point due to the laser is the sum of the temperature rise due to the above two heat sources.

8.3.1 Temperature rise due to a moving disk source with variable intensity:

Solution to the instantaneous ring heat source is given by (Jaeger, 1942) :

$$\theta_m = \frac{Q_{rg}}{c\rho(4\pi a\tau)^{3/2}} \cdot \exp\left(\frac{-(r_i^2 + r^2 + z^2)}{4a\tau}\right) \cdot I_0\left(\frac{rr_i}{2a\tau}\right)$$

where,

θ_m = Temperature rise at any point M (x,y,z) in the Cartesian coordinate system

Q_{rg} = Heat liberated by a ring heat source at time t

c = Specific heat

ρ = Density of the material

$r = \sqrt{x^2 + y^2}$

r_i = Beam radius

a = Thermal diffusivity

I_0 = Modified Bessel function of the first kind and zeroth order

A moving ring heat source continuously liberates heat q_{rg} (cal/sec) and moves along z-axis with velocity v (cm/sec) (Figure 8.3.1.1).

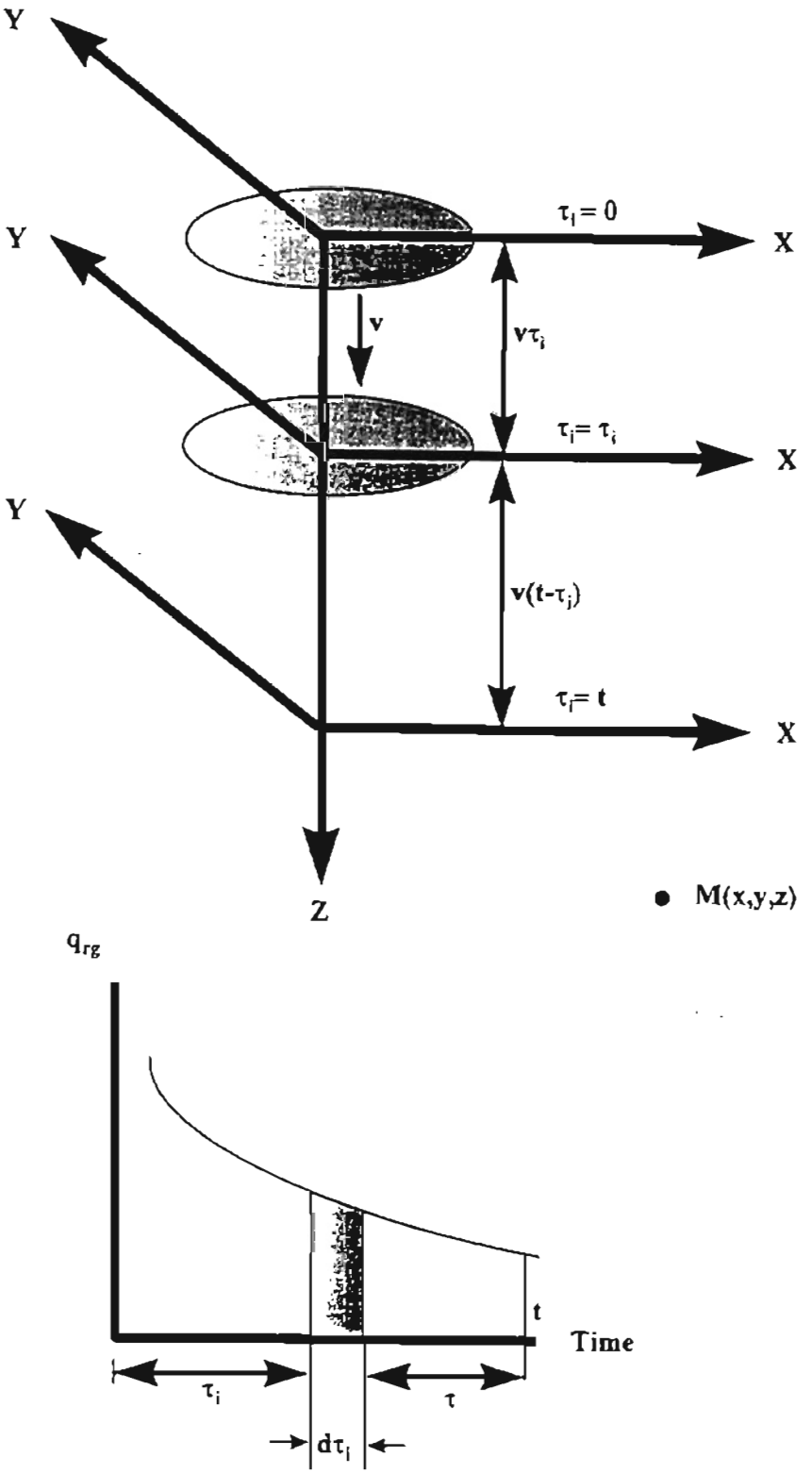

Figure 8.3.1.1 Moving Ring Heat Source With Variable Intensity

The total time interval from $\tau_i = 0$ (the moment when the heat source begins to work) to $\tau_i = t$ can be considered as a combination of a series of infinitesimal time intervals, $d\tau_i$. In this time interval, the amount of heat liberated by the heat source is $q_{rg} \cdot d\tau_i$ cal. This amount of heat can be considered as liberated instantaneously. The heat liberated in the small time interval $d\tau_i$ at moment τ_i will cause a certain temperature rise at point M at time t, given

by:

$$d\theta_m = \frac{Q_{rg} d\tau_i}{c\rho(4\pi a\tau)^{3/2}} \cdot \exp\left(\frac{-(r_i^2 + r^2 + (z - v\tau_i)^2}{4a\tau}\right) \cdot I_0\left(\frac{rr_i}{2a\tau}\right)$$

where,

$$Q_{rg} = \frac{2\pi W r_i dr_i}{\pi r_0 (2v\tau_i + r_0)}$$

The total temperature rise at point M at time t, caused by the ring heat source from $\tau_i = 0$, to $\tau_i = t$ is :

$$d\theta_m = \frac{2 W r_i dr_i}{c\rho(4\pi a)^{3/2} r_0} \int_0^t \frac{d\tau_i}{\tau^{3/2} (2v\tau_i + r_0)} \cdot \exp\left(\frac{-(r_i^2 + r^2 + (z - v\tau_i)^2}{4a\tau}\right) \cdot I_0\left(\frac{rr_i}{2a\tau}\right)$$

With some substitutions

$$\tau_i = t - \tau ; \qquad d\tau_i = -d\tau ; \qquad z - v\tau_i = z - vt + v\tau$$

when $\tau_i = 0$ $\tau = t$; when $\tau_i = t$ $\tau = 0$;

$$d\theta_m = \frac{2 W r_i dr_i}{c\rho(4\pi a)^{3/2} r_0} \int_0^t \frac{d\tau}{\tau^{3/2} (2vt - 2v\tau + r_0)} \cdot I_0\left(\frac{rr_i}{2at}\right)$$

$$\cdot \exp\left(\frac{-(r_i^2 + r^2 + (z - vt + v\tau)^2}{4a\tau}\right)$$

Moving disc heat source is a combination of a series of concentric moving ring heat sources with radii ranging from $r_i = 0$ to $r_i = r_0$. Thus the

temperature rise at any point M(x,y,z) due to a moving disc heat source moving in the z-direction is given by:

$$\theta_m = \frac{2W}{c\rho(4\pi a)^{3/2} r_0} \int_0^{r_0} r_i \, dr_i \int_0^t \frac{d\tau}{\tau^{3/2}(2vt - 2v\tau + r_0)} \cdot I_0\left(\frac{rr_i}{2at}\right)$$

$$\cdot \exp\left(\frac{-(r_i^2 + r^2 + (z - vt + v\tau)^2}{4a\tau}\right)$$

The total temperature rise at a point M due to the original heat source and the image source is :

$$\theta_m = \frac{2W}{c\rho(4\pi a)^{3/2} r_0} \int_0^{r_0} r_i \, dr_i \int_0^t \frac{d\tau}{\tau^{3/2}(2vt - 2v\tau + r_0)} \cdot I_0\left(\frac{rr_i}{2at}\right)$$

$$\cdot \left(\exp\left(\frac{-(r_i^2 + r^2 + (z - vt + v\tau)^2}{4a\tau}\right) + \exp\left(\frac{-(r_i^2 + r^2 + (z + vt - v\tau)^2}{4a\tau}\right)\right) \quad \text{Eq (1)}$$

8.3.2 Temperature rise due to a cylindrical heat source with variable length and variable intensity:

Heat liberated per unit surface area by a barrel heat source is given by:

$$q_{br} = \frac{W}{2\pi r_0 v(t_{oi} + \tau_i) + \pi r_0^2}$$

where,

t_{oi} = time at which the barrel heat source is initiated

(Ref Figure 8.3.2.1).

In the time interval $d\tau_i$, the amount of heat liberated by the heat source is $q_{rg} \cdot d\tau_i$ cal.

where,

$$q_{rg} = \frac{2W}{2v(t_{oi} + \tau_i) + r_0} \bullet dL_i$$

$$L_i = v \bullet t_{oi}$$

and

$$\theta_{rg} = q_{rg} \bullet d\tau_i = \frac{2W}{(2v(t_{oi} + \tau_i) + r_o)} \bullet dL_i \bullet d\tau_i$$

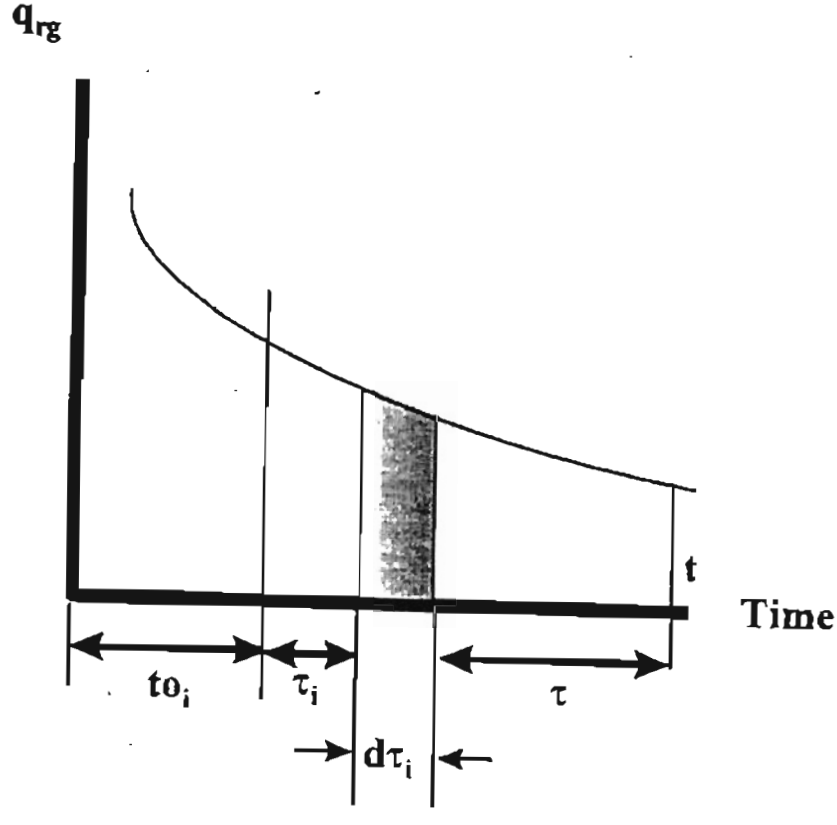

Figure 8.3.2.1 Moving Cylindrical Heat Source With Variable Intensity

The heat liberated in the small time interval $d\tau_i$ at moment τ_i will cause a certain temperature rise at point M at time t, given by:

$$d\theta_m = \frac{2W}{c\rho\,(4\pi a)^{3/2}\,\tau^{3/2}(2v(t_{oi} + \tau_i) + r_o)} \bullet dL_i \bullet d\tau_i \bullet I_0\left(\frac{rr_0}{2a\tau}\right)$$

$$\bullet \exp\left(-\left(\frac{r_0^2 + r^2 + (z - L_i)^2}{4a\tau}\right)\right)$$

Moving cylindrical heat source is a combination of a series of cylinders with radius r_0 and length varying from $L_i = o$ to $L_i = vt$. Thus the temperature rise at any point M(x,y,z) due to a moving disc heat source moving in the z-direction is given by:

$$\theta_m = \frac{2W}{c\rho\,(4\pi a)^{3/2}} \int_0^{vt} dL_i \int_0^{t-t_{oi}} \frac{d\tau_i}{\tau^{3/2}(2v(t_{oi} + \tau_i) + r_o)} \bullet I_0\left(\frac{rr_0}{2a\tau}\right)$$

$$\bullet \exp\left(-\left(\frac{r_0^2 + r^2 + (z - L_i)^2}{4a\tau}\right)\right)$$

The temperature rise at any point M(x,y,z) due to a continuous cylindrical heat source with variable length and variable intensity in a body of semi-infinite dimensions is given by:

$$\theta_m = \frac{2W}{c\rho\,(4\pi a)^{3/2}} \int_0^{vt} dL_i \int_0^{t-t_{oi}} \frac{d\tau_i}{\tau^{3/2}(2v(t_{oi} + \tau_i) + r_o)} \bullet I_0\left(\frac{rr_0}{2a\tau}\right)$$

$$\bullet \left(\exp\left(-\left(\frac{r_0^2 + r^2 + (z - L_i)^2}{4a\tau}\right)\right) + \exp\left(-\left(\frac{r_0^2 + r^2 + (z + L_i)^2}{4a\tau}\right)\right)\right) \qquad \text{Eq (2)}$$

The total temperature rise at any point M(x,y,z) is due to the moving disc heat source with variable intensity and the continuous cylindrical heat

source with variable length and variable intensity given by the sum of the Eqs (1) and (2).

The equation for the temperature rise was solved by numerical integration using Simpson's rule. A code was developed in C language for the same. For the convenience of further mathematical derivations for the moving heat source problem, the function $I_o(p)$ was approximated as follows (Hou and Komanduri, 1997) :

when $p > 0$ and $p < 1.6$	$I_o(p) \approx 0.935\, e^{0.352\, p}$	(with error < 6.5 %)
when $p \geq 1.6$ and $p \leq 3$	$I_o(p) \approx 0.5293\, e^{0.7348\, p}$	(with error < 1.7 %)
when $p > 3$	$I_o(p) \approx e^{p} / (2\pi p)^{0.5}$	(with error < 5 %)

8.4 Results and Discussion

Theoretical results were computed for the case of laser drilling on hot pressed silicon nitride workpiece. The thermal properties of Si_3N_4 used for the theoretical calculations are given in Table 8.4.1.

Table 8.4.1 Thermal Properties of Si_3N_4 (Ziegler et al, 1987)

Vaporization Temperature	1900 ° C
Theoretical Density	3.19 g/cm^3
Thermal Conductivity	0.15 W/cm-K
Thermal Diffusivity	0.17 cm^2/sec

Temperature distribution was calculated as a function of the radial distance and depth from the center of the hole, for a given pulse duration.

One very practical result of this model is the ability to predict the profile of the laser drilled hole. This profile is determined using the isotherm at the vaporization temperature. Figure 8.4.1 shows the isotherms for different pulse durations for adiabatic boundary conditions. It can be seen that at the end of 0.1 sec the hole depth is 4.86 mm and the hole diameter is ~ 3.5 mm. Figure 8.4.2 shows the dimensions of the drilled hole obtained experimentally. The mismatch in the hole diameters can be attributed to the fact that the effect of molten material ejecting from the hole is not considered in the theoretical model. The recast layer also contributes to the decrease in the hole dimension at the inlet, the effect of which is not considered in the theoretical model.

To analyze the effect of boundary conditions on the hole dimensions, the calculations were repeated with a factor h = 0.1 and h = 0.01, multiplied to the exponential term of the image heat source. In the physical sense this would imply a convective boundary condition. As seen from Figures 8.4.3 and 8.4.4 this causes the hole diameter to come closer to the experimental value without affecting the dimensions of the hole depth. Thus more realistic value of hole dimensions could be obtained by selecting an appropriate value of this factor.

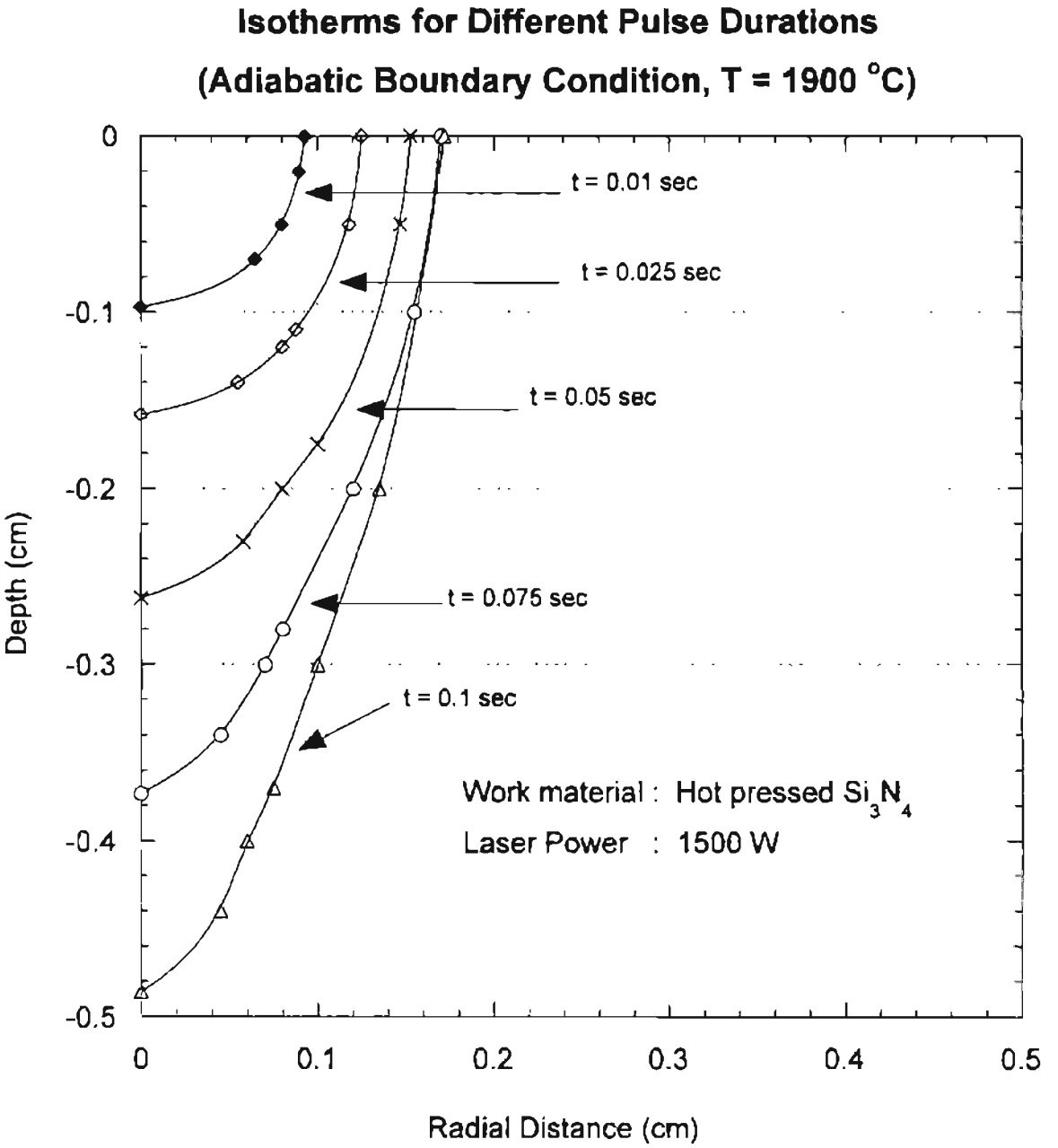

Figure 8.4.1 Isotherms for Different Pulse Durations

Dimensions of the experimentally drilled hole at 0.1sec pulse duration, 1500 W power

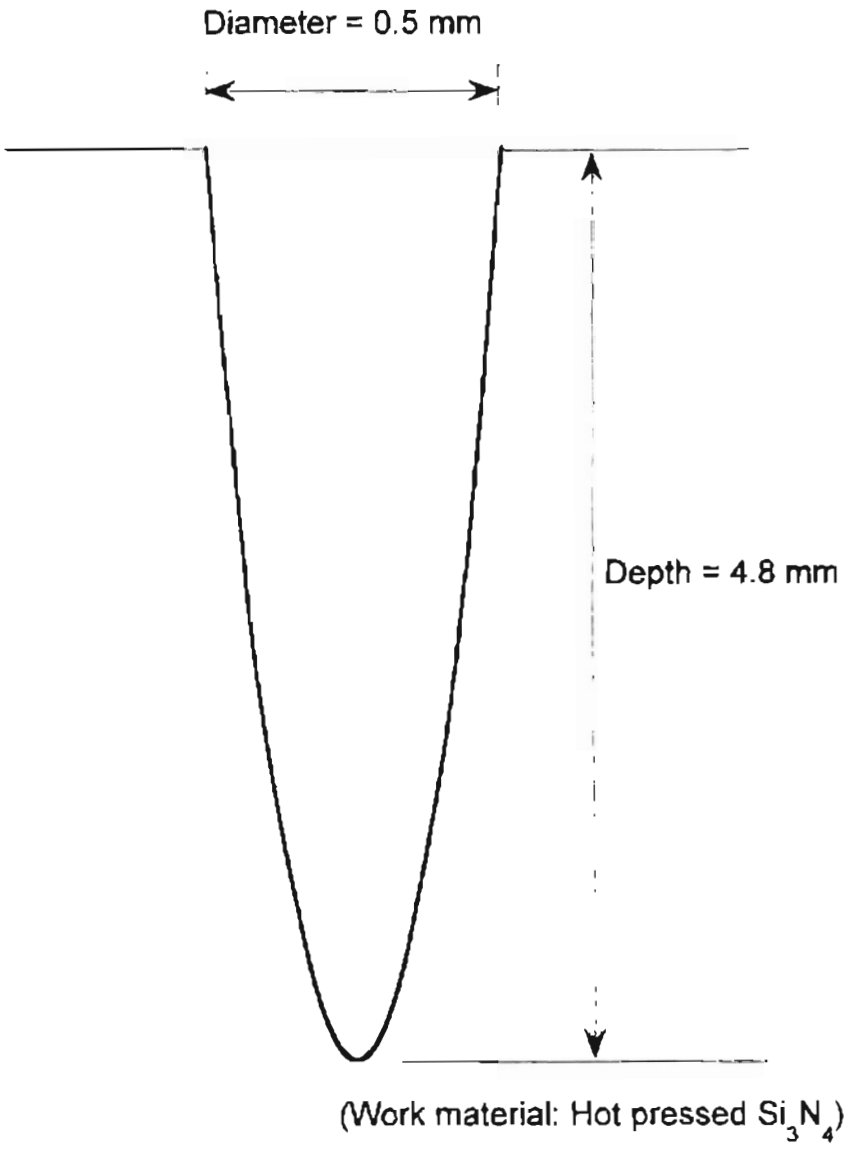

Figure 8.4.2 Dimensions of the Drilled Hole Obtained Experimentally

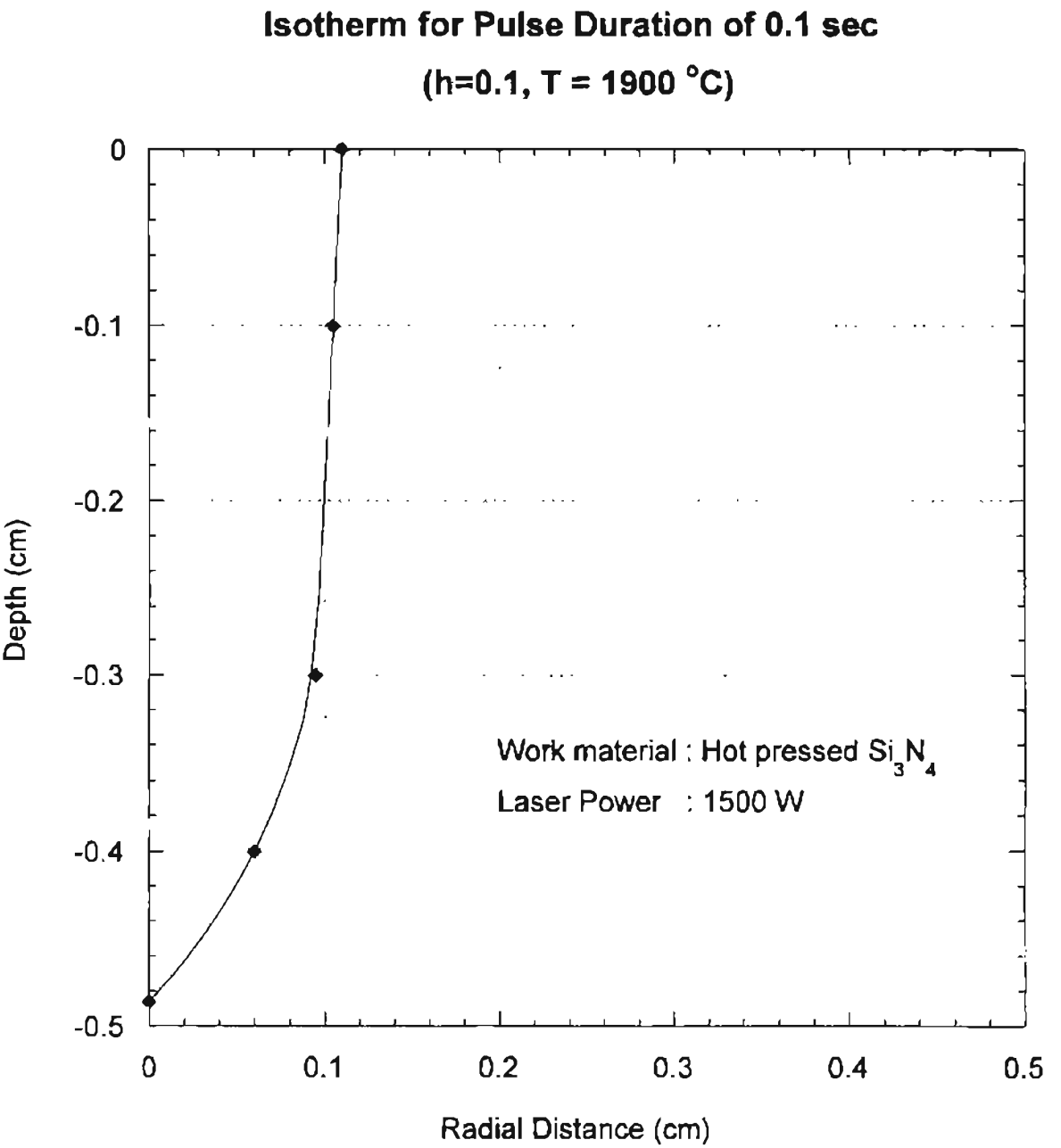

Figure 8.4.3 Isotherm for a Pulse Duration of 0.1 sec and h = 0.1

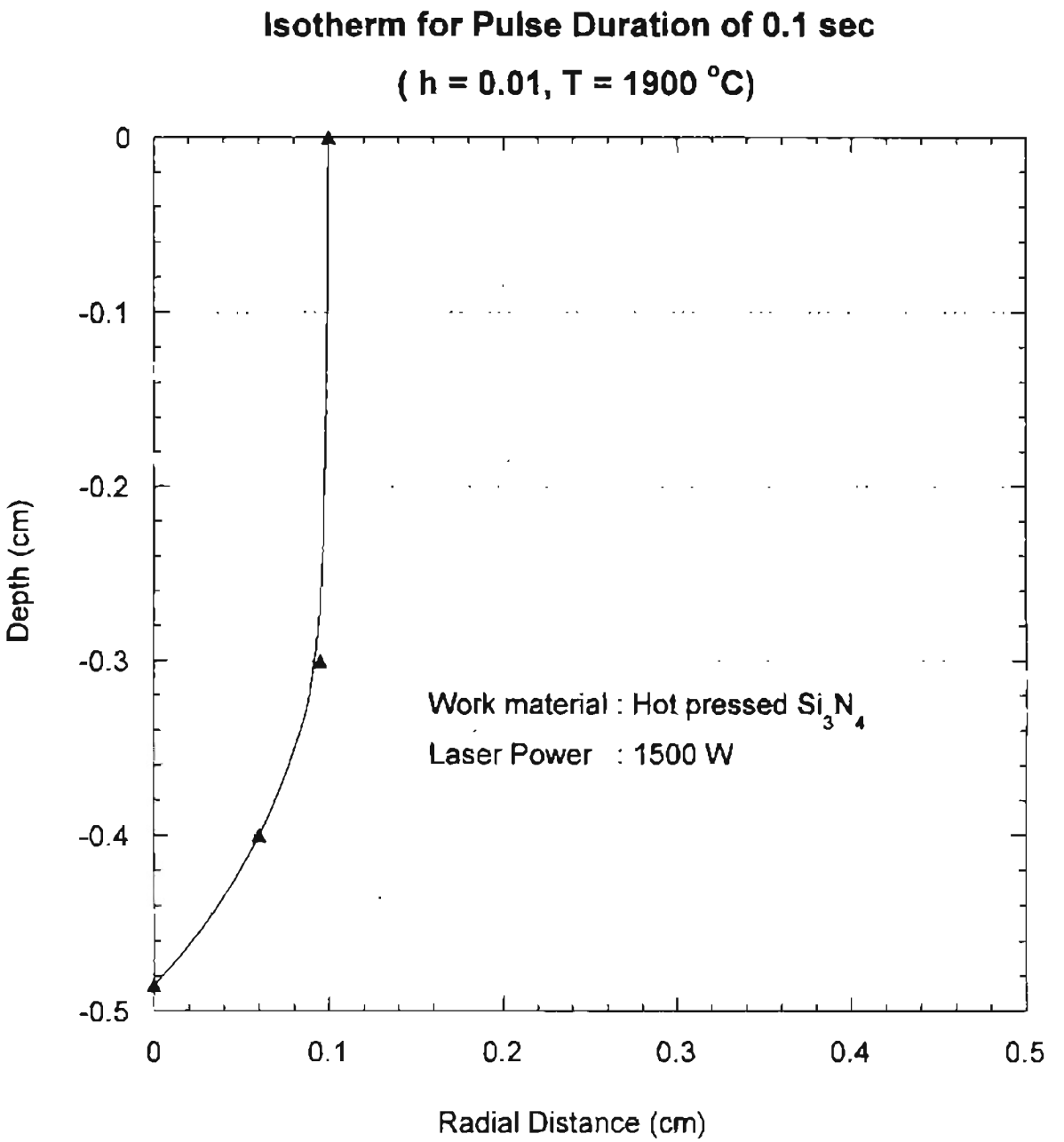

Figure 8.4.4 Isotherm for a Pulse Duration of 0.1 sec and h = 0.01

CHAPTER 9

LASER ASSISTED MACHINING

9.1 Introduction

Laser assisted machining (LAM) uses a laser beam positioned directly in front of the cutting tool to heat and soften the work material near the shear zone before machining. The schematic of LAM is shown in Figure 9.1.1. This process can boost metal removal rates in some high performance steels, superalloys such as nickel base and cobalt base alloys and titanium alloys which are difficult to mill or turn conventionally. As the laser heats the material in the shear plane, there is a decrease in the shear strength of the work material, which can be exploited to increase the material removal rate. Ceramic materials can be shaped by forming a groove or shallow hole at the surface by vaporization (Copley et al.,1979). Thus, shaping operations such as turning, facing, thread cutting and milling have been carried by overlapping the grooves or holes through laser beam or workpiece manipulation. Copley et al (1979) have reported increase in the material removal rate of 100% in Ti-6Al-4V, without decreasing tool life. Potential advantages of laser assisted machining (LAM) are summarized as follows: (Copley et al, 1979):

- In LAM, the laser is used as the heat source. It heats the material in the shear plane as the chip is formed. Heating the material in the shear plane decreases the cutting forces, increases the material removal rate and increases the tool life. There is also an improvement in the surface conditions of the workpiece in

terms of smoothness and improved stress distribution.

- In LAM, as the material is heated in the shear plane, the mode of chip formation may change from discontinuous to continuous, with the possibility of a decrease in built-up edge. This would give better surface finish and minimize flaws on the machined surface.

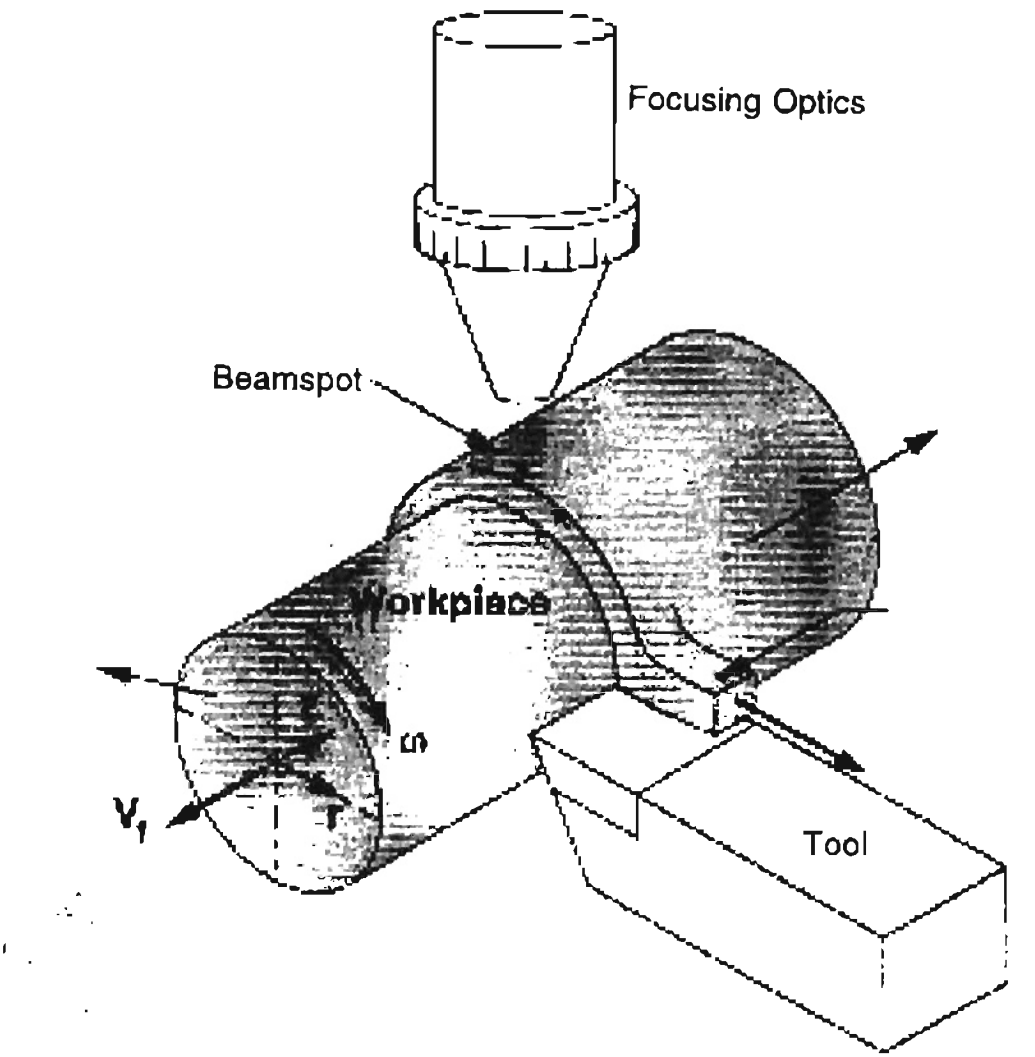

Figure 9.1.1 Schematic of Laser Assisted Machining

The most important reason for heating the material in the shear zone is to decrease the shear strength of the work material. This effect is anticipated in precipitation hardened alloys where the yield stress of the material decreases markedly with increasing temperature. Komanduri et al. (1985) have reported that with ceramic tools turning an Inconel 718 workpiece, LAM (with laser power 15 kW) has provided 40 % less tool wear and 18 % less cutting force at a metal removal rate 33 % greater than in conventional turning.

LAM has been successfully attempted at the Fraunhofer Institute of Production Technology IPT (Aachen, Germany) on hard materials such as tempered 30 NiCrMo 16 6 steel, which has a strength near 1800 N/mm^2 (hardness 58 R_c), and cobalt based Stellite 6 alloy (1995). They have reported three times increase in the material removal rates in the case of 30 NiCrMo 16 6 steel. In Stellite 6 work material, they have reported a drop in the cutting forces by 70% and a reduction in tool wear by 90% compared to conventional machining.

Komanduri et al. (1982) have reported an improved laser assisted machining process for difficult-to-machine materials, such as titanium alloys and other high temperature superalloys. As shown in Figure 9.1.2 a series of holes were drilled on the rotating workpiece using a pulsed Nd-YAG laser ahead of the cutting process so that the tool removes the rest of the weaker material with relative ease. They have reported a decrease in the cutting forces, breakage of the chip to a manageable size, and reduced tool wear.

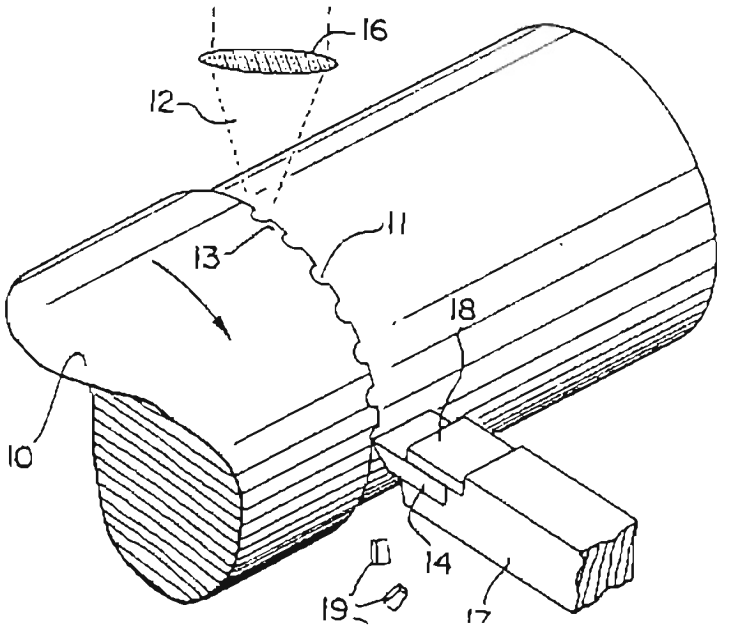

Figure 9.1.2 Improved LAM Process for Ti and High Temperature Super Alloys. (after Komanduri et al., 1982)

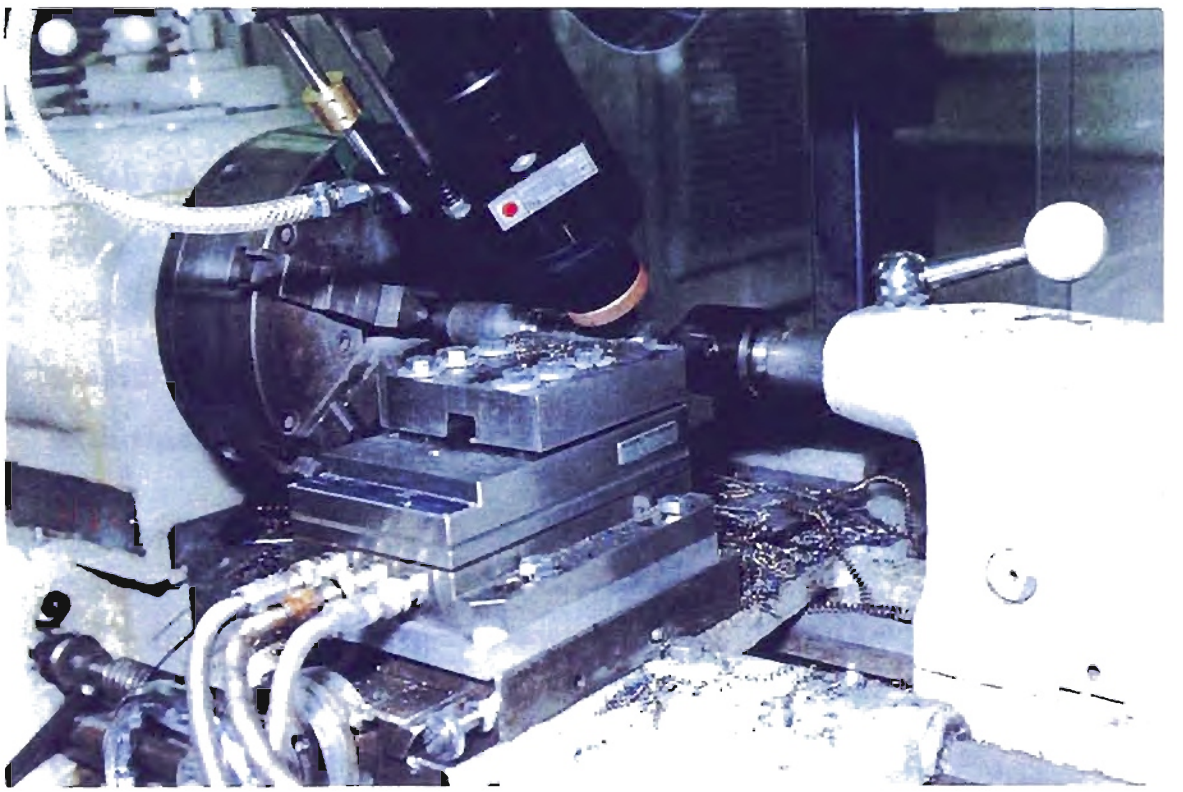

Figure 9.2.1 Experimental Setup for LAM

9.2 Experimental setup for Laser Assisted Machining (LAM)

Figure 9.2.1. is the photograph of the arrangement used for Laser assisted machining (LAM). It consists of a beam delivery system which directs the laser beam onto the workpiece, a distance δ in front of the edge of the cutting tool. The focusing optics which is attached to the beam delivery system is held by a fixture mounted on the tool carriage of the lathe. This fixture allows the focusing optics to be moved in the X, Y, Z, and θ direction. The beam delivery system, in the form of an articulated arm, consists of 7 water cooled mirrors and 8 ball bearing rotary joints which gives total flexibility in the movement of the arm with the motion of the tool carriage. A special fixture was made to hold the tool onto the dynamometer. A three-component piezoelectric dynamometer (Kistler,Type 9257A) was used for measuring the three components of tool forces perpendicular to each other. The tool forces set up a proportional electrical charge in the dynamometer which is fed into a charge amplifier where they are converted into proportional voltages. Using a data acquisition system, the voltages are converted into equivalent force values and are displayed as real time graphics. Thus on-line monitoring of the tool forces was made possible with this system.

Experiments were carried out with the following variable factors:

- Incidence angle of the laser beam on the workpiece.
- Distance between the impingement point of the laser and the cutting tool edge.
- Coatings to increase the absorptivity of the laser beam into the

workpiece material.

- Laser Power
- Cutting velocity
- Different materials

9.3 Results and Discussion

9.3.1 Incidence Angle of the Laser Beam

To obtain the optimum incidence angle, experiments were carried out with the focusing optics placed at angles of 90, 80, 70, 60, 50, 40, 30 degrees with respect to the cutting tool as shown in Figure 9.3.1.1. In these experiments tool forces were considered as the response variables. The other parameters were kept constant and are given in Table 9.3.1.1.

Table 9.3.1.1 Test Conditions for Varying Beam Incidence Angle

Workpiece Material	Steel 5150
Tool Material	Multi coated tool (Al_2O_3+TiC+TiCN) TP 100 Carboloy
Coating on Workpiece	Manganese Phosphate
Laser Power	650 W, CW mode
Cutting Speed	110 sfpm
Feed Rate	0.0021 in/rev
Depth of Cut	0.1 in.

It was observed from the experiments carried out on AISI steel 5150 that at incidence angles between 50 to 60 degrees, the cutting forces on the

tool were minimum. The same experiments were attempted on AISI steel 1018 with laser power at 1500 W and identical results were obtained. It was not possible to adjust the focusing optics at intermediate angles between 50 and 60 degrees, to further optimize the conditions, due to the limitation of the fixture holding the optics. Figure 9.3.1.2 gives the result of varying the beam incidence angle on AISI steel 5150.

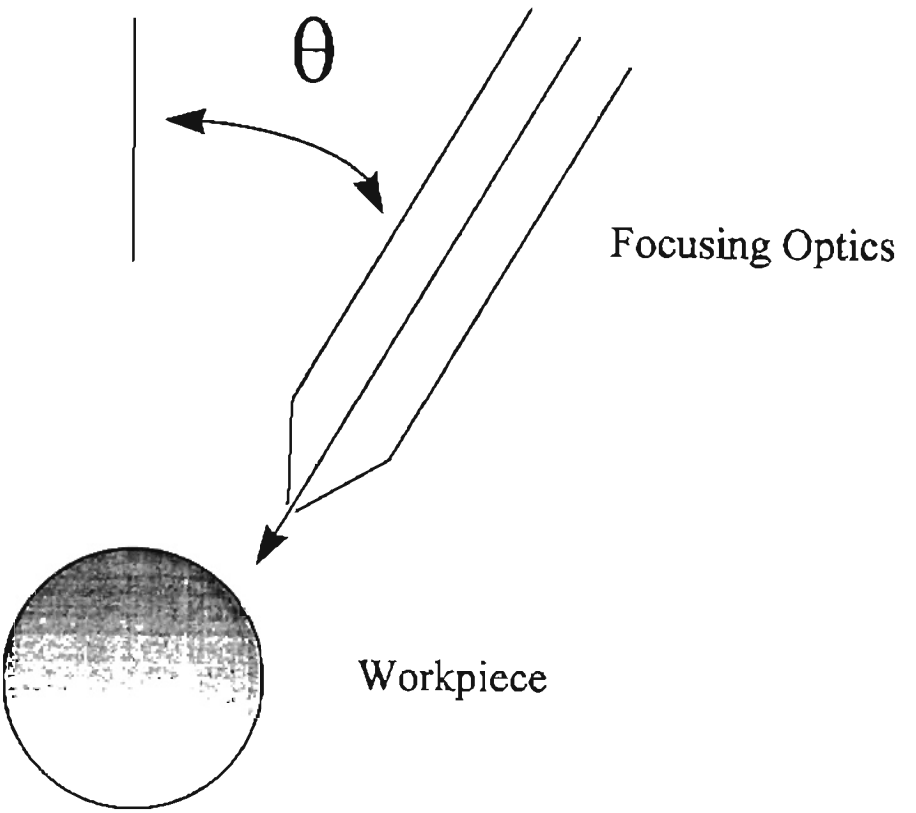

Figure 9.3.1.1 Schematic Showing the Angular Position of the Focussing head Relative to the Workpiece

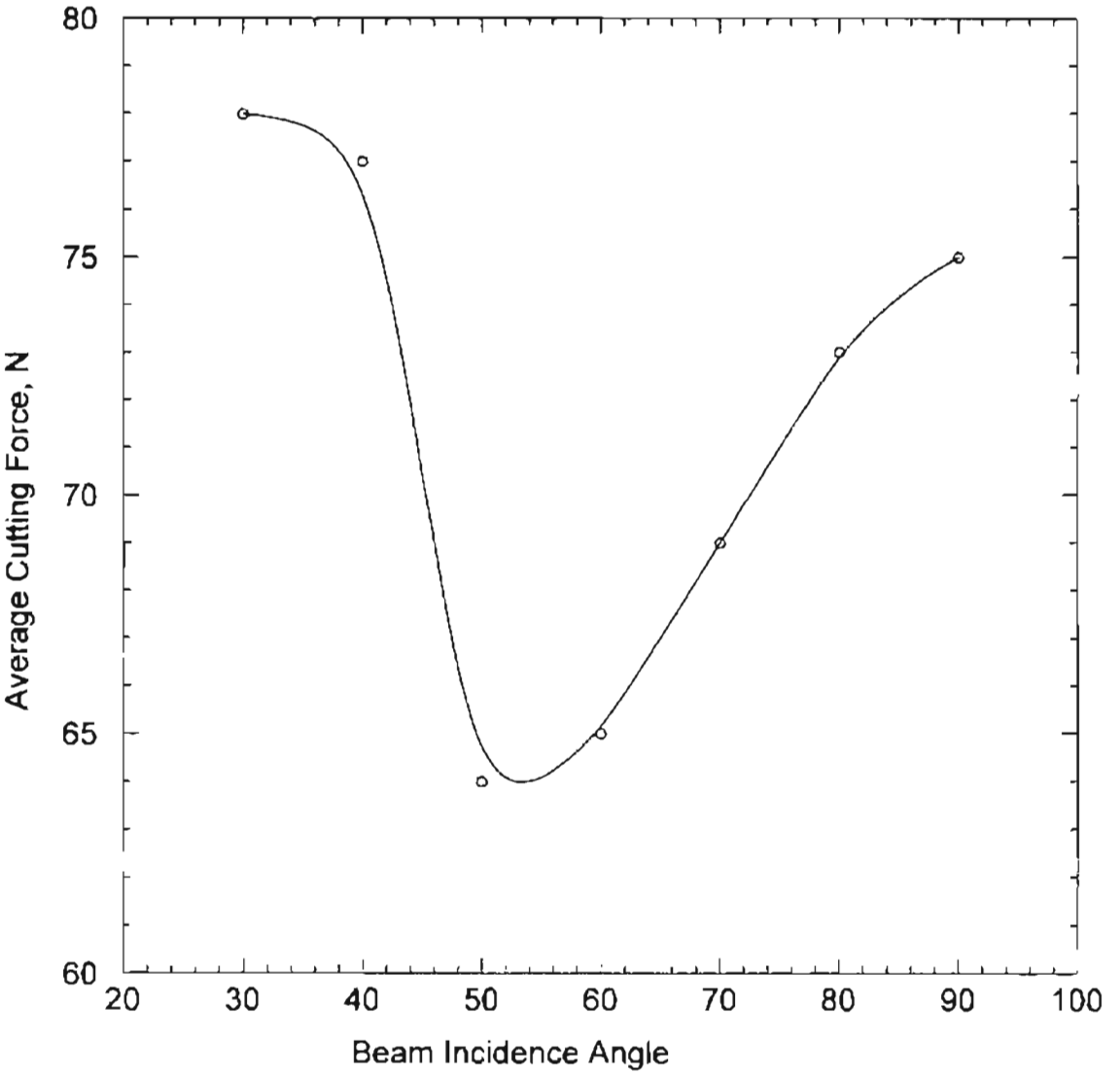

Figure 9.3.1.2 Plot Showing the Variation of Force with Beam Incidence Angle

9.3.2 Distance between impingement point of the beam and the cutting edge

The distance between the impingement point of the laser beam on the workpiece and the tool cutting edge, δ, plays a very important role in varying the cutting forces. The other test conditions were maintained the same (refer Table 9.3.1.1). It was observed that the maximum reduction in the cutting forces occurs in the range δ = 3 to 4 mm. At distances less than this range, it is thought that chip interference may account for the decrease in the force reduction. Besides, the tool gets heated and thermal damage occurs due to this. At distances greater than this range, the material cools down in the shear plane and hence the effect of laser heating is minimized. Figure 9.3.2.1 shows the results of varying the distance between the impingement point of the laser beam and the cutting tool edge.

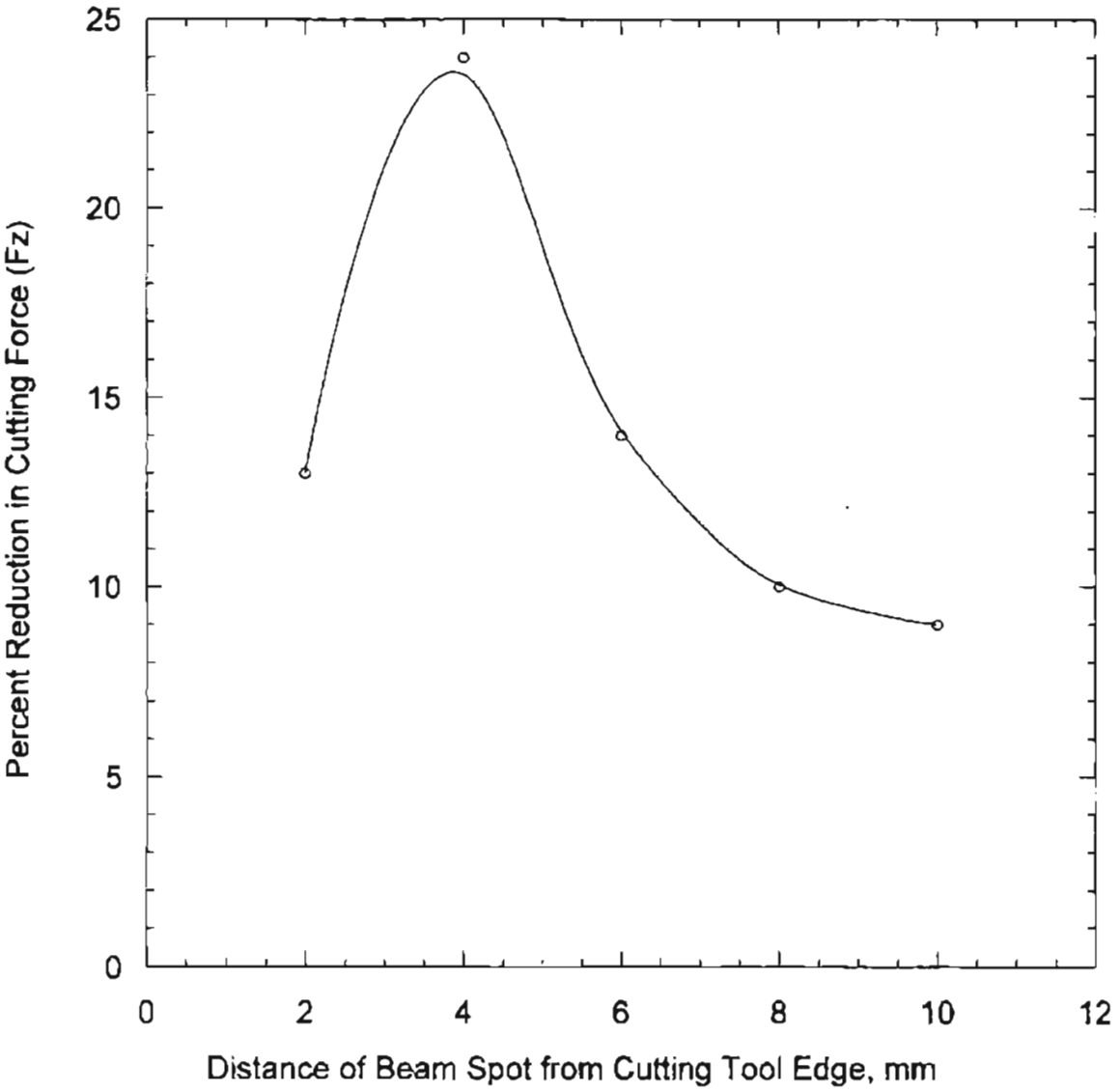

Figure 9.3.2.1 Plot Showing the Variation of Force with Distance of Beam Spot from Tool Cutting Edge

9.3.3 Use of Absorptive Coating

The intensity with which a material reflects the laser radiation is defined by the material reflectivity that varies with the wavelength of

radiation. Metals heavily reflect the CO_2 laser beam at the wavelength of 10.6 μm. The coupling efficiency of the laser energy can rise significantly with changes in the surface finish of the workpiece or its chemical composition. For instance, a metal powder coating or a paint coating can increase the absorptivity quite appreciably. The approach involving an increase in the surface roughness to raise the absorption efficiency not always justifies the effort from the technological viewpoint. Hence the use of absorbent coatings on the surfaces has become indispensable in most laser treatments. Table 9.3.3.1 gives the absorptivity of different materials as a function of wavelength.

Table 9.3.3.1 Absorptivity of Different Materials as a Function of Wavelength (after, Hecht, 1992)

	Laser/Wavelength			
Material	Argon 500 nm	Ruby 694 nm	Nd-YAG 1064 nm	CO_2 10.6 μm
Aluminum	9%	11%	8%	1.9%
Copper	56%	17%	10%	1.5%
Human skin (dark)	88%	65%	60%	95%
Human skin (light)	57%	35%	50%	95%
Iron	68%	64%	–	3.5%
Nickel	40%	32%	26%	3%
Sea water	*	*	*	90%
Titanium	48%	45%	42%	8%
White paint	30%	20%	10%	90%

*At these wavelengths, sea water transmits most light not reflected at the surface

An applied coating must be able to strongly absorb the laser radiation. In addition, it must be easy to use, inexpensive, stable in long storage, adhere well to metals, have reasonably high melting and vaporization temperatures, and readily conduct heat. The coatings that would equally satisfy the above requirements are yet to be found. Researchers have used (Grigoryants,1994) :

- Chemical coatings obtained by manganese or zinc phosphatizing, sulfurizing, and oxidizing.
- Paints containing Al and Zn oxides
- Colloidal solutions of carbon in acetone and alcohol
- Sprayed oxides of metals and
- Soot of resin, oil etc.

Whatever the type of coating material, it cannot be completely free of shortcomings. For example, the soot deposited on the surface does not provide a uniform coat and colloidal solutions give coats that adhere poorly to metals (Grigoryants,1994). Also, oxides sprayed on metal surfaces call for a complex and costly spraying process. Hence it can be noted that much work has still to be done to develop more efficient, cheaper and more practicable coating.

Several coatings were used to enhance the absorptivity of the CO_2 laser beam on the steel and aluminum materials used in the LAM tests. Results obtained from the tests are as shown in Figure 9.3.3.1. It can be noted that the use of potassium silicate gives the best result in terms of reduction in cutting forces followed by the coatings of manganese phosphate, graphite and black varnish. However, there are several

practical problems associated with the use of these coatings. Potassium silicate (50% aqueous solution) has to be sprayed on the shoulder region of the workpiece during LAM (Figure 9.3.3.2). This causes splashing of the chemical onto the focusing lens causing considerable damage. Manganese phosphate is insoluble in water and soluble in mineral acids. Hence the solution is prepared by dissolving the phosphate in phosphoric acid. Metal sample dipped in the solution of manganese phosphate develops a black lustrous coating. However, this coating was found to be ineffective on aluminum samples. Graphite powder would not adhere well to the metal sample, hence was "glued" to the metal sample using sprayed adhesive. Black varnish and other black paints (high temperature barbecue paints) could not withstand the temperature of the laser beam and vaporized on contact.

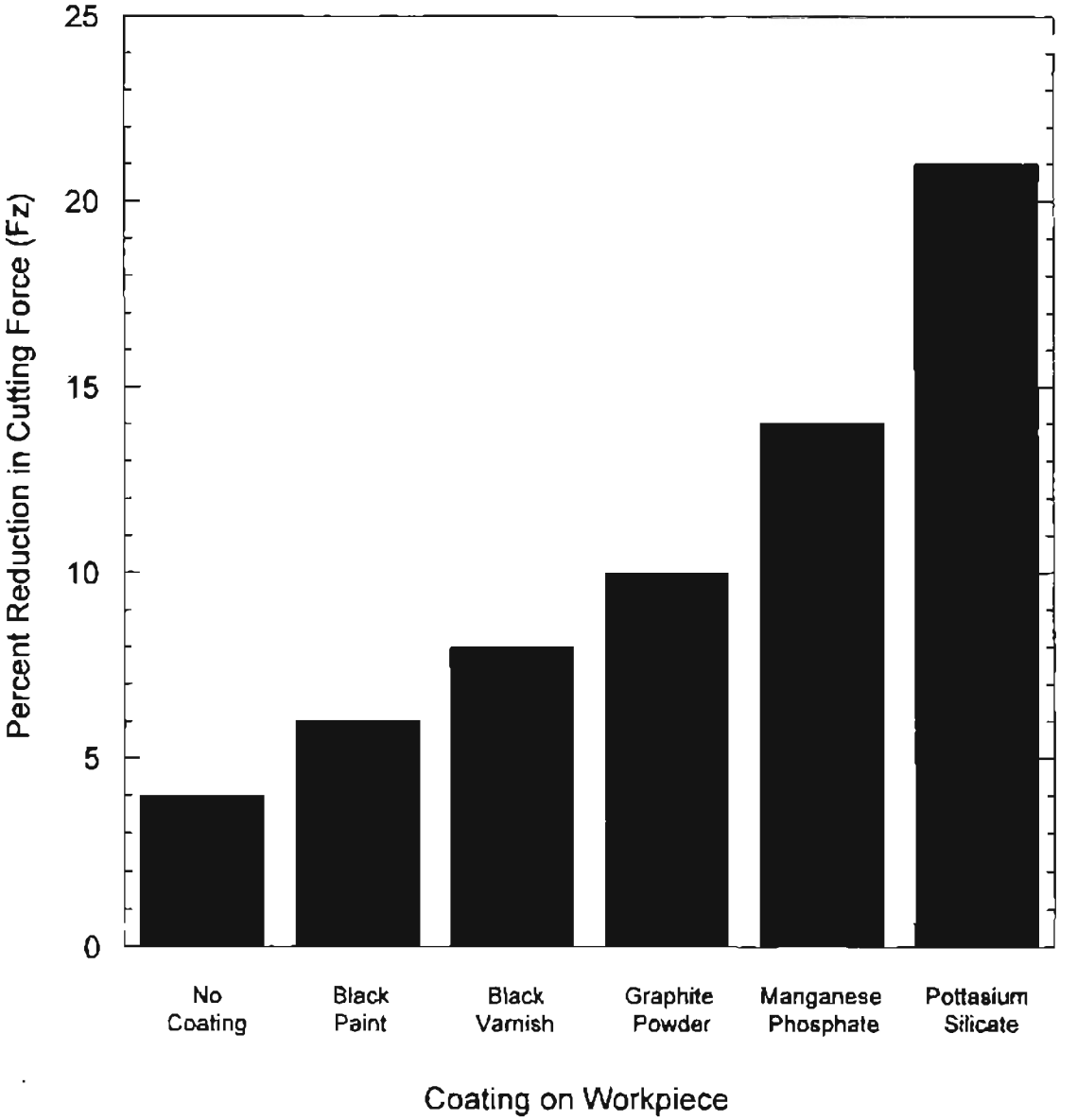

Figure 9.3.3.1 Histogram Showing Variation of Force with Different Absorptive Coating on Workpiece

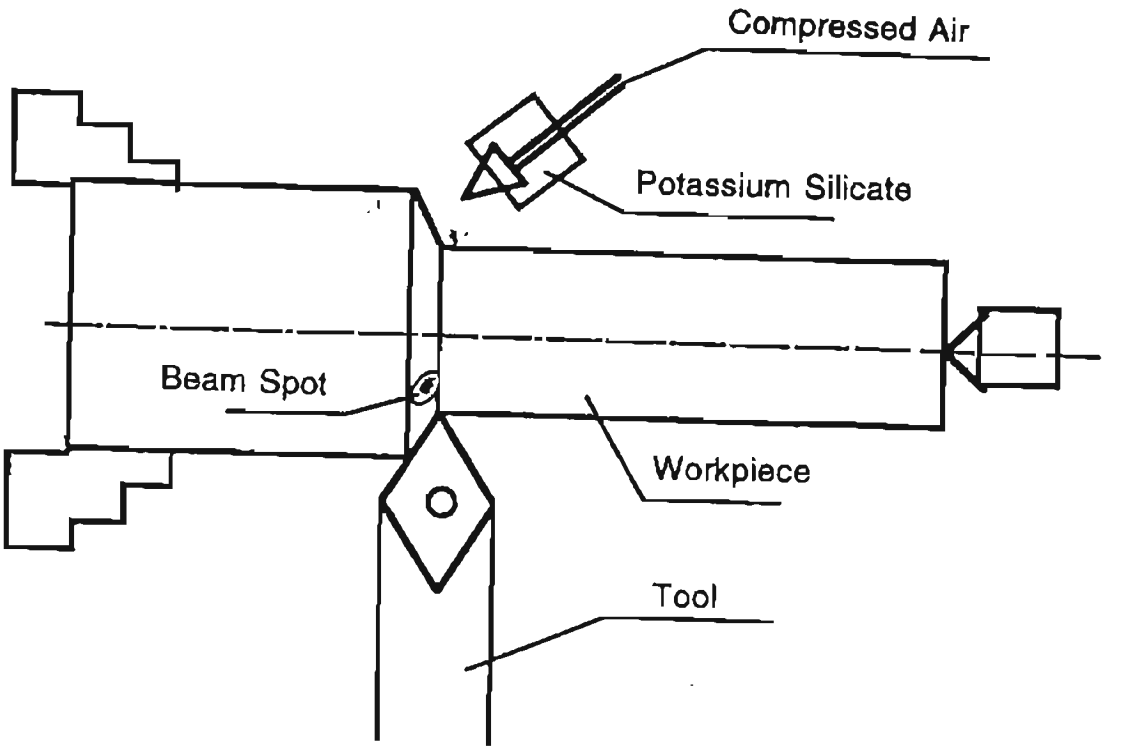

Figure 9.3.3.2 Pottasium Silicate Sprayed on Shoulder Region of Workpiece During LAM

9.3.4 Effect of Laser Power

From Figure 9.3.4.1, it can be seen that increasing the incident power increases the magnitude of force reduction. However, at cutting speeds of over 150 sfpm on steels it was not possible to obtain a significant force drop with the available incident beam power.

It was observed during these experiments that the cutting forces at high cutting speeds (> 130 sfpm) occasionally increased and the force changes were not reproducible. A possible explanation for this may be due to an unstable built-up edge at high cutting speeds which might increase the effective rake angle resulting in an increased cutting force. The force increase associated with the loss of the built up edge could outweigh the decrease in force due to laser heating the material on the shear plane which may account for the lack of reproducibility in the force change and the occasional increase in the force induced by the laser heating.

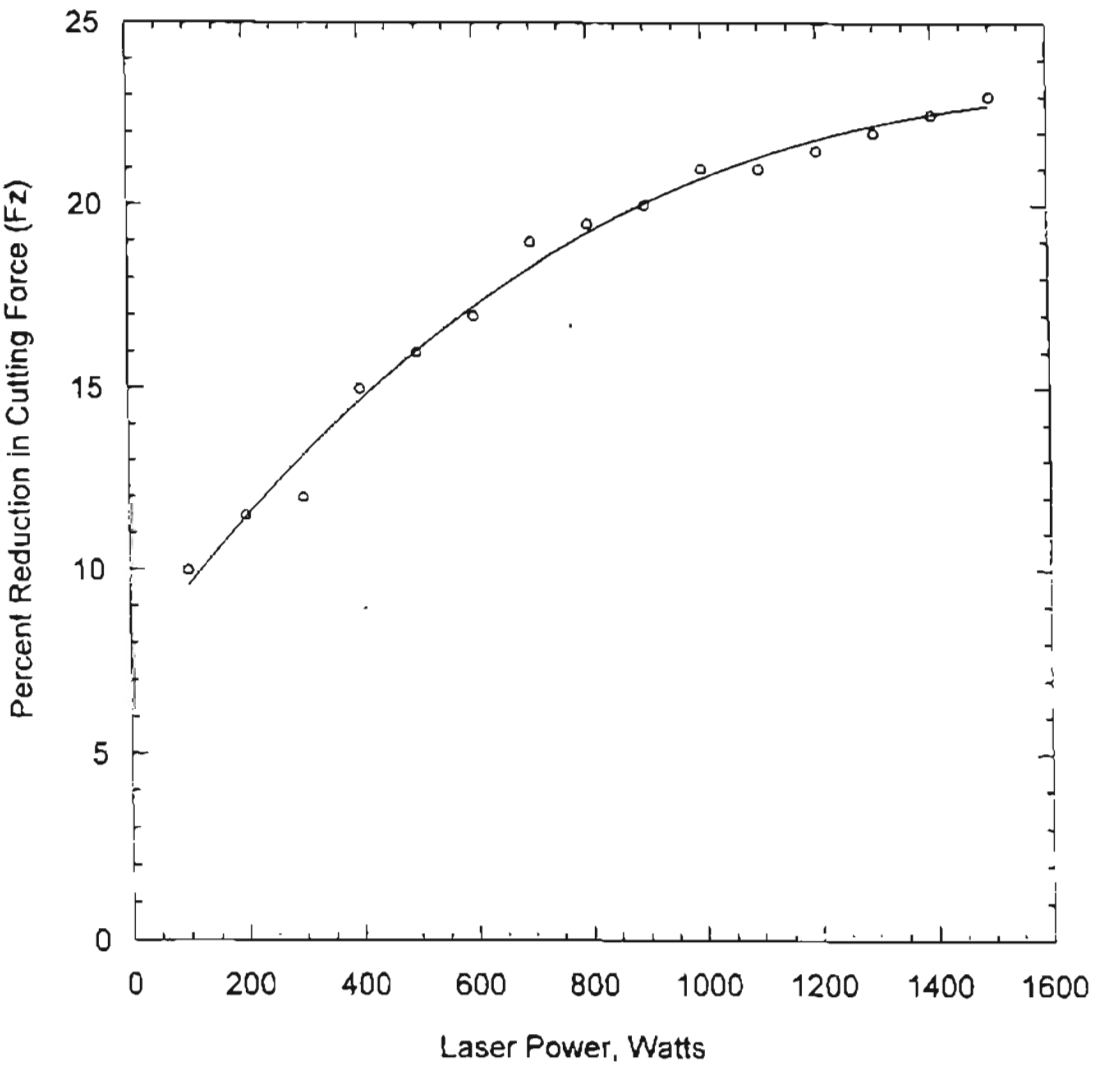

Figure 9.3.4.1 Variation of Cutting Force with Laser Power

9.3.5 Cutting Velocity

From the Figure 9.3.5.1, it can be observed that maximum reduction in the cutting forces can be obtained at a speed ~ 120 sfpm. At lower speeds (< 100 sfpm), or at higher speeds (> 130 sfpm) the reduction in forces is not very significant. A possible reason for this at higher speeds may be due to unstable built-up edge as mentioned in the previous section and also due to the fact that there is less time for the absorbed power of the laser beam to heat the material on the shear plane.

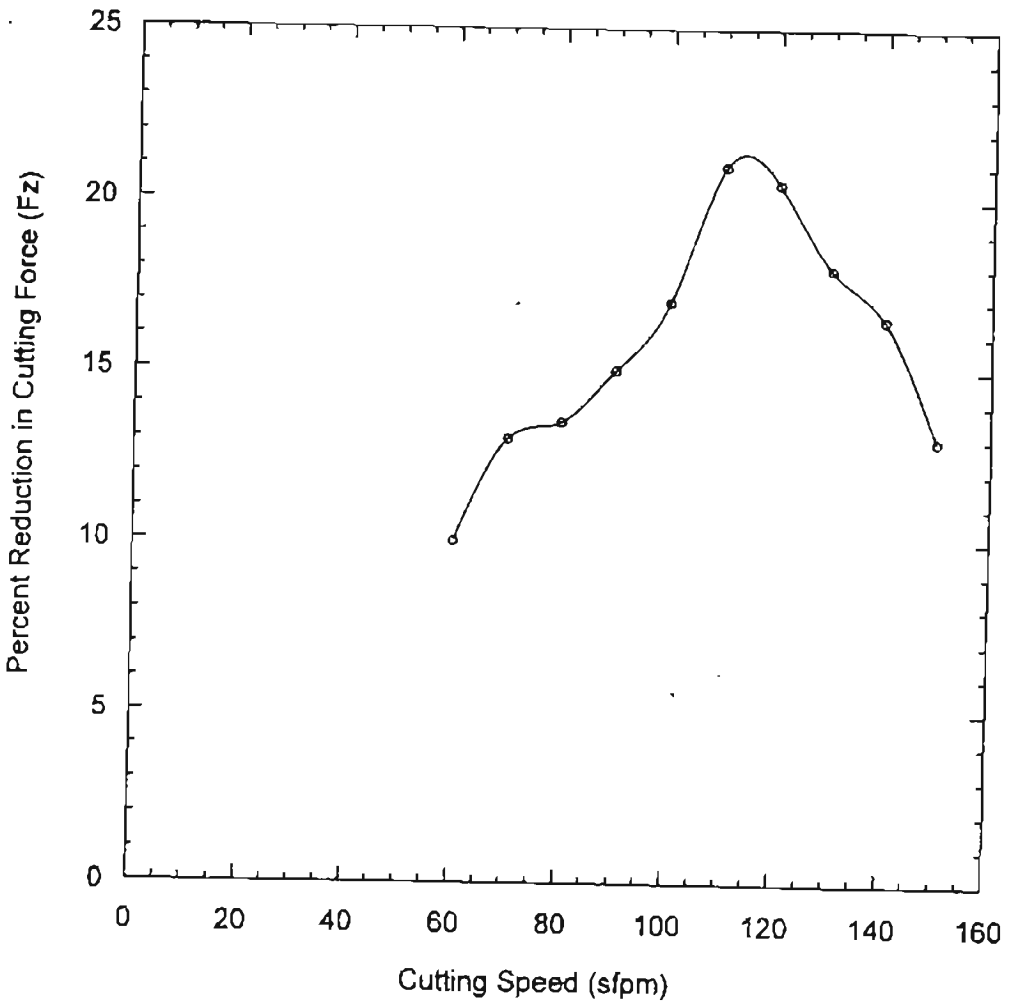

Figure 9.3.5.1 Variation of Cutting Force with Cutting Speed.

9.3.6 Type of Material used

Aluminum has a very high reflectivity of ~ 97% while steel has reflectivity of ~ 95 % to the CO_2 laser beam at 10.6 μm wavelength (Duley, 1983). The difference is observed in the response of these two materials in terms of reduction in the cutting forces. There is a mere 5% reduction in cutting force in the case of aluminum whereas about 20% reduction is observed in the case of steel. Besides, manganese phosphate coating was found to be ineffective in the case of aluminum whereas it gave a black, lustrous, absorptive coating on the steel sample which may also contribute to the more reduction in cutting forces. Figure 9.3.6.1 gives the comparative value in force reduction with the different materials used in these experiments.

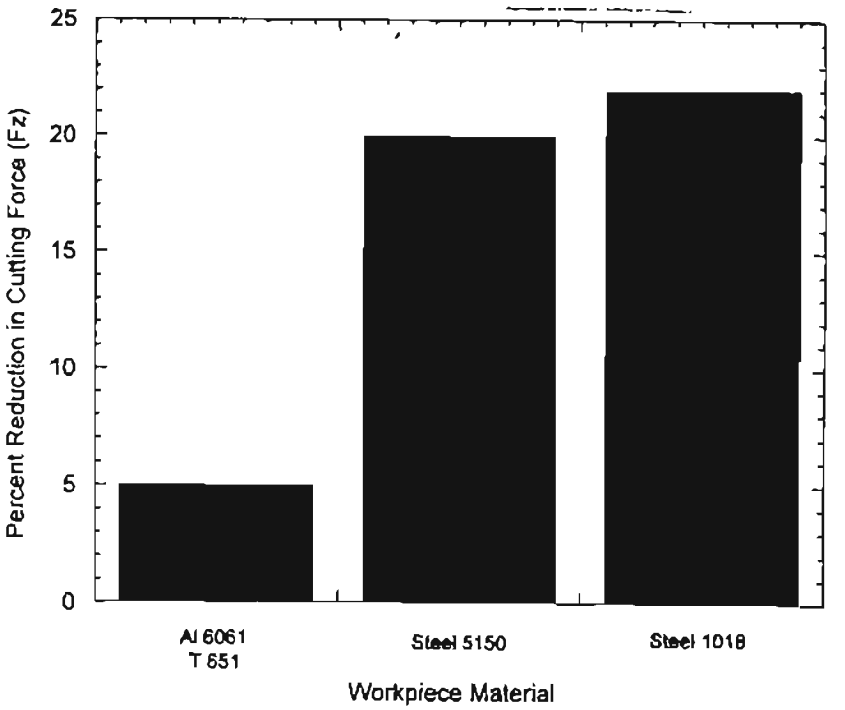

Figure 9.3.6.1 Histogram Showing the Reduction in Force for Different Workpiece Materials

CHAPTER 10

RECAST LAYER FORMATION IN LASER MACHINING

10.1 Introduction

Due to their high hardness and brittleness, ceramics are difficult to shape by conventional machining. Laser machining is an excellent method to produce holes, grooves and odd shaped cavities in ceramics. However, a major limitation in the machining of ceramics by laser is the formation of a recast layer that adversely affects the surface finish and depth of cut, and is responsible for the crack formation on the machined surfaces. The recast layer is formed principally by the condensation of the vaporized material as well as the solidification of the molten material during laser processing.

Laser machining of silicon nitride has been investigated by several researchers but limited data is available on the mechanics of formation of the recast layer (Ray, 1995). During laser machining, silicon nitride decomposes into Si which subsequently melts and resolidifies as the recast layer. If oxygen is used as the assist gas, molten silicon would oxidize to form SiO_2 which contributes to an increase in the recast layer. In laser hole drilling of ceramics, due to the limited size of the hole, most of the molten material is not blown out by the assist gas. Hence, it solidifies quickly due to high thermal diffusivity across the hole and increases the surface roughness.

Maruo et al. (1990) studied the mechanisms of material removal during laser machining of silicon nitride using CO_2 and pulsed excimer laser. They observed that wavelength of the laser beam had a significant effect on the decomposition of silicon nitride and consequently on the formation of the recast layer. In CO_2 (λ=10.6 μm) laser machining, the silicon nitride is decomposed into liquid silicon and adheres to the walls of the machined surface. In contrast, silicon nitride decomposed into silicon vapors in excimer laser (λ=248 nm) resulting in a much cleaner surface. Solomah (1991) investigated the laser cutting of hot-pressed silicon nitride using nitrogen and oxygen as assist gases. X-ray analysis of the recast layer revealed that only silicon was present when nitrogen was used as the assist gas while a mixture of Si and SiO_2 were identified when oxygen was used as the assist gas.

The formation of a recast layer in laser machining depends on several factors including (Ray, 1995):

- oxidation, decomposition and melting of the material.
- viscosity and surface tension of the molten layer.
- type of machining (drilling, grooving, cutting)
- assist gas flow parameters (pressure and flow rate)

Figure 10.1.1 is a schematic showing the formation of recast layer during blind hole drilling, grooving and cutting using a pulsed laser. The initial pulses generate a shallow blind hole within which the flow rate of the assist gas is high enough that most of the molten layer is blown away. However, as the number of pulses increase and the hole depth increases, the assist gas flow rates in the hole are reduced as the pressure gradient

becomes lower. This allows more recast layer to be formed until a through hole is achieved after which the assist gas can readily eject most of the molten layer through the bottom of the hole. Grooving differs from drilling in that, an open channel is left in the wake of the moving laser beam.

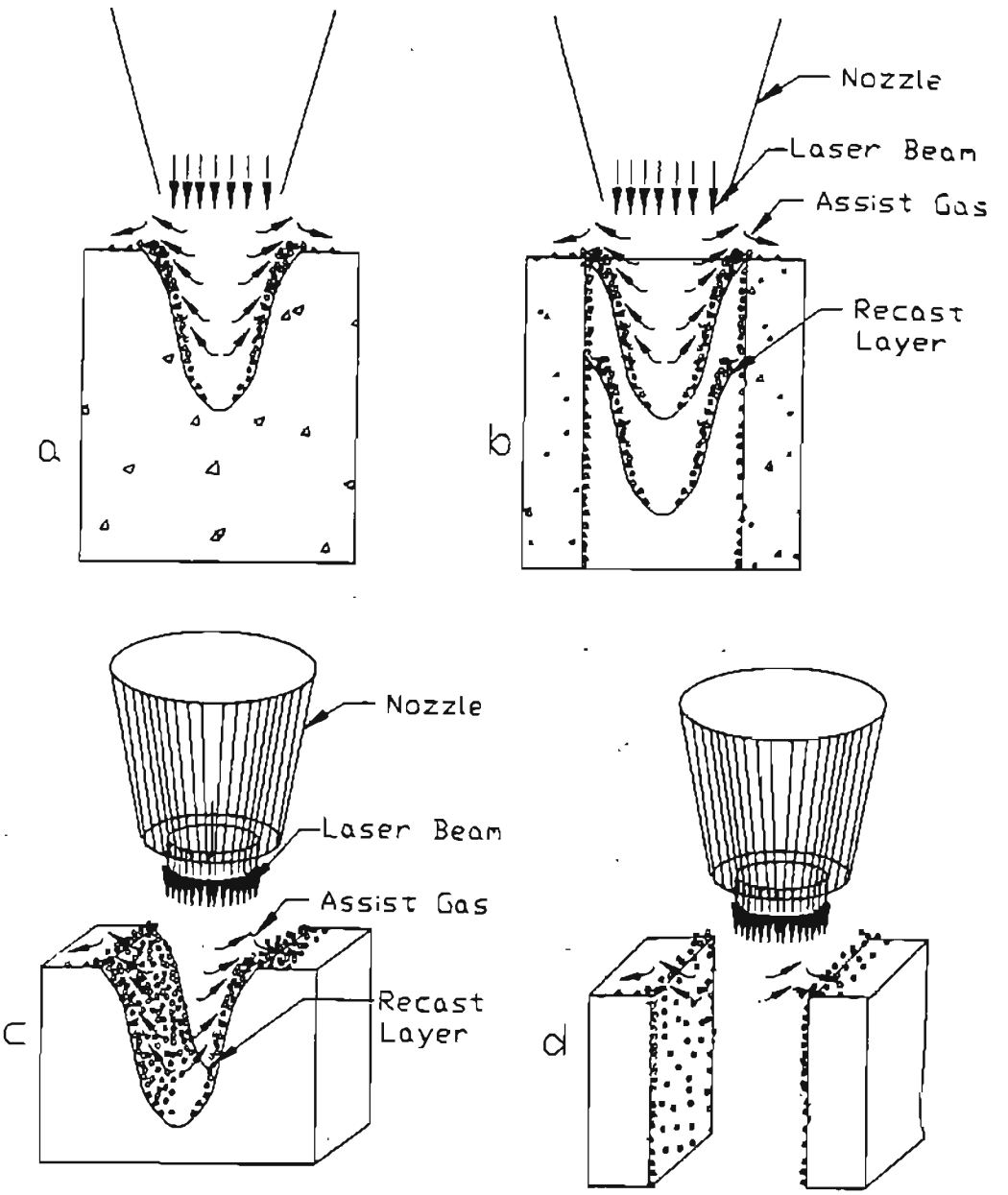

Figure 10.1.1 Formation of Recast Layer for a) Laser Drilling of a Blind Hole, b) Laser Drilling of a Through Hole, c) Laser Grooving and d) Laser Cutting (after Ray, 1995)

The less confined geometry provides a ready path for assist gas flow and allows for more effective removal of the molten slag and less recast layer formation than during drilling for the same depth.

Laser cutting is a process involving drilling to produce a through hole and grooving to produce a trailing, open cut. In this case, the confined geometry for the cut results in low assist gas flow rates and hence cannot remove the molten slag completely. Besides, the molten slag adheres to the parent material, thus leading to a coarser surface finish than for simple laser drilling. This would obviously imply that as the thickness of the material increases, more recast layer would be obtained along the sidewall of the cut as the gas flow rates would further decrease

To understand the mechanism of formation of recast layer, experiments were carried out on silicon nitride, SiAlON, Al_2O_3 and multi-coated tools. The 1500 W CO_2 laser was used to generate holes in silicon nitride specimen. The composition and location of the recast layer were evaluated as a function of laser power. The effects of the recast layer on the surface finish and crack formation were determined. The results of the grooving tests along with the material removal mechanism in silicon nitride are discussed separately in Chapter 11.

10.2 Results and Discussion

A continuous wave CO_2 laser was focused on the workpiece surface. Drilling was performed at different laser powers with oxygen and helium gas. The coaxial assist gas, was blown into the machining zone through a gas-jet nozzle.

The specimen were examined under an optical microscope and with a scanning electron microscope (SEM) to determine recast layer thickness and crack formation. An energy dispersive X-ray analyzer attached to the SEM was used to identify the composition of the recast layer. XRD was also performed to identify the phases present.

Figures 10.2.1 (a) and 10.2.1 (b) show the sectional view of the laser drilled holes in silicon nitride. Figures 10.2.2 (a) and 10.2.2 (b) show the cross-section of the laser drilled holes in SiAlON. Figures 10.2.3 (a) and 10.2.3 (b) show the cross-section of Al_2O_3 specimen. For comparison between ceramics and cemented carbides, tests were conducted on TiC coated WC and multi coated cemented WC tools. The micrographs of the two samples are shown in Figures 10.2.4 (a) and 10.2.4 (b), respectively.

It can be seen from the micrographs that the recast layer builds up with increasing groove depth. It can also be observed that the recast layer is mostly formed along the walls of the groove/hole. This may be due to the reduction in the gas flow rate along the walls, which causes the viscous molten layer to adhere to the parent material. In case of Si_3N_4, formation of dendritic structures can be observed in the recast layer. These dendritic structures, were identified as β-Si_3N_4 grains from XRD analysis. However

similar phase transformation is not evident in the recast layer of other materials.

It can also be observed that the crack in the specimen seem to originate from the recast layer. In case of ceramics, these cracks propagate in the radial direction. In case of cemented carbides these cracks propagate in the axial direction.

The recast layer did not form at the bottom of the groove. The scouring action of the direct impingement of the assist gas, at the bottom of the groove, seems to be effective in sweeping away the molten material.

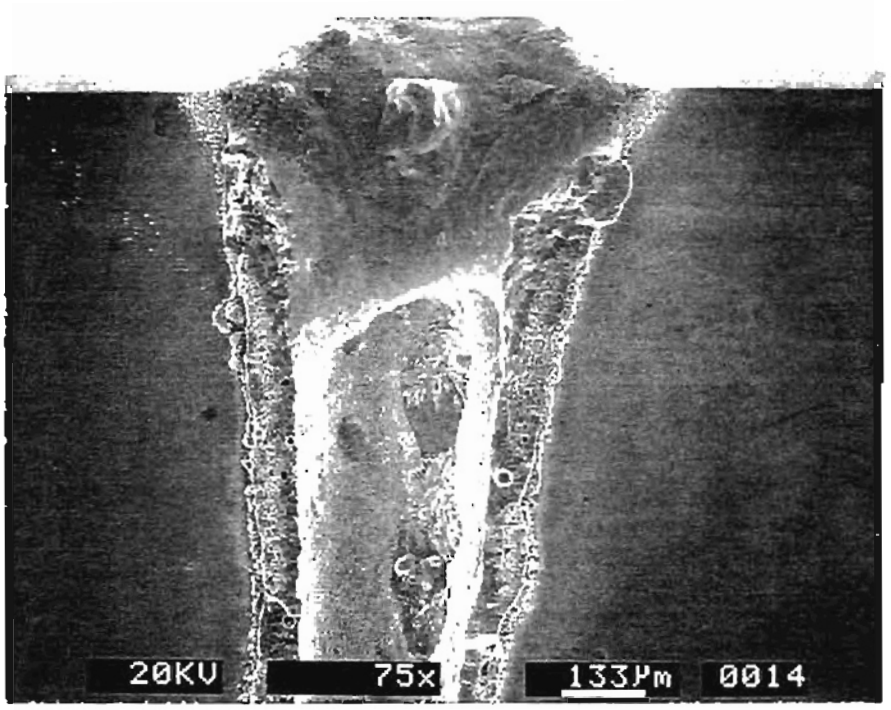

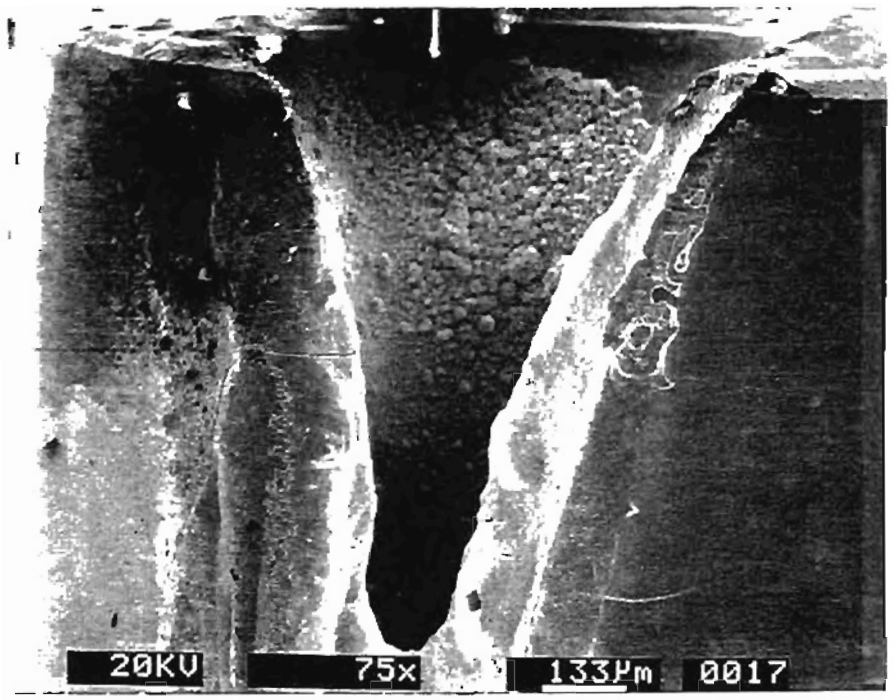

Figure 10.2.1 Laser Drilled Hole in Si_3N_4 at a) Low Power b) High Power

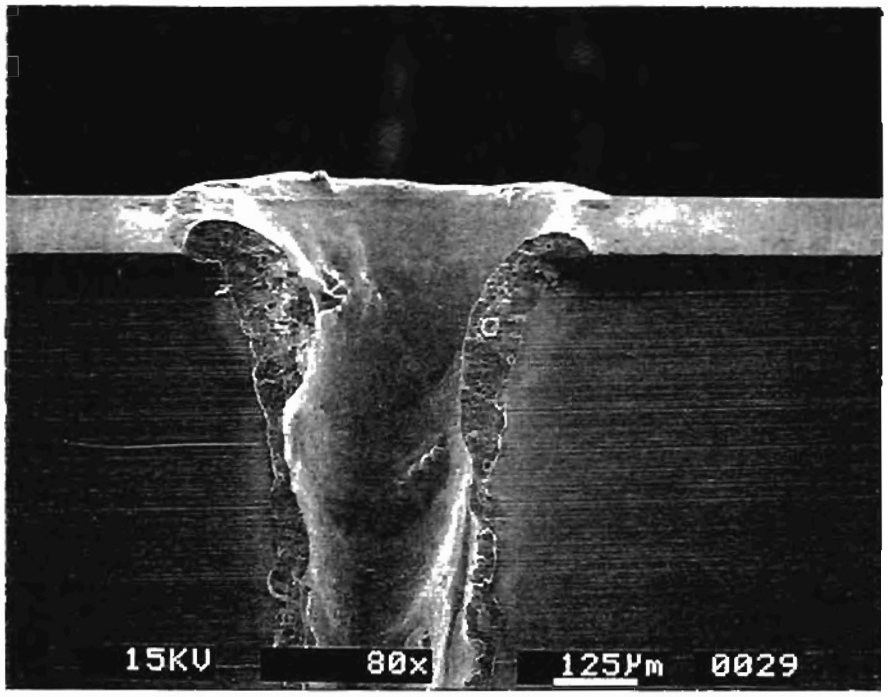

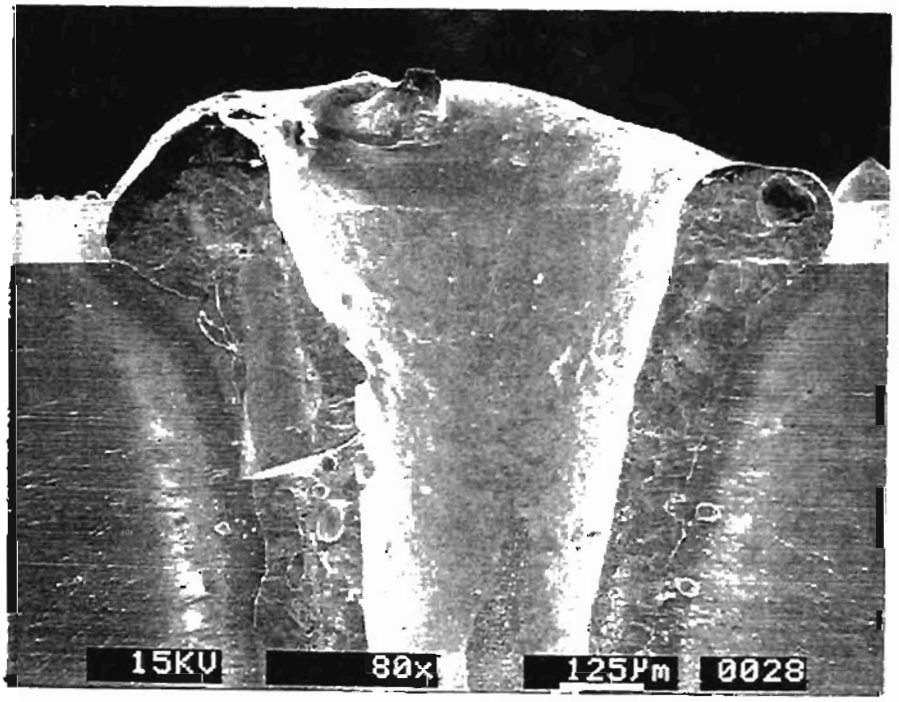

Figure 10.2.2 Laser Drilled Hole in SiAlON at a) Low Power
b) High Power

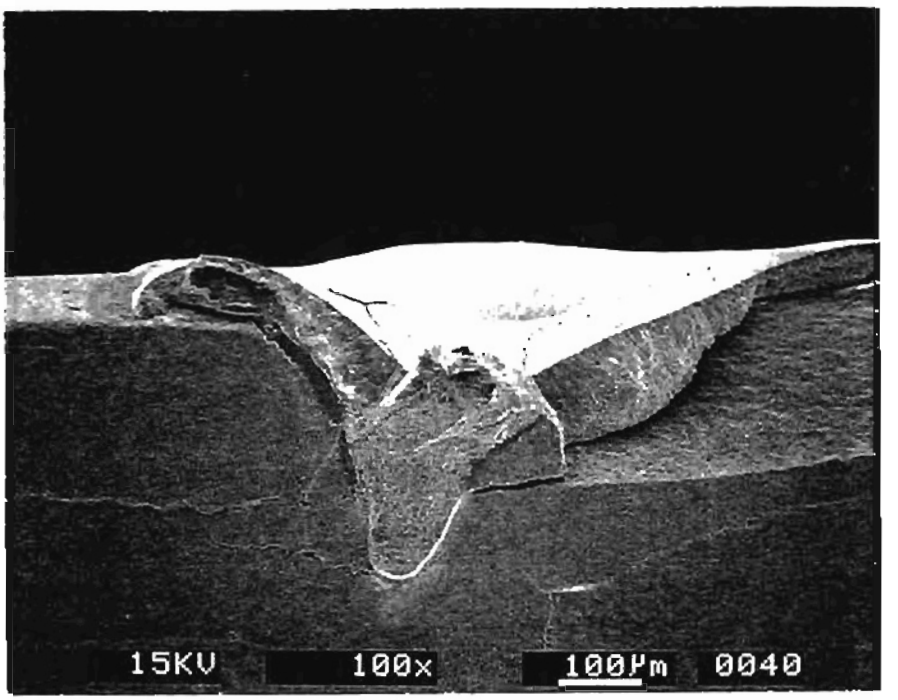

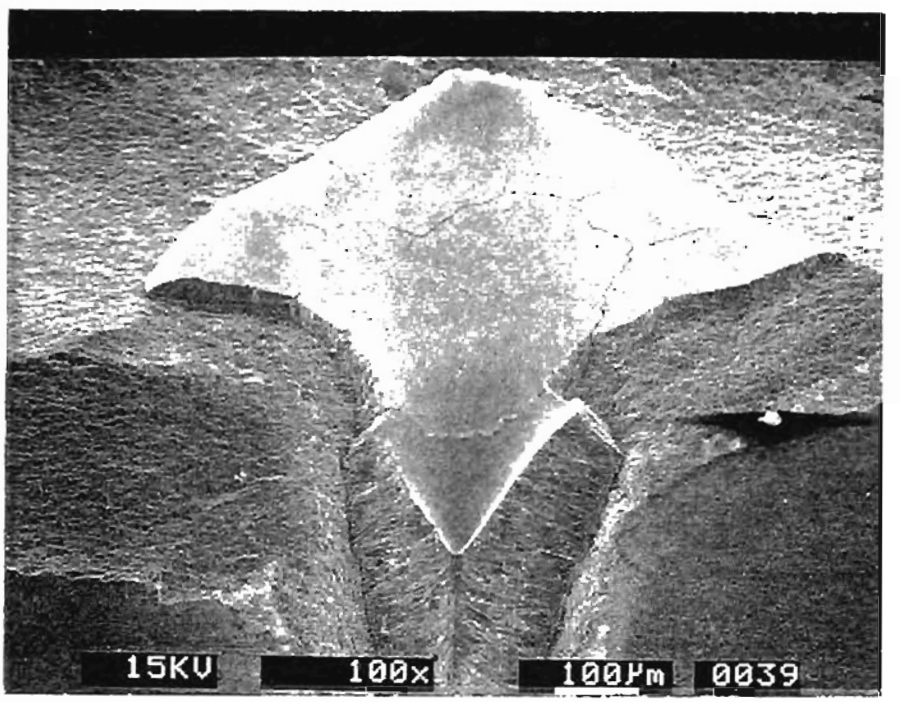

Figure 10.2.3 Laser Drilled Hole in Al_2O_3 at a) Low Power b) High Power

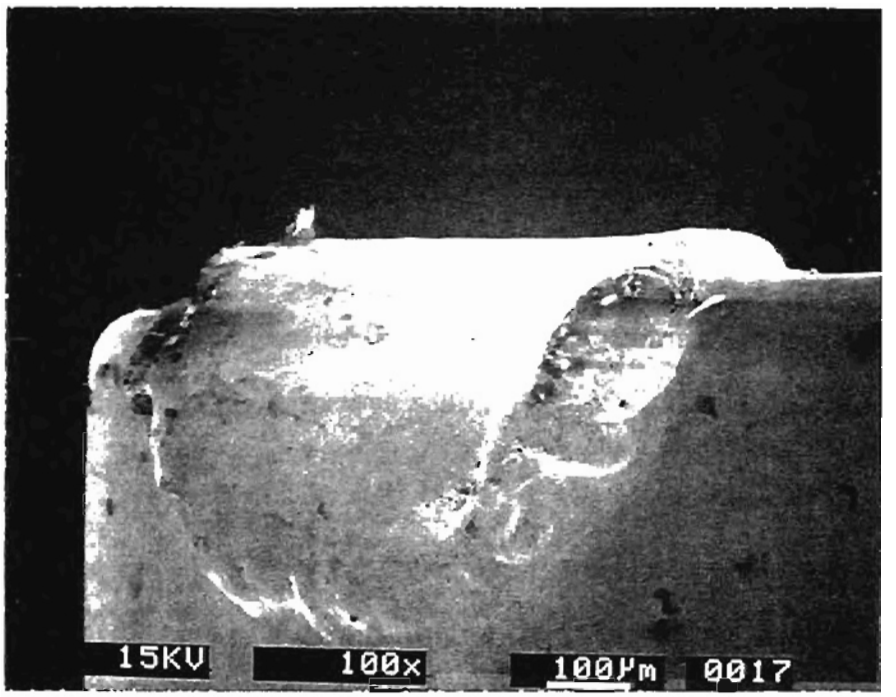

Figure10.2.4 a) Laser Drilled Hole at High Power in TiC Coated WC

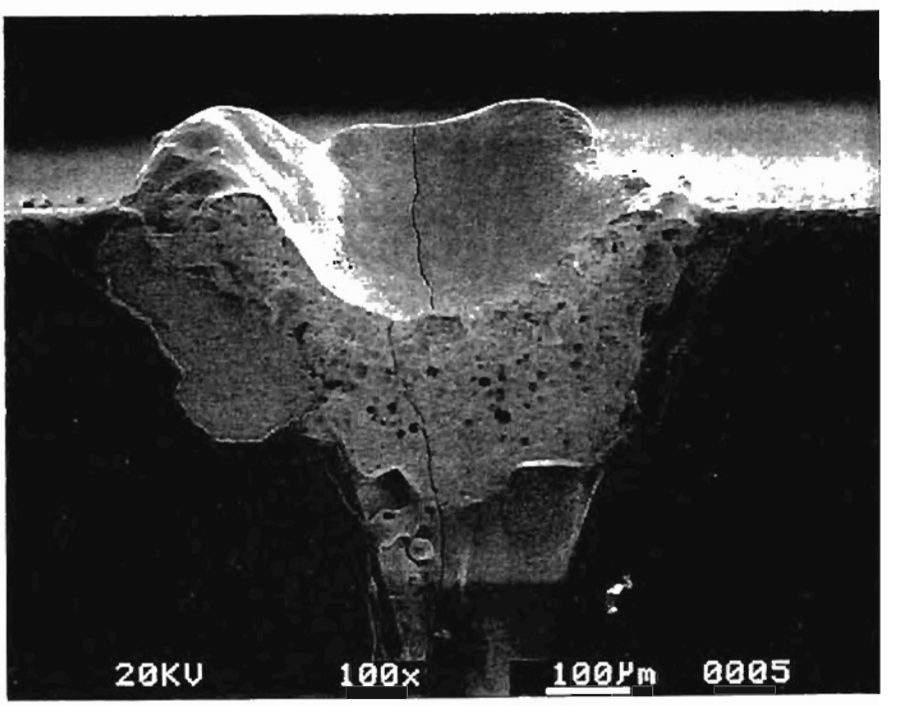

Figure 10.2.4 b) Laser Drilled Hole at High Power in Multi Coated Tool

10.3 Conclusions

The following conclusions are drawn from the observations:

- The build-up of the recast layer with increasing groove depth may be explained by the reduction in gas flow rate which does not permit the ejection of the molten material out of the groove.

- The scouring effect of the direct impingement of the assist gas on the bottom of the hole/groove seems to be very effective in removing the molten material.

- The recast layer was formed mostly along the walls of the groove/hole mainly because of the reduction in the gas flow rate along the walls, causing the viscous molten layer to adhere to the parent material. The net result is the formation of the recast layer that has an increasing thickness toward the top of the groove.

- The crack in the specimen seem to originate from the recast layer. Cracks are found to propagate in the radial direction, in case of ceramics and in the axial direction in the case of cemented carbides.

- An α to β phase transformation via the intermediate dendritic structure formation occurs in the recast layer of Si_3N_4. However similar phase transformation was not evident in the recast layer of other materials.

CHAPTER 11

ON THE MATERIAL REMOVAL MECHANISMS IN SILICON NITRIDE

11.1 Introduction

Hot pressed silicon nitride (Si_3N_4) was used for carrying out grooving tests. This material is reported to contain about 3 % wt. MgO and other non-specified amounts of sintering additives. The specimen were mounted on an x-y translation stage as shown in Figure 11.1 and moved at three different scanning speeds, 13.95, 6.97 and 4.017 in/min. The laser was operated in both pulsed and continuous wave modes to irradiate the specimen surface.

During the drilling tests with Si_3N_4, it was found that high power levels caused shattering of the specimen. Hence, low power levels were employed. The laser power was fixed at 215 W in the pulsed mode and at 750 W in the continuous mode. Helium and oxygen were used as assist gases. The microstructural features of the grooves and the surface near the grooves were examined by SEM. XRD was employed to identify the phases present inside the groove surface.

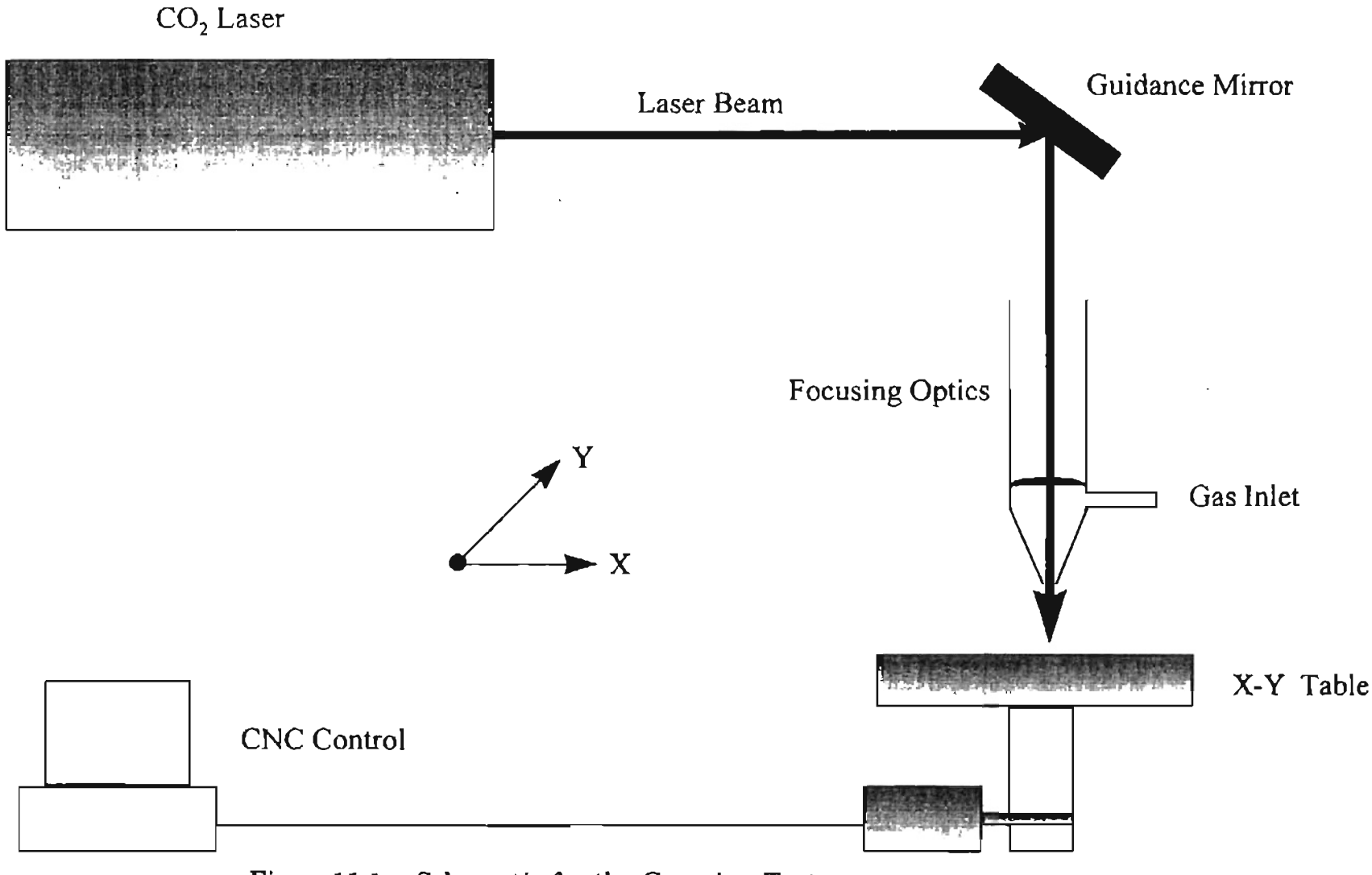

Figure11.1 Schematic for the Grooving Tests

11.2 Results

11.2.1 Microstructure and morphology of the groove at and near the surface

Figure 11.2.1.1 shows the ground surface of Si_3N_4, before the grooving tests. Figure 11.2.1.2 shows the microstructure of the same specimen before irradiation by a laser. The specimen was etched in hydrofluoric acid for 15 minutes to reveal the microstructure. From the micrograph, it can be seen that the microstructure consists of interlocking elongated β-Si_3N_4 grains, with a residual secondary phase at the grain boundaries. After laser irradiation, a different morphology was found in the groove, on the edges of the groove and on the surface outside the groove.

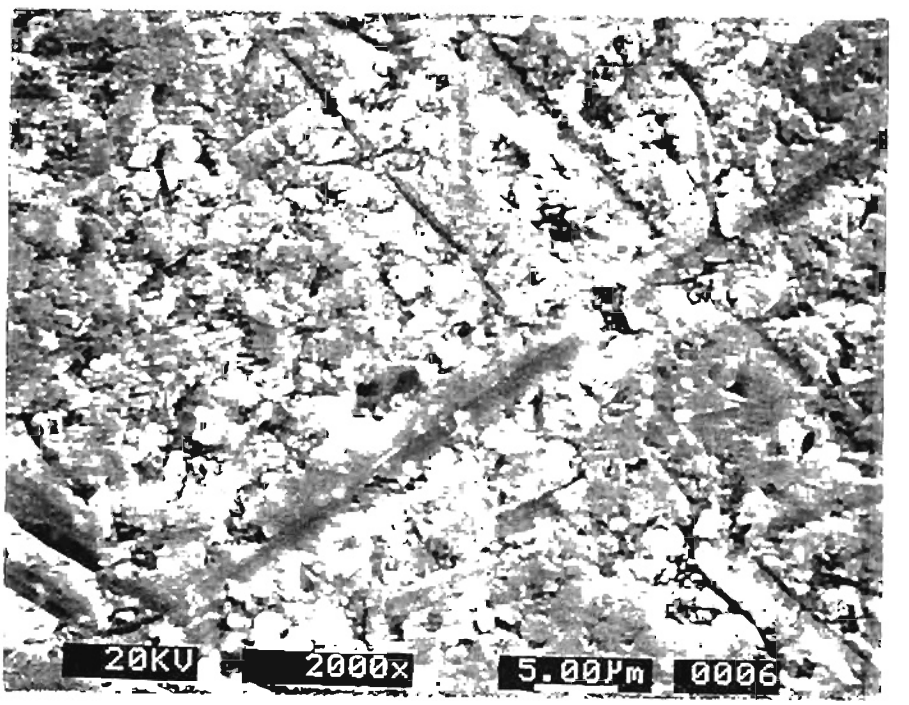

Figure11.2.1.1 Micrograph Showing Ground Surface of Si_3N_4

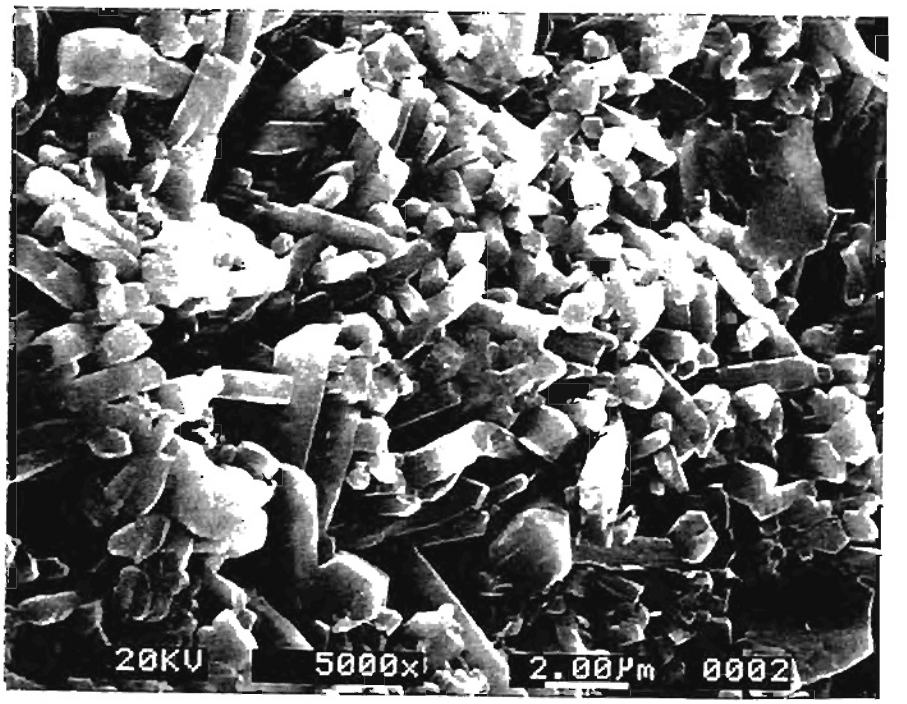

Figure11.2.1.2 Micrograph Showing the Etched Surface of Si_3N_4

Figures 11.2.1.3 (a), (b), and (c) show the micrographs of silicon nitride irradiated by the laser at different scanning speeds. Figure 11.2.1.3 (a) shows ball shaped agglomerates in the groove at a scanning speed of 4.017 in/min. The size of these agglomerates range between 1-5 µm. These particles appear to have grown by condensation from the vapor phase. As the translation speed increases, these small particles combine to form columnar grains.

Figure 11.2.1.3 (b) shows the microstructure inside the groove at medium scanning speed of 6.97 in/min. Such columnar grains were also observed at the edge of the groove. As the translation speed increases further, these columnar grains become larger and only elongated columnar grains are observed inside and on the edge of the groove. Figure 11.2.1.3 (c) clearly indicates the formation of elongated grains at a scanning speed of 13.95 in/min.

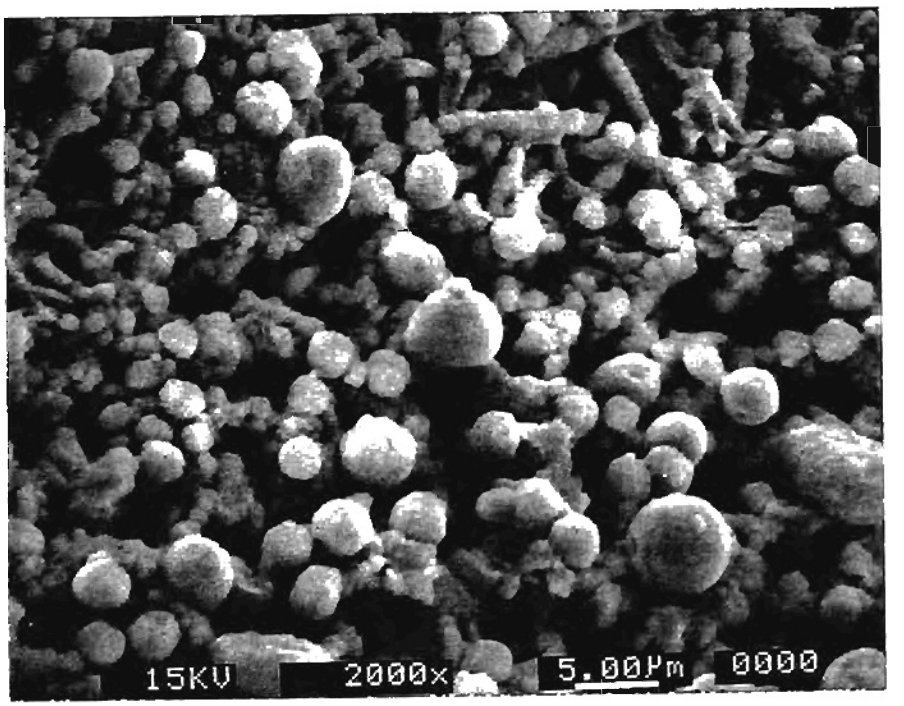

Figure11.2.1.3 (a) Micrograph Showing Ball Shaped Agglomerates in the Groove at a Scanning Speed of 4.017 in/min

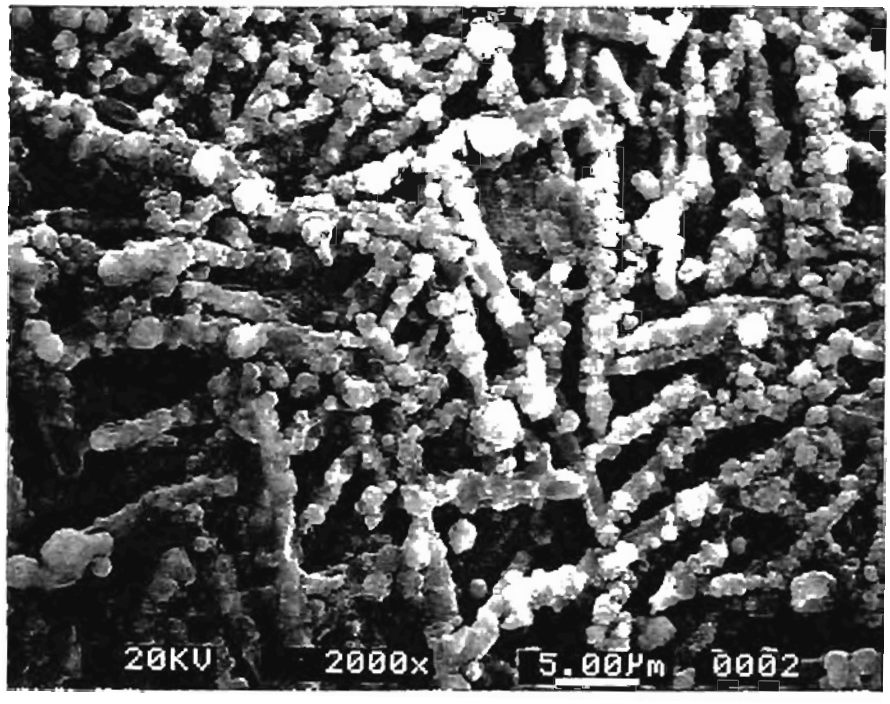

Figure11.2.1.3 (b) Micrograph Showing the Formation of Columnar Structures at a Scanning Speed of 6.97 in/min

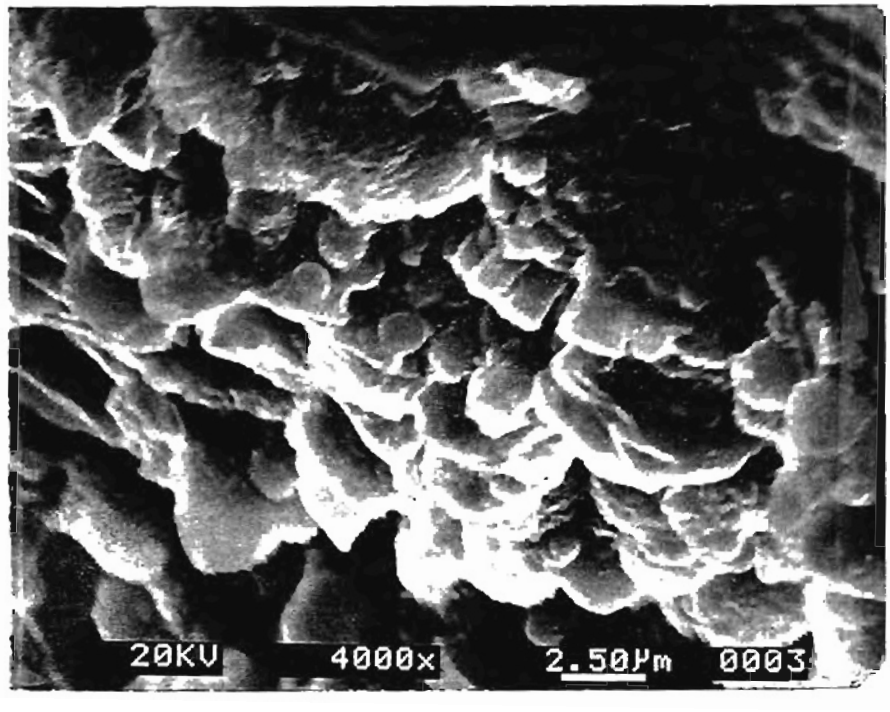

Figure11.2.1.3 (c) Micrograph Showing Elongated Grains at the Scanning Speed of 13.95 in/min (Side View)

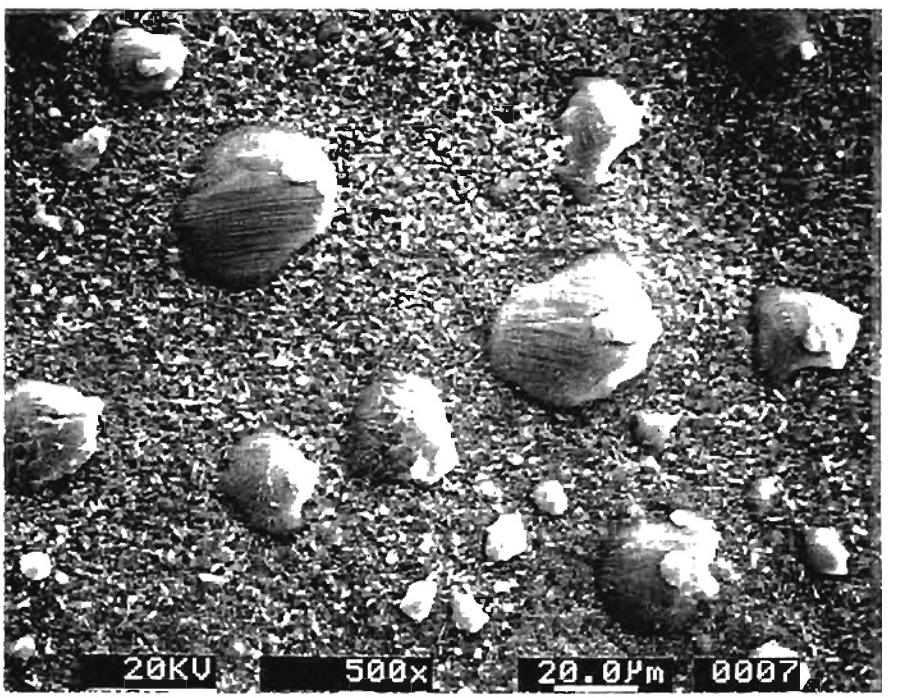

Figure11.2.1.4 Micrograph Showing Molten Silicon in the Groove

On laser heating, silicon nitride evaporates and decomposes above 1900° C (Solomah, 1993). Figure 11.2.1.4 shows large melt bumps inside the groove. These molten bumps appear to have formed by the coalescing of fine droplets. XRD analysis of these bumps reveals the presence of silicon in these molten bumps. Figures 11.2.1.5 (a) and (b) show the micrographs

at low and high magnifications which reveal the glassy secondary phase inside the groove at low scanning speed. As the scanning speed is increased, this glassy phase (MgO in this case) interacts with the liquid silicon to form compounds of silicon oxide. Figures 11.2.1.6 (a) and (b) show micrographs of the groove surface at medium speed. It can be seen that the glassy phase interacts with the molten bumps leading to secondary nucleation of very small sized droplets on the molten glassy phase. As the scanning speed is increased further, the nucleating compounds of molten oxides condense into sub-micron sized grains (< 0.5 μm). Figures 11.2.1.7 (a) and (b) show the sub-micron sized grains of the molten oxides at low and high magnification formed in the specimen at a scanning speed of 13.95 in/min.

During continuous wave irradiation of the specimen surface with the CO_2 laser, a different observation was made. During CW mode, the molten silicon appears to resolidify rapidly by self quenching, leading to the formation of dendritic structures (Figure 11.2.1.8). However, secondary nucleation of sub-micron sized particles can be observed even in CW mode. Figure 11.2.1.9 shows the dendritic crystallization along with the secondary nucleated particles inside the groove at a scanning speed of 6.97 in/min in CW mode.

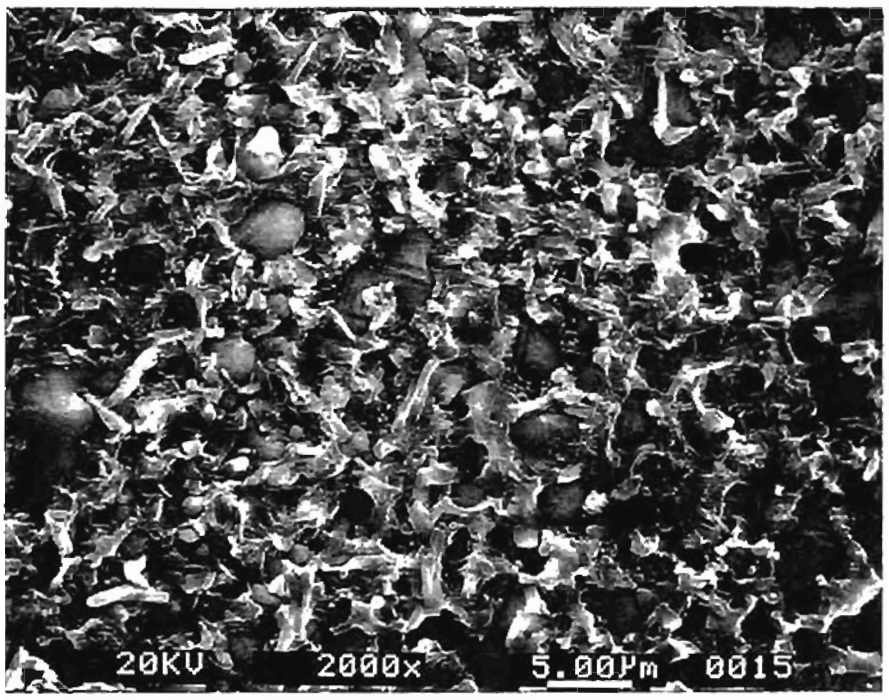

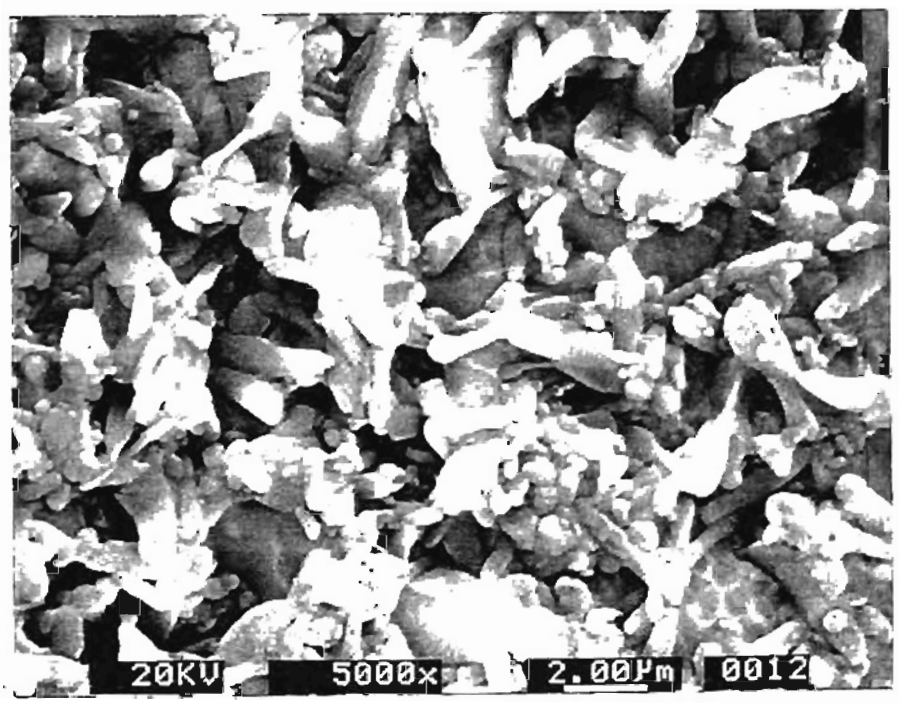

Figure11.2.1.5 Micrographs Showing the Secondary Glassy Phase in the Groove at Low Speed a) Low Magnification
b)High Magnification

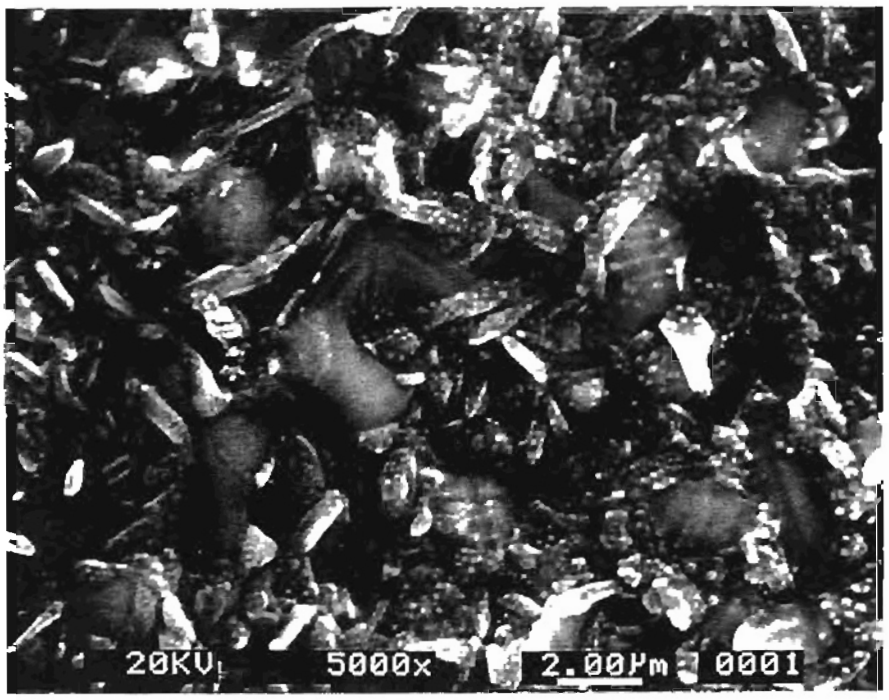

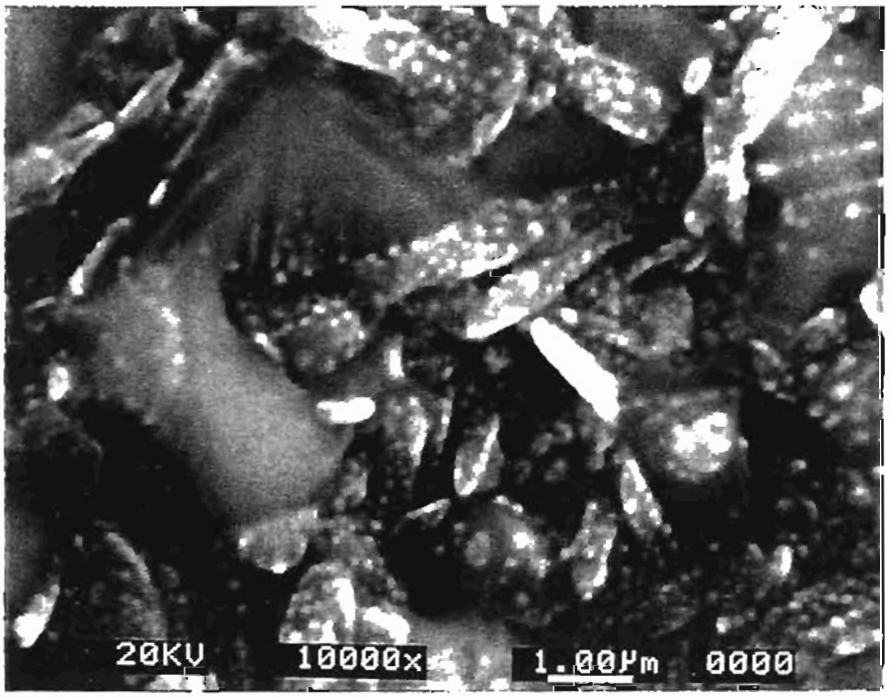

Figure 11.2.1.6 Micrographs Showing Secondary Nucleation in the Groove at Medium Speed a) Low Magnification b) High Magnification

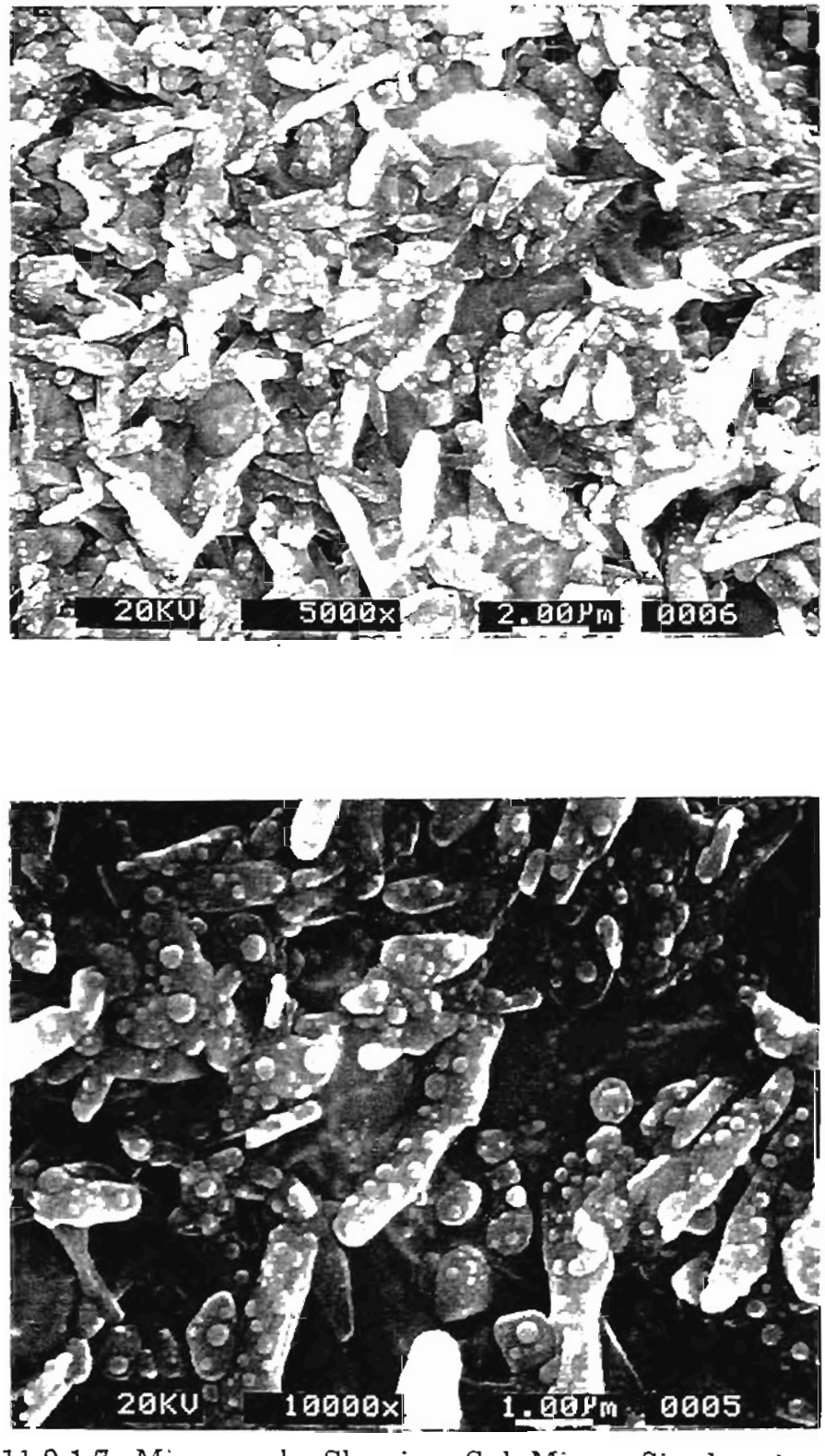

Figure 11.2.1.7 Micrographs Showing Sub-Micron Sized grains of the Molten Oxides in the Groove at High Speed
a) Low Magnification b) High Magnification

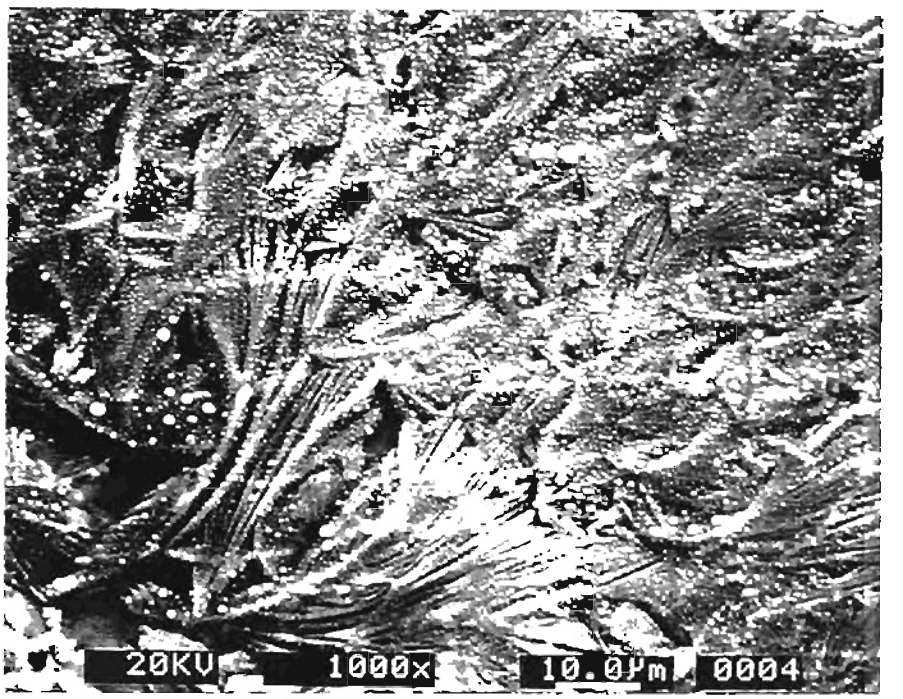

Figure 11.2.1.8 Micrograph Showing Dendritic Structure in the Groove in CW Mode

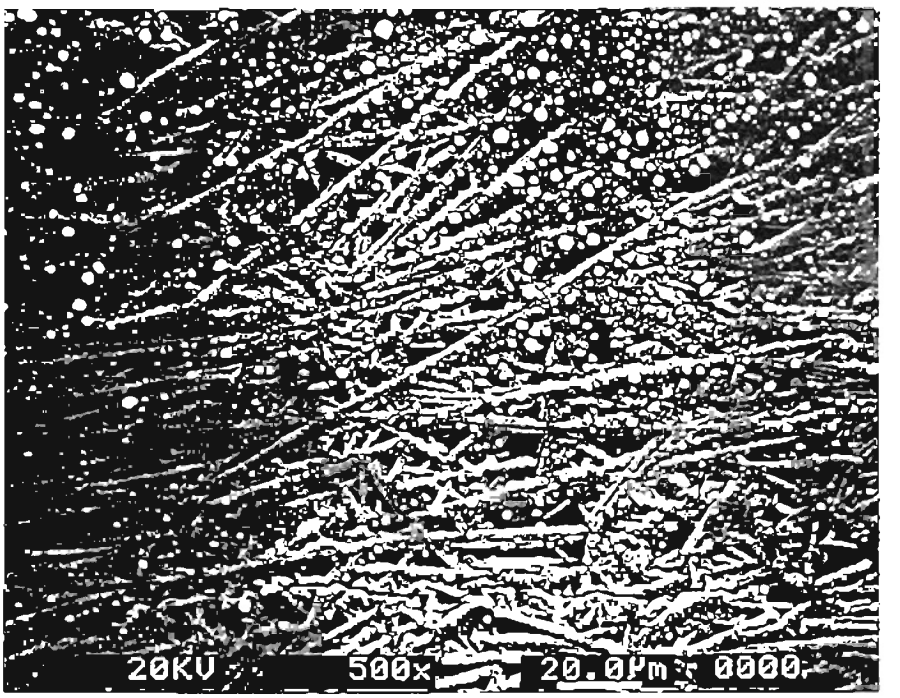

Figure 11.2.1.9 Micrograph Showing Secondary Nucleated Particles in the Groove in CW Mode

11.2.2 Identification of phases using XRD

X-Ray diffraction analysis was conducted to identify the phases present inside the groove surface. Figure 11.2.2.1 shows the XRD spectra of Si_3N_4 before laser irradiation. The spectra reveals β-Si_3N_4 as the major phase along with small amounts of SiO_2. It can be seen that the peak due to SiO_2 is very small, indicating that the phase is present in amorphous form. Figure 11.2.2.2 shows the XRD spectra of Si_3N_4 inside the groove using oxygen assist gas. Considerable amount of SiO_2 was found along with α- and β-Si_3N_4. The intensity of peaks corresponding to SiO_2 were considerably greater than the previous one taken on the ground surface. This is due to oxidation of silicon nitride in the presence of oxygen assist gas.

Figure 11.2.2.3 shows the XRD spectra of Si_3N_4 inside the groove surface at high translation speed using helium assist gas. Major amounts of silicon and $MgSiO_3$ were found in addition to the α and β phases of Si_3N_4. At low translation speed,only silicon was present in major amounts in the groove surface (Figure 11.2.2.4).

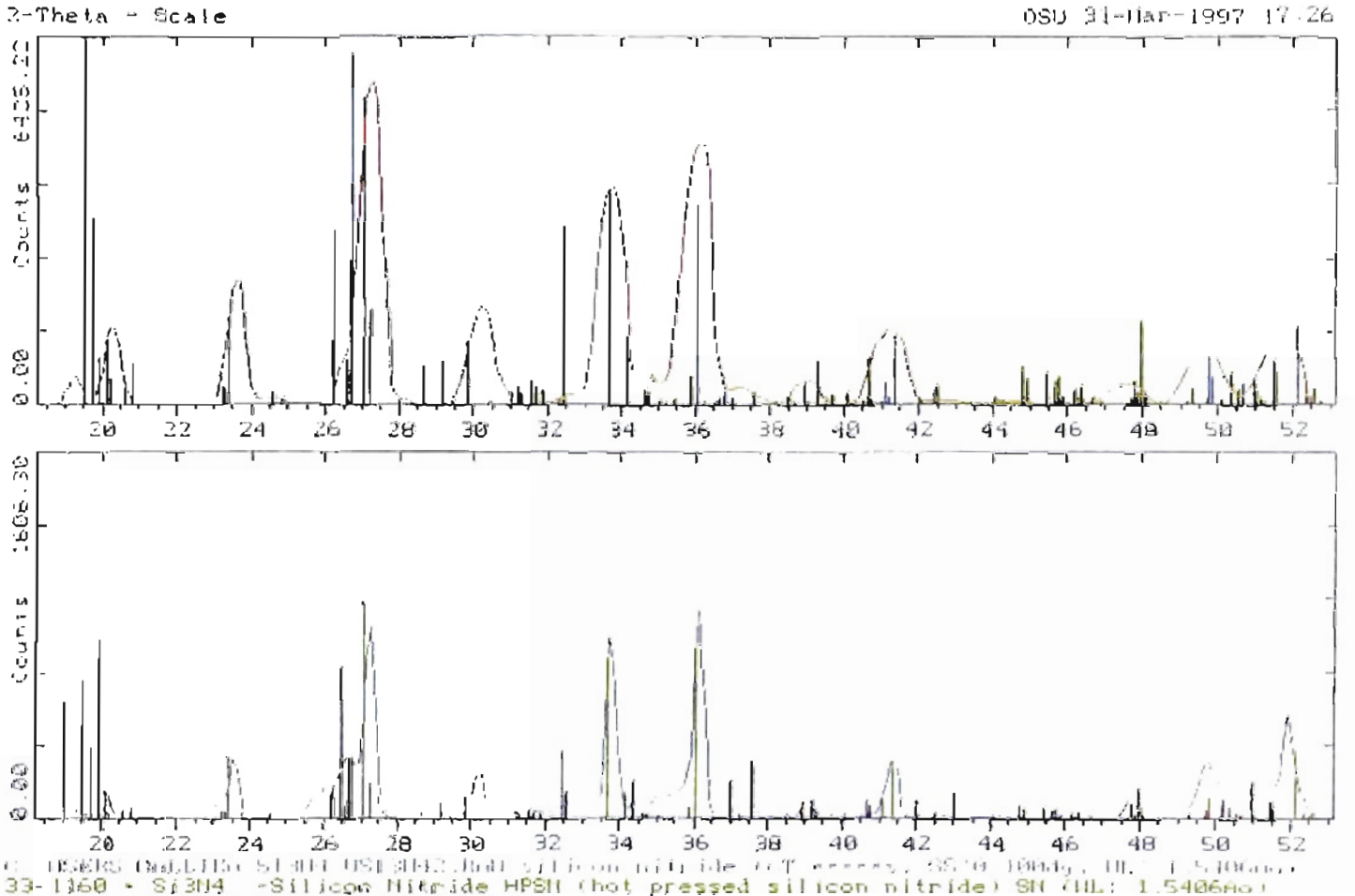

Figure 11.2.2.1 XRD Spectra of Ground Si_3N_4 Showing β-Si_3N_4 as a Major Phase

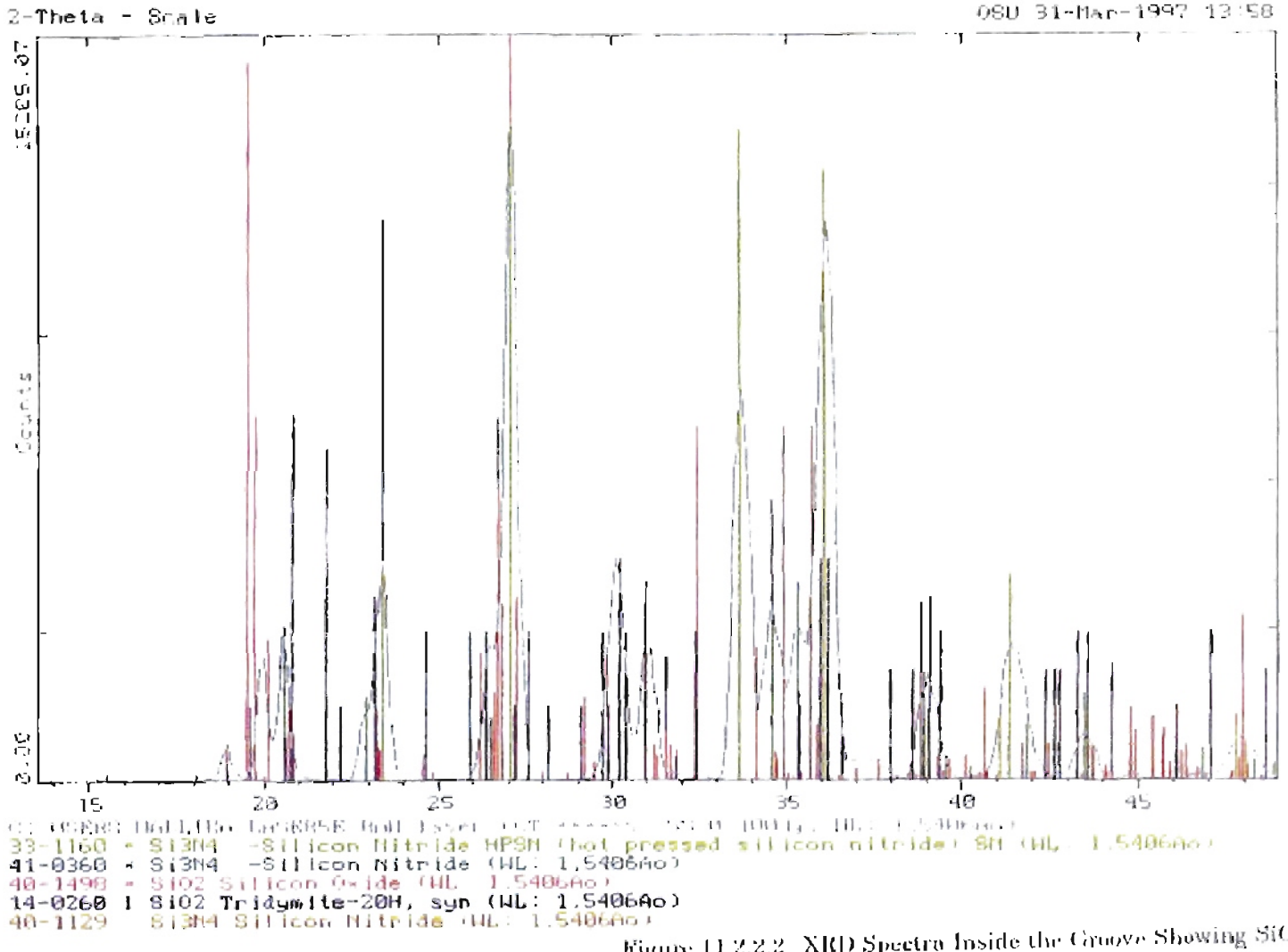

Figure 11.2.2.2 XRD Spectra Inside the Groove Showing SiO_2 Along with α and β Si_3N_4

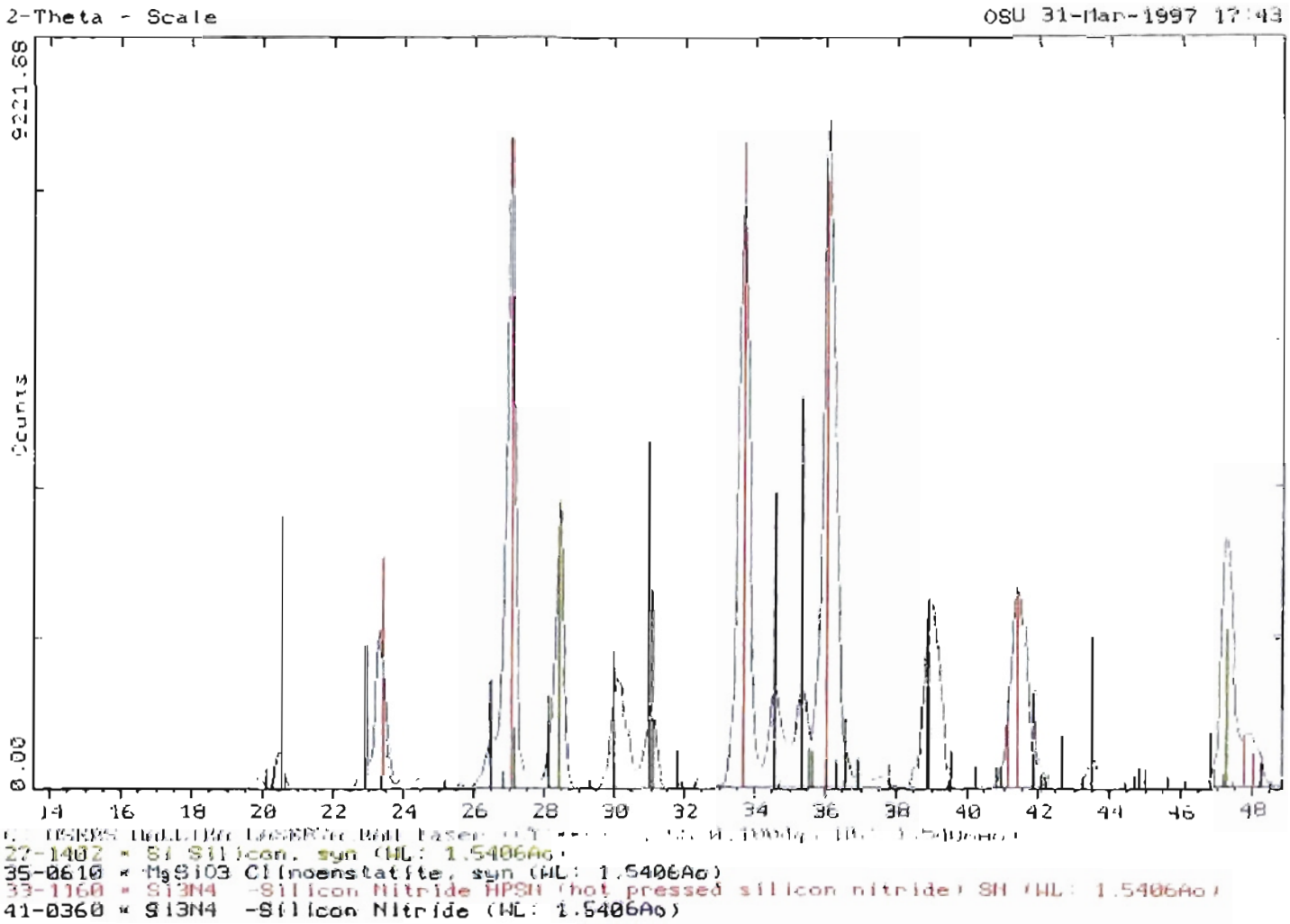

Figure 11.2.2.3 XRD Spectra Inside the Groove Showing the Presence of Silicon and $MgSiO_3$

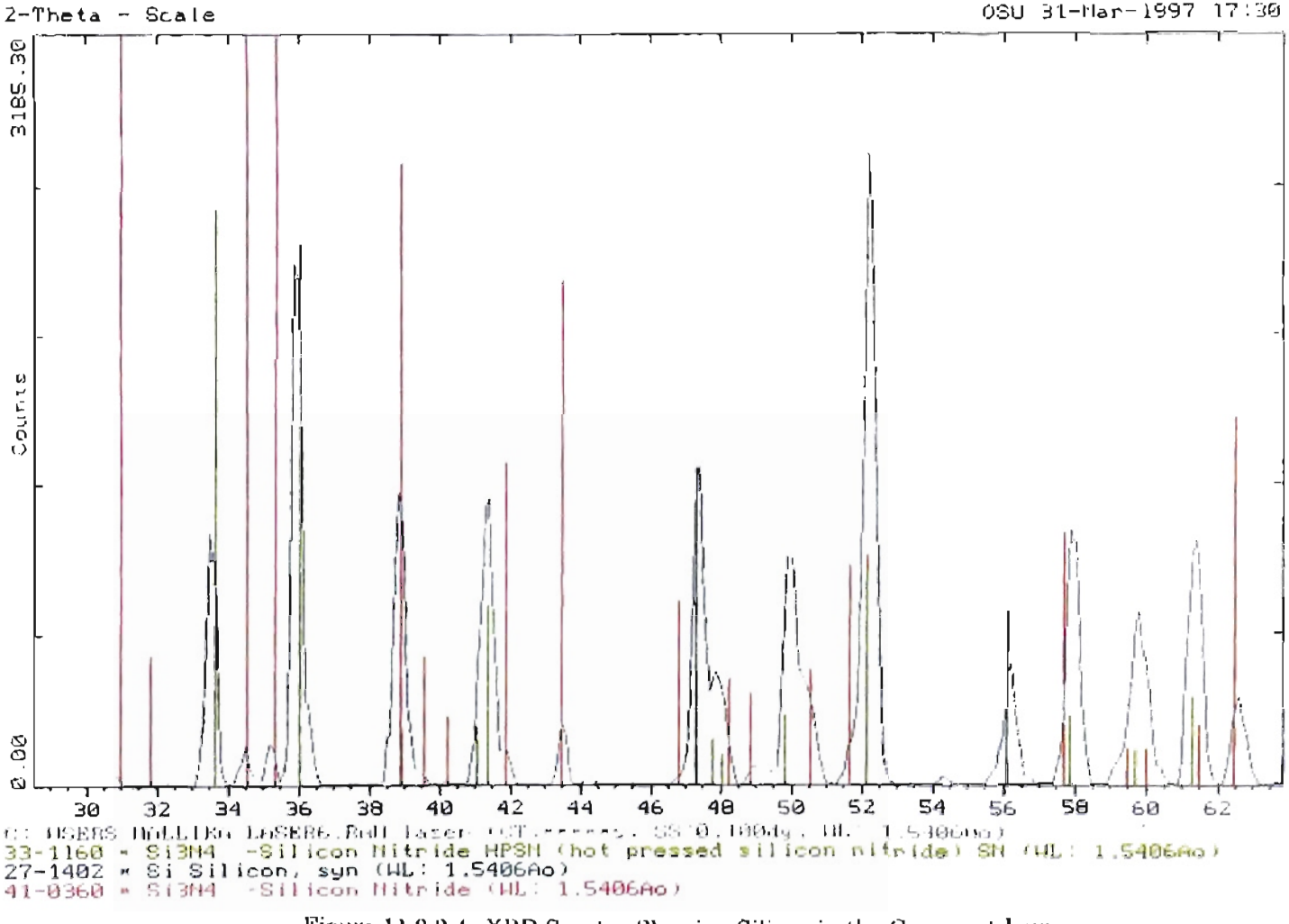

Figure 11.2.2.4 XRD Spectra Showing Silicon in the Groove at Low Translation Speed

11.3 Discussion and Conclusion

According to Solomah (1993), oxidation of Si_3N_4 takes place as follows:

$$2Si_3N_4 + 7O_2 \text{ --------> } 6SiO + 8NO$$

$$6SiO + 3O_2 \text{ ----------> } 6SiO_2$$

In the presence of oxygen assist gas, it can be observed that oxidation of molten silicon nitride takes place, generating SiO which is further converted into SiO_2 consuming more oxygen. Major amount of SiO_2 was hence detected by XRD analysis in the groove.

In the presence of an inert assist gas like helium, the decomposition of silicon nitride takes place according to the reaction (Solomah, 1993):

$$Si_3N_4 \text{ ----------> } 3Si_{(l)} + 2N_2$$

The molten silicon reacts with MgO to form magnesium silicate which was detected in the groove when helium was used as assist gas. The formation of compounds seem to proceed via the following reactions:

$$Si_3N_4 \text{ ----------> } 3Si + 2N_2$$

$$Si + O_2 \text{ ----------> } SiO_2$$

$$SiO_2 + MgO \text{ ---------> } MgSiO_3$$

$$2Si + 2MgO + 2O_2 \text{ --> } 2MgSiO_3$$

In summary, it can be concluded that the mechanism of material removal from Si_3N_4 by CO_2 laser heating is a vaporization process. Some of the vapor condenses inside the groove and reacts with the sintering

additives leading to formation of glassy silicates. Formation of these glassy silicates is enhanced at high translation speed. Morphology of the irradiated surface is also found to change with the translation speed, indicating the formation of columnar grains at higher translation speeds. Phases inside and outside the groove are influenced considerably by the type of assist gas used. However the microstructure is not affected by the type of the assist gas used.

CHAPTER 12

CONCLUSIONS

In the present investigation a CO_2 laser machining system was set up to provide flexibility for conducting a range of experiments without major modifications and ease of operation with a sturdy equipment giving accurate results and good repeatability.

For the preliminary laser assisted machining tests, a beam delivery system was designed and fabricated indigenously in the lab. A vinyl protection screen was provided around the test area to protect the operating personnel from stray reflections of the laser beam. To dispose off any gases liberated during laser machining of metals, ceramics and composites, an exhaust system was connected to the laser machining center. The CO_2 laser machining center was designed to conduct drilling, grooving, or laser assisted machining tests with minor modifications if any, to the existing system. An articulated arm was later integrated to the lathe to provide flexibility of motion and to carry out a wide range of machining tests.

This research has focused on the problems related to the laser machining of ceramics, cemented carbides and metals. Theoretical modelling has been presented for laser drilling process which is applicable for ceramics, metals or composites. This model is less computationally intensive while retaining a degree of accuracy comparable to the scatter in the experimental data associated with laser drilling.

Simple experimental setups have been devised to measure the material removal temperature and the focused beam spot size.

Experiments were conducted to determine the hole characteristics during laser drilling. The results thus obtained were compared to the theoretical values from the model and were found to be in good agreement. Grooving tests were performed on hot pressed silicon nitride to investigate the material removal mechanisms due to laser irradiation. Laser assisted machining tests were carried out on steel and aluminum work materials. A reduction in cutting force by 20 % was obtained during the tests on steel. These tests, however, highlighted the need for an absorptive coating on metal samples to increase the absorptivity to the 10.6 μm CO_2 laser beam.

Specific conclusions that can be drawn from this study are as follows:

- The measurements presented in this thesis for material removal temperature for silicon nitride is substantially in agreement with values available in the literature.

- The technique for determining the beam profile and focused beam spot size appears to be adequate for its application in modelling calculations.

- The heat transfer model for laser drilling is in good agreement with experimental results.

- The grooving tests on silicon nitride specimen enables a good understanding of the material removal mechanism and products of laser irradiation on the specimen surface.

- Laser assisted machining tests have highlighted the importance of absorptive coating on metal samples to achieve a significant reduction in cutting forces and increase in the tool life.

CHAPTER 13

FUTURE WORK

Future work in the following areas needs to be focused to understand laser machining better:

- During laser processing of various materials, heating rates close to 10^6 K/sec are encountered. Accurate temperature and absorptance measurements need to be undertaken to understand the effects of ionization, plasma formation etc. on the machining process.

- Investigation on the occurrence of plasma plume during laser machining of ceramics needs to be undertaken to understand its effects in the laser ablation process.

- Micro and macrocracking in ceramics is the main obstacle for the use of lasers to machine these materials. This thermal fracturing problem could possibly be solved by preheating and post heating the specimen and also by the use of pulsed laser beams. Extensive study needs to be undertaken to evaluate these possibilities.

- Calculation of thermal stresses during laser machining of ceramics would provide substantial insight into the reasons for thermal fracture and possible methods to prevent it.

- Laser assisted machining tests should be conducted on ceramics. This area has not been explored much and holds much promise for shaping of ceramics in future.

- Laser machining of composite materials is another area where more efforts need to be directed. Laser machining of wood, for example, has been studied quite extensively in the past. However, the tests have resulted in charred ends on the laser irradiated surfaces. These tests were carried using low power lasers. With the advent of multikilowatt CO_2 lasers and fast translating x-y tables, it should be possible to cut wood without leaving any charred ends.

- The role of assist gas in laser machining tests needs further investigation. Inert assist gases perform functions such as blowing away debris, cooling the material, maintaining an inert atmosphere near the lased material, thus preventing oxidation etc. Reactive gases help in exothermically reacting with the material. The effect of assist gases should be investigated in future heat transfer models to take advantage of the appropriate assist gas.

REFERENCES

Abakians, H., and M. F. Modest,"Evaporative Cutting of a Semi-Transparent Body with a Moving CW Laser," ASME Journal of Heat Transfer, 110, (1988) 924-930.

Affolter, P., and H. G. Schmid,"Processing of New Ceramic Materials with Solid State Laser Radiation," In High Power Lasers, 801, SPIE, (1987) 120-129.

Allcock, G., Dyer, P. E., Elliner, G., and H. V. Snelling,"Experimental Observations and Analysis of CO_2 Laser Induced Microcracking of Glass," J. Appl. Phys., 78(12), (1995) 7295-7303.

Arata, Y., Abe, N., and N. Tsujii,"Fundamental Phenomena during Vacuum Laser Welding," In Proceedings of the Materials Processing Symposium ICALEO '84, (1984) 1-7.

Arnot, R. S., and C. E. Albright,"Plasma Plume Effects in Pulsed Carbon Dioxide Laser Spot Welding," In Proceedings of ICALEO '83, 38,(1983) 51-58.

Atanasov, P. A., and S. I. Gendjov,"Laser Cutting of Glass Tubing- A Theoretical Model," J. Phys. D: Appl. Phys., 20, (1987) 597-601.

Baird, J. D., and A. Taylor,"Reaction Between Silica and Carbon and the Activity of Silica in Slag Solution," Transactions of the Faraday Society, 54, (1958) 526-539.

Bang, S. Y., and M. F. Modest,"Multiple Reflection Effects on Evaporative Cutting with a Moving CW Laser," ASME Journal of Heat Transfer, 113(3), (1991) 663-669.

Bang, S. Y.,"Effects of Multiple Reflections and Beam Polarization on Laser Grooving of Hard Ceramics," PhD thesis, The Pennsylvania State University, University Park, PA, (1991).

Bang, S. Y., and M. F. Modest,"Evaporative Cutting with a Moving CW Laser- Effects of Specular Reflections," In Fundamentals of Radiation Heat Transfer, HTD-160, ASME, (1991) 69-78.

Bang, S. Y., and M. F. Modest,"Evaporative Scribing with a Moving CW Laser - Effects of Multiple Reflections and Beam Polarization," In Proceedings of ICALEO '91, Laser Materials Processing, 74, (1992) 288-304.

Bar-Isaac, and C., U. Korn,"Moving Heat Source Dynamics in Laser Drilling Processes," Applied Physics, 3, (1974) 45-54.

Barnekov, V. G., McMillin, C. W., and H. A. Huber,"Factors Influencing Laser Cutting of Wood," Forest Products Journal, 36(1), (1986) 55-58.

Batanov, V. A., Bunkin, F. V., Prokhorov, A. M., and V. B. Fedorov, "Evaporation of Metallic Targets caused by Intense Optical Radiation," Soviet Phys- JETP, 36, (1973) 311-322.

Batha, H. D., and E. D. Whitney,"Kinetics and Mechanism of the thermal Decomposition of Si_3N_4," Journal of the American Ceramic Society,56,(1973) 365-369.

Biyikli, S., and M. F. Modest,"Beam Expansion and Focusing Effects on Evaporative Laser Cutting," ASME Journal of Heat Transfer, 110, (1988), 529-532.

Borkin, A. G., Drobyazko, S. V., Levchenko, E. B., Senatorov, Y. M., and A. Y. Turygin,"Self focusing and Waveguide Propagation of Radiation in the case of Deep Penetration of a Metal by a Laser Beam," Soviet Journal of Quantum Electronics,15, (1985) 1515-1523.

Borsch-Supan, W., Hunter, L. W., and J. R. Kutter,"Endothermic Gasification of a Solid by Thermal Radiation Absorbed in Depth," International Journal of Heat and Mass Transfer, 27, (1984) 1171-1182.

Brugger, K.,"Exact Solutions for the Temperature Rise in a Laser Heated Slab," Journal of Applied Physics, 43, (1972) 577-583.

Carslaw, H. S., and J. C. Jaeger,"Conduction of Heat in Solids," Oxford University Press, 2nd edition, (1959).

Chen, X., Lotshaw, W. T., Ortiz, A. L., Staver, P. R., Erikson, C. E., McLaughlin, M. H., and T. J. Rockstroh,"Laser Drilling of Advanced Materials: Effects of Peak Power, Pulse Format, and Wavelength," Journal of Laser Applications, 8, (1996) 233-239.

Chryssolouris, G.,"Laser Machining: Theory and Practice," Springer-Verlag, 1991.

Chun, M. K., and K. Rose,"Interaction of High Intensity Laser Beams with Metals," Journal of Applied Physics, 41(2), (1970) 614-620.

Copley, S. M., Bass, M., and R. J. Wallace,"Shaping Silicon Ceramics With Continuous Wave Carbon Dioxide Laser," In Proceedings of the Second International Symposium on Ceramic Machining and Finishing, NBSA Publication No. 562, (1979) 283-292.

Dabby, F. W., and U. C. Paek,"High-Intensity Laser-Induced Vaporization and Explosion of Solid Material," IEEE Journal of Quantum Electronics, QE-8, (1972) 106-111.

DeBastiani, D., Modest, M. F., and V. S. Stubican,"Mechanisms of Reactions during CO_2 laser Processing of Silicon Carbide," Journal of the American Ceramic Society, 73(7), (1990) 1947-1952.

Dobrovol'skii, I. P., and A. A. Uglov,"Analysis of the Heating of Solids by Laser Radiation Allowing for the Temperature Dependence of the Absorptivity," Soviet Journal of Quantum Electronics, 4, (1974) 788-790.

Drowart, J., De Maria, G., and M. G. Inghram,"Thermodynamic Study of SiC Utilizing a Mass Spectrometer," Journal of Chemical Physics,29,(1958) 1015-1021.

Duley, W. W.,"CO_2 lasers: Effects and Applications," Academic Press, New York, (1976).

Duley, W. W., and J. N. Gonsalves,"CO_2 Laser Cutting of Thin Metal Sheets with gas Jet Assist," Optics and Laser Technology, 6, (1974) 78-81..

Duley, W. W.,"Laser Processing and Analysis of Materials," Plenum Press, New York, (1983).

Durand, C., Ramulu, M., Pierre, R., and J. Machan,"An Experimental Analysis of a Nd-YAG Laser Cutting Process for Machining Silicon Nitride," International Journal of Prod. Res., 34(5), (1996) 1417-1428.

Eberl, G., Hildebrand, P., Kuhl, M., Sutor, and U., P. Wrba,"New Developments in the LASERCAV Technology,"In Proceedings of ICALEO '91, Laser Materials Processing, 74, San Jose, CA, (1992) 1-14.

Engin, D., and K. W. Kirby,"Development of an Analytical Model for the Laser Machining of Ceramic and Glass-Ceramic Materials," J. Appl. Phys., 80(2), (1996) 681-690.

Fieret, J., Terry, M. J., and B. A. Ward,"Overview of Flow Dynamics in Gas-Assisted Laser Cutting," In High Power Lasers, 801, SPIE,(1987) 243-250.

Finucane, M. A., and I. Black,"CO_2 Laser Cutting of Stained Glass," Int. J. of Adv. Manuf. Technology, 12, (1996) 47-59.

Gonsalves, J. N., and W. W. Duley,"Cutting thin Metal Sheets with the CW CO_2 Laser," Journal of Applied Physics, 43, (1972) 4684-4687.

Gonsalves, J. N., and W. W. Duley,"Interaction of CO_2 laser radiation with Solids I. Drilling of Thin Metallic Sheets," Canadian Journal of Physics, 49, (1971) 1708-1713.

Gonsalves, J. N., and W. W. Duley,"Interaction of CO_2 laser radiation with Solids II. Drilling of Fused Quartz," Canadian Journal of Physics, 50, (1972) 216-221.

Gregersen, O., and F. O. Olsén,"Beam Analyzing System for CO_2 Lasers," In Proceedings of Laser Materials Processing, ICALEO,(1990) 27-35.

Grigoryants, A. G."Basics of Laser Material Processing," Mir Publishers, 1994.

Grum, J., and D. Zuljan,"Analysis of Heat Effects in Laser Cutting of Steels," Journal of Materials Processing and Performance, 5(4), (1996) 526-537.

Hachfeld, K. D.,"Laser Beam Quality and Brightness Impacts Industrial Applications," in The Industrial Laser Annual Handbook, PennWell Books, Tulsa, Oklahoma, (1992).

Hecht, J.,"Laser Guidebook," Optical and Electro-Optical Series, 2nd Edition, (1992).

Hecht, J.,"Understanding Lasers: An Entry Level Guide," IEEE Press Understanding Science and Technology Series, 2nd Edition, (1992).

Herziger, G., Beyer, E., Kramer, R., Loosen, and P., F. Ruhl,"Diagnostic System for Measurement of the Focus Diameter of High Power CO_2 Lasers," In International Conference on Laser Advanced Materials Processing-Science and Applications, High Temperature Society of Japan, Japan Laser Processing Society, Japan,(1987) 37-41.

Ilavarasan, P. M., and P. A. Molian,"Laser Cutting of Thick Sectioned Steels Using Gas Flow Impingement on the Erosion Front," Journal of Laser Applications, 7, (1995) 199-209.

Jaeger, J. C.,"Some Problems Involving Line Sources in Conduction of Heat," Phil. Mag., 35 (7), (1942) 169-179.

Kirichenko, N. A., and B. S. Luk'yanchuk,"Laser Activation of Oxidizing Reactions on the Surfaces of Metals," Soviet Journal of Quantum Electronics, 13, (1983) 508-511.

Kocher, E., Tshudi, L., Steffen, and J., G. Herziger,"Dynamics of Laser Processing in Transparent Media," IEEE Journal of Quantum Electronics, QE-8, (1972) 120-125.

Komanduri, R., Flom, D. G., and M. Lee,"Highlights of the DARPA Advanced Machining Research Program," Journal of Engineering for Industry, 107, (1985) 325-335.

Komanduri, R., Flom D. G., Thomson, R. A., Jones, M. G., and R. J. Douglas,"Pulse Laser Pretreated Machining," United States Patent No. 4,356,376, (1982).

Kunz, T. D., Menefee, R. F., Krenek, B. D., Fredin, L. G., and M. J. Berry, "Laser Probe Absorption Spectroscopy Measurements on Laser Induced Plumes," High Temperature Science,27, (1990) 459-472.

Lax, M.,"Temperature Rise Induced by a Laser Beam," Journal of Applied Physics, 50, (1971) 1761-1789.

Lijun Li, and J. Mazumder,"A Study of the Mechanism of Laser Cutting of Wood," Forest Products Journal, 41(10), (1991) 53-59.

Lim, G. C., and W. M. Steen,"Measurement of the Temporal and Spatial Power Distribution of a High Power CO_2 Laser Beam," Optics and Laser Technology, (1982) 149-153.

Longfellow, J,"High Speed Drilling in Alumina Substrates with a CO2 Laser," Ceramic Bulletin, 50(3), (1971) 251-253.

Lukacs, M., Sayer, and M., H. Bisset,"Copper Vapour Laser Machining of Ceramics," Canadian Ceramics Quarterly, (1995) 148-151.

Lunau, F. W., Paine, E. W., Richardson, M., and M. D.Wijetunge,"High Power Laser Cutting using a Gas Jet," Optics Technology, 1, (1969) 255-258.

**********,"Laser Assist for Machining," Manufacturing Engineering, (Nov 1995) 26-27.

Maruo, H., Miyamoto, I., Ooie, T., and Y., Horiguchi,"Laser Machining of Ceramic-Machining Mechanism and Quality," In Advanced Technology in Welding, Materials Processing and Evaluation, 5th International Symposium in J. W. S., Tokyo, (1990) 251-256.

Maydan, D,"Micromachining and Image Recording on Thin Films by Laser Beams," Bell System Technical Journal,50, (1971) 1761-1789.

Mazumder, M., and W. M. Steen,"Heat Transfer Model for CW Laser Material Processing," J. Appl. Phys., 51(2), (1980) 941-947.

McMillin, C. W., and J. E. Harry,"Laser Machining of Southern Pine," Forest Products Journal, 21(10), (1971) 34-37.

Modest M. F., and H. Abakians,"Heat Conduction in a Moving Semi-Infinite Solid Subjected to Pulsed Laser Irradiation," ASME Journal of Heat Transfer, 108, (1986) 597-601.

Modest, M. F., and H. Abakians,"Evaporative Cutting of a Semi-Infinite Body with a Moving CW Laser," ASME Journal of Heat Transfer, 108, (1986) 602-607.

Modest, M. F.,"Laser Processing of Materials-The Present and Future," In Proceedings of the XXII ICHMT International Symposium on Manufacturing and Materials Processing, Dubrovnik, Yugoslavia, 1990.

Modest, M. F., and S. Ramanathan,"Laser Machining of Ablating Materials-Overlapped Grooves and Entrance/Exit Effects," ICALEO, (1994) 303-312.

Molian, P. A,"Dual-Beam CO_2 Laser Cutting of Thick Metallic Materials," Journal of Materials Science, 28, (1993) 1738-1748.

Nissim, Y. I., Lietoila, A., Gold, R. B., and J. F. Gibbons,"Temperature Distributions Produced in Semiconductors by a Scanning Elliptical or Circular CW Laser Beam," Journal of Applied Physics, 51, (1980) 274-279.

Paek, U. C., and F. P. Gagliano,"Thermal Analysis of Laser Drilling Process," IEEE Journal of Quantum Electronics,QE-8, (1972) 112-119.

Paek, U. C., and V. J. Zaleckas,"Scribing of Alumina Material by YAG and CO_2 Lasers," The American Ceramic Bulletin, 54, (1975), 585-588.

Peters, C. C., and C. M. Banas,"Cutting Wood and Wood-Base Products with a Multikilowatt CO_2 Laser," Forest Products Journal, 27(11), (1976) 41-45.

Powell, J., King, T. G., and I. A. Menzies,"Cut Edge Quality Improvement by Laser Pulsing," In 2nd International Conference of Lasers in Manufacturing, Birmingham, UK, (1985) 37-45.

Ramanathan, S., and M. F. Modest,"High Speed Photographic Studies of Laser Drilling of Ceramics and Ceramic Composites," Journal of Laser Applications, 7, (1995) 75-82.

Ray, A.,"Laser Machining and its Thermal Effects on Silicon Nitride and Steel," Phd thesis, Iowa State University, Ames, (1995).

Ready, J. F,"Development of Plume of Material Vaporized by Giant Pulse Laser," Applied Physics Letters, 3(1), (1963) 11-13.

Ready, J. F,"Effects Due to Absorption of Laser Radiation," Journal of Applied Physics, 36(2), (1965) 462-468.

Risch, T. K., and B. Laub,"General Model for Thermochemical Ablation into a Vacuum," Journal of Thermophysics and Heat Transfer, 4(3), (1990) 278-284.

Roy, S., and M. F. Modest,"Three-Dimensional Conduction Effects During Evaporative Scribing with a CW Laser," Journal of Thermophysics and Heat Transfer, 4(2), (1990) 199-203.

Roy, S., Bang, S. Y., Modest, M. F., and V. S. Stubican,"Measurement of Spectral, Directional Reflectivities of Solids at High Temperatures Between 9 and 11 mm," In Proceedings of the ASME/JSME Engineering Joint Conference, 4, (1991) 19-26.

Rykalin, N. N., Uglov, A. A., and I. Y. Smurov,"Nonlinearities of Laser Heating of Metals ," Soviet Physics-Doklady, 27, (1982) 970-972.

Saifi, M. A., and R. Borutta,"Optimization of Pulsed CO_2 Laser Parameters for Al_2O_3 Scribing," Ceramic Bulletin, 54(11), (1975) 986-989.

Sami, M., and B. S. Yilbas,"A Kinetic Theory Approach for Laser Pulse Heating Process," Optics and Lasers in Engineering, 24, (1996) 319-337.

Schellhorn, M., Nowack, and R., G. Roth,"Optical Diagnostics of Laser-Metal Interaction during Welding," In 3rd International Conference of Lasers in Manufacturing, Paris, France, (1986) 97-105.

Schenck, P. K., Bonnell, D. W., and J. W. Hastie,"In Situ Analysis of Laser Induced Vapor Plumes," High Temperature Science, 27, (1990), 483-501.

Schuocker, D,"Theoretical Model of Reactive Gas Assisted Laser Cutting including Dynamic Effects," In High Power Lasers and Their Industrial Applications, 560, SPIE, (1986), 210-219.

Sheng, P. S., and Ko-Wang Liu,"Laser Machining for Secondary Finishing Applications," Journal of Engineering for Industry, 117, (1995) 629-636.

Singhal, S. C,"Thermodynamic Analysis of the High-Temperature Stability of Silicon Nitride and Silicon Carbide," Ceramurgia International,2,(1976) 123-130.

Solomah, A. G,"Laser Machining of Silicon Nitride," Annals of CIRP, 87, (1991), 543-546.

Steen, W. M,"Laser Materials Processing," Springer Verlag, 1991.

Sturmer, E., and M. Von Allmen,"Influence of Laser Supported Detonation Waves on Metal Drilling with Pulsed CO_2 lasers," Journal of Applied Physics, 49, (1978) 5648-5654.

Thomassen, F. B., and F. O. Olsen,"Experimental Studies in Nozzle Design for Laser Cutting," In 1st International Conference of Lasers in Manufacturing, Brighton, UK, (1983) 169-180.

Trubelja, M. F., Ramanathan, S., Modest, M. F., and V. S. Stubican, "Carbon Dioxide Laser Cutting of a Carbon-Fiber-Silicon Carbide-Matrix Composite," Journal of American Ceramic Society, 77(1), (1994) 89-96.

Trubelja, M. F., Ramanathan, S., Modest, M. F., and V. S. Stubican, "Carbon-Dioxide Laser Cutting on Laser Advanced Materials Processing-Science and Applications," Nagaoka, Japan, (1992) 633-638.

Tuersley, I. P., Hoult, A. P., and I. R. Pashby,"The Processing of a Magnesium-Alumino-Silicate Matrix, SiC Fibre Glass-Ceramic Matrix Composite Using a Pulsed Nd-YAG Laser," Chapman and Hall, (1996) 4111-4119.

Uglov, A. A., and A. N. Kokora,"Thermophysical and Hydrodynamic Effects in Laser Beam Processes of Materials (Review)," Soviet Journal of Quantum Electronics, 7, (1977) 671-678.

Uglov, A. A., Smurov, I. Y., and A. A. Volkov,"Calculation of Heating of Metals by Continuous Laser Radiation in an Oxidizing Atmosphere," Soviet Journal of Quantum Electronics, 13, (1983) 154-156.

Von Allmen, M., Blaser, P., Affolter, and K., E. Sturmer,"Absorption Phenomena in Metal Drilling with Nd-YAG lasers," IEEE Journal of Quantum Electronics, QE-14, (1978) 85-88.

Von Allmen, M.,"Laser Drilling Velocity in Metals," Journal of Applied Physics, 47, (1976) 5460-5463.

Von Allmen, M.,"Laser-Beam Interactions with Materials," Springer Series in Materials Science, 2, Springer Verlag, Berlin, (1987).

Wallace, R. J.,"A Study of the Shaping of Hot Pressed Silicon Nitride With a High Power CO_2 laser," PhD Thesis, University of Southern California, Los Angeles, CA,(1983).

Wallace, R. J., Bass, M., and S. M. Copley,"Curvature of Laser Machined Grooves in Si_3N_4," Journal of Applied Physics, 59, (1986) 3555-3560.

Wallace, R. J., Bass, M., and S. M. Copley,"Curvature of Laser-Machined Grooves in Si_3N_4," Journal of Applied Physics, 59(10), (1986) 3555-3560.

Wallace, R. J., and S. M. Copley,"Laser Machining of Silicon Nitride: Energetics," Advanced Ceramic Materials, 1(3), (1986) 277-283.

Watanabe, T., Yoshida, and Y., T. Arai,"Reflectivity and Meltability of Aluminum Alloys with YAG laser beams," In International Conference on Laser Advanced Materials Processing-Science and Applications, Japan, (1992) 505-510.

Wei, P. S., and J. Y. Ho,"Energy Considerations in High-Energy Beam Drilling," International Journal of Heat and Mass Transfer, 33(10), (1990) 2207-2216.

Yakovlev, E. B,"Changes in the Properties of Glass Heated by a Laser," J. Opt. Technology, 63(2), (1996) 105-108.

Yamamoto, J., and Y. Yamamota,"Laser Machining of Silicon Nitride," In International Conference on Laser Advanced Materials Processing-Science and Applications," High Temperature Society of Japan, Japan Laser Processing Society, Osaka, Japan, (1987) 297-302.

Yilbas, B. S., and A. Z. Al-Garni,"Some Aspects of Laser Heating of Engineering Materials," Journal of Laser Applications, 8, (1996) 197-204.

Yilbas, B. S.,"Laser Heating Process and Experimental Validation," Int. J. Heat Mass Transfer, 40(5), (1997) 1131-1143.

Yue, T. M., Jiang, C. Y., Xu, J. H., and W. S. Lau,"Laser Fantasy: From Machining to Welding," Journal of Materials Processing Technology, 57, (1996) 316-319.

Zhang, J. H., Lee, T. C., Ai, X., and W. S. Lau,"Investigation of the Surface Integrity of Laser-Cut Ceramic," Journal of Materials Processing Technology, 57, (1996) 304-310.

Zhen Bing, Hou., and R. Komanduri,"A Thermal Model of Magnetic Float Polishing of Ceramic Balls," to be published in J. Tribology, 1997.

Ziegler, G., Heinrich, J., and G. Wotting,"Review - Relationships Between Processing, Microstructure and Properties of Dense and Reaction Bonded Silicon Nitride," J. Mat. Sci., 22, 1987, 3041 - 3086.

APPENDIX

/* Program to calculate temperature rise at any point in laser drilling */

```
#include <stdio.h>
#include <math.h>
#include <stdlib.h>
#include <string.h>
double tddisk(double , double);
double tdbar(double , double);
double simpson2(double (*)(double),double (*)(double),int,double,double,int,
  double (*)(double,double));
double simpson1(double,double,double,int,double (*)(double,double));
double fltd(double);
double futd(double);
double fltb(double);
double futb(double);


FILE *of1, *of2, *of3;
double W,lm,a,r0,t,x,y,z,pi,v,r,d,tem,l;
double tem1,tem2;
int flag;

main()
  {
        printf ("Enter W = ");
        scanf("%lf",&W);
        printf( " Enter lamda = ");
          scanf("%lf", &lm);
        printf("enter a = ");
```

```
    scanf("%lf", &a);
   printf("Enter t = ");
    scanf("%lf", &t);
   printf("enter r0 = ");
    scanf("%lf", &r0);
   printf("Enter x =  ");
     scanf("%lf", &x);
   printf("enter y = ");
     scanf("%lf", &y);
   printf("enter z = ");
    scanf("%lf", &z);
   printf("enter velocity = ");
     scanf("%lf",&v);
   printf("enter density of material = ");
     scanf("%lf", &d);
   pi = 3.1415927;
    l = v*t;
    r = sqrt(x*x +y*y);

  tem1 =  simpson2(fltd,futd,100,0.00001,r0,30,tddisk) ;
  tem2  =  simpson2(fltb,futb,100,0.00001,l,30,tdbar);
          tem = tem1 +tem2;
 printf("temperature = %lf\n",tem);

      }

double tddisk (double T, double ri)


  {
    double t1, t2, t3, t4,t5,t6,p;
    t5 =  (ri*ri +r*r + (z-(v*t) + (v*T))*(z-(v*t)+(v*T)));
```

```
    t1 =  t5/(4*a*T);
    t6 =  (ri*ri + r*r+(z+(v*t)-(v*T))*(z+(v*t)-(v*T)));
    t2 =  t6/(4*a*T);
     p = ri*r/(2*a*T);
     if (p<1.6)
          t3 = 0.935 * (exp(0.352*p - t1) + exp (0.352 *p - t2));
        else if ((p >= 1.6) && (p <=3.0))
          t3 = 0.529 * (exp(0.735*p - t1) + exp(0.735*p -t2));
           else
           t3 = (exp(p-t1) + exp(p-t2))/sqrt(2*pi*p);
           t4 = T*sqrt(T)*((2*v*t) - (2*v*T) + r0);
        t3 *= 2*W*ri / (t4*(r0*8*lm*pi*sqrt(a*pi)));
           return(t3);

     }


double tdbar(double T,double li)

  {
    double t1,t2,t3,t4,p;
    t1 = (r0*r0 + r*r +(z-li)*(z-li))/(4*a*T);
    t2 = (r0*r0 +r*r +(z+li)*(z+li))/(4*a*T);
     p = r*r0/(2*a*T);

 if (p<1.6)
          t3 = 0.935 * (exp(0.352*p - t1) + exp (0.352 *p - t2));
        else if ((p >= 1.6) && (p <=3.0))
          t3 = 0.529 * (exp(0.735*p - t1) + exp(0.735*p -t2));
           else
           t3 = (exp(p-t1) + exp(p-t2))/sqrt(2*pi*p);
           t4 = T*sqrt(T)*(2*v*(t-T) + r0);
```

```
        t3 *= 2*W/(8*pi*lm*sqrt(pi*a)*t4);
        return(t3);
    }


double simpson2 (double (*flx)(double), double (*fux)(double),int hx,double lowy,
                    double upy, int hy, double (*f)(double,double))
    {
        double deltx, delty,temp1,temp2,tempy;
         int i,j,k;
        delty = (upy - lowy)/ (double) hy;
         temp2 = simpson1((*flx)(lowy), (*fux)(lowy),lowy,hx,f) +
        simpson1((*flx)(upy),(*fux)(upy),upy,hx,f);
            temp2 = simpson1((*flx)(lowy), (*fux)(lowy),lowy,hx,f) +
                        simpson1((*flx)(upy),(*fux)(upy),upy,hx,f);


             for(i=1;i<=hy-1;i+=2)
        {
               tempy = lowy +(double) i*delty;
               temp2 += 4*simpson1((*flx)(tempy),(*fux)(tempy),tempy,hx,f);
         }
             for(i=2;i<=hy-2;i+=2)
       {
             tempy = lowy +(double) i*delty;
             temp2 += 2*simpson1((*flx)(tempy),(*fux)(tempy),tempy,hx,f);
        }
            return(temp2*delty/3.0);
    }
```

```
double simpson1(double lowx, double upx, double y, int hx,
                                double (*f)(double,double))
  {
       double temp2, deltx;
        int i;
        if(lowx >= upx) return(0);
         deltx = (upx -lowx)/ (double) hx;
        temp2 = (*f)(lowx,y) + (*f)(upx,y);
        for(i=1;i<=hx-1; i+=2)
      temp2 += 4*(*f)(lowx + (double) i*deltx,y);
         for(i=2;i<=hx-2; i+=2)
      temp2 += 2*(*f)(lowx + (double) i*deltx,y);
       return(temp2*deltx/3.0);

 }
double fltd(double c) { return(0.00001);}

double futd(double c) { return(t);}

double fltb(double k) {return(0.00001);}

double futb(double li) {return(t - li/v);}
```

VITA

Rajesh Iyer

Candidate for the Degree of

Master of Science

Thesis: MATERIAL PROCESSING USING A CO_2 LASER

Major Field: Mechanical Engineering

Biographical:

Education: Received Bachelor of Engineering degree in Mechanical Engineering from Visvesvaraya Regional Engineering College, Nagpur, India.
Completed the requirements for the Master of Science degree with a major in Mechanical Engineering at Oklahoma State University in May, 1997.

Experience: Employed as Commissioning Engineer (Power Plants) by Thermax Babcock and Wilcox Ltd., Pune, India (1991-95); Graduate research assistant at Oklahoma State University, Department of Mechanical and Aerospace Engineering, 1995 to present.